ANALYSIS OF THE OBSERVED EARTHQUAKE RESPONSE OF A MULTIPLE SPAN BRIDGE

Thesis by

John Charles Wilson

In Partial Fulfillment of the Requirements
for the Degree of
Doctor of Philosophy

California Institute of Technology
Pasadena, California

1984

(Submitted May 23, 1984)

ACKNOWLEDGMENTS

I wish to express my thanks to my advisor, Professor P.C. Jennings, for his guidance and encouragement throughout the course of my Ph.D. studies at Caltech. His numerous suggestions and ideas were especially valuable contributions to many stages of my research. I would also like to thank Professor J.L. Beck for the interesting discussions we had on the application of system identification to bridge structures. The assistance provided by Mr. James Gates of the California Department of Transportation and Mr. John Ragsdale, formerly of the California Division of Mines and Geology was very helpful.

The financial support of a Postgraduate Scholarship from the Natural Sciences and Engineering Research Council of Canada is gratefully acknowledged. I am also appreciative of the support from the California Institute of Technology in the form of Graduate Research Assistantships, Graduate Teaching Assistantships and tuition scholarships.

Special thanks go to Gloria Jackson and Sharon Beckenbach for their skillful typing of this thesis, and to Cecilia Lin for her assistance in preparation of several of the figures.

I finally wish to mention my family; my parents and brother who have provided continual encouragement throughout my education, and my wife, Anne-Marie, who has made such a valuable contribution through her support, encouragement and understanding. This thesis is dedicated to these people.

ABSTRACT

Accelerograms obtained during the 1979 Coyote Lake, California earthquake are used to examine the response of a multiple-span, steel girder bridge to strong earthquake loading. The structure studied, the San Juan Bautista 156/101 Separation Bridge, is typical of many highway bridges in seismic regions of the United States. Although the bridge was not damaged, the strong-motion records are of significant engineering interest as they are the first to be recorded on such a structure.

An engineering seismology study suggests that long-period ground displacements at the bridge site were caused by Rayleigh waves. A three-second period, pseudostatic response of the superstructure is attributed to small amounts of differential support motion induced by the surface waves.

A time-domain technique of system identification is used to determine linear models which can closely replicate the observed bridge response. Using time-invariant models, two structural modes at 3.50 and 6.33 Hz, are identified in the horizontal direction. Each mode, having approximately ten-percent damping, involves coupled longitudinal and transverse motions of the superstructure. Time-variations of frequency and damping in the horizontal response are also identified using a moving-window analysis.

A three-dimensional finite element model which includes soil-structure interaction predicts several important features of the dynamic response of the bridge. The first two computed horizontal frequencies are found to be in excellent agreement with the observed responses provided the model's expansion joints are locked, preventing relative translational motions from occurring across the joints. Locking is confirmed by the observed deformations of the structure in the fundamental mode. Fundamental vertical frequencies of the individual spans, predicted by the finite element model, are in very good agreement with ambient vibration test data. Results of the strong-motion data analysis and the finite element modeling are used to recommend a plan for expansion of the strong-motion instrumentation array on the bridge.

TABLE OF CONTENTS

TABLE OF CONTENTS (CONTINUED)

TABLE OF CONTENTS (CONTINUED)

CHAPTER I

INTRODUCTION

1.1 GENERAL INTRODUCTION AND OVERVIEW

Bridges are an essential and integral part of local and national highway systems. Throughout the world, many thousands of highway bridges are located in areas of moderate to high seismicity. The safety of these bridges, and the functional capability of the associated transportation routes in the aftermath of a major earthquake, are highly dependent upon the seismic resistance of the bridge structures.

In the United States, the seismic vulnerability of highway bridges was made dramatically evident by the failure of many of these structures during the 1971 San Fernando earthquake. This earthquake provided a stimulus to investigate the seismic response of highway bridges, in much the same way as the 1933 Long Beach earthquake stimulated research on the earthquake response of buildings.

The purpose of the research described in this dissertation is to investigate the earthquake response of a multiple-span bridge, typical of many highway bridge structures in North America. The bridge studied is the San Juan Bautista 156/101 Separation Bridge in California. The study is based heavily upon a set of multiple-channel recordings of the strong-motion response of the bridge during the 1979 Coyote Lake earthquake.

The remainder of this first chapter is devoted to a discussion of the damage sustained by bridge structures in past earthquakes, to previous research on bridge earthquake engineering, and to a brief outline of the main contents of this dissertation.

1.2 DAMAGE TO HIGHWAY BRIDGES IN PAST EARTHQUAKES

A study of the damage sustained by engineering structures in past earthquakes provides one of the best means of evaluating the seismic resistance of various types of structures, and serves as the ultimate test for assessing the adequacy of seismic design procedures.

The greatest number of bridges damaged by past earthquakes has been in Japan. The 1923 Kanto earthquake (local magnitude, $M_L \simeq 7.9$) was the first earthquake to cause large scale damage and destruction to modern facilities in Japan. Prior to the Kanto earthquake, Japan did not have regulations which required the consideration of seismic forces in the design of structures. After the earthquake, however, seismic design regulations were quickly imposed for future construction.

The Kanto earthquake damaged more than two thousand bridges, although for some the damage from subsequent fires was more severe than the direct effects of the earthquake. Since 1923, numerous other earthquakes have also inflicted considerable damage to highway bridges in Japan. Iwasaki, et al., (1972)* provide a detailed discussion of damage sustained by many different types of bridges during nine major Japanese earthquakes from 1923 to 1968. For the most part, seismic damage was a

* References appear at the end of each chapter.

result of failures of either bridge substructures or the surrounding soils. In very few instances did vibrational effects of the bridge account for appreciable levels of damage. When superstructure damage was found to occur, it was generally possible to trace the cause of the damage back to a failure of the substructure or soil.

Japanese experience indicates that most damage has occurred to abutments, piers, bridge girders and supports. In many instances, large differential movement between the superstructure and substructure has been ascribed as the cause of collapse of single-span bridges; in essence, girders were displaced from their supports. Loss of foundation support in the form of bearing failures (including liquefaction), soil settlements, or excessive horizontal movements of the soil were often found to be significant contributors to the failure of abutments and piers.

In addition to those Japanese bridges which sustained overall failure, many others have been observed which showed signs of distress or complete failure of individual structural components. These include: (1) excessive displacement of the end supports of girders, (2) displacement and/or failure of bearings, (3) anchor bolt damage, (4) settlement of approach fills at the abutments, rendering the bridge inaccessible, and (5) damage to abutments and wingwalls by excessive cracking and crushing of concrete.

In the United States, numerous highway bridges were damaged during the 1964 Alaska earthquake (Sturman, 1973). The causes and types of damage to most Alaskan bridges were generally similar to the

observations from the Japanese earthquakes, namely failure of soils or substructures; little damage was associated with vibrational effects on the bridge structures themselves.

The perception of the way in which highway bridges respond to earthquake shaking was dramatically changed by the 1971 San Fernando earthquake. For the first time, vibrational effects on the structures were seen to be a principal cause of the failure of bridges. Although failure and heavy damage to freeway structures was confined to the epicentral region, the total collapse of five high overcrossing structures at three major freeway interchanges clearly indicated that the dynamic behavior of such structures must be considered in the seismic design process.

Some of the major deficiencies which led to collapse of the high overcrossing structures in the San Fernando earthquake were: (1) inadequate width of seats at expansion joints, (2) adjacent spans not tied together to prevent excessive relative movement across the joints, (3) inadequate column reinforcing, and (4) unstable configuration of spans in which only one column was placed between expansion joints.

Damage to many of the shorter span, lower height bridges was observed to occur in a similar but less spectacular fashion, but the effects of vibration were still evident in many of the damaged structures. Shear failure of short columns, rotation of skewed superstructures, evidence of longitudinal and lateral movements, and signs of soil-bridge interaction, especially at abutment failures, were

noticeable in many bridges. Jennings and Wood (1971) provide a discussion of the damage to several freeway structures during the San Fernando earthquake. A comprehensive investigation of damage to freeway bridges was conducted for the California Department of Transportation by Elliott and Nagai (1973). Their report documents the most extensively damaged bridges, and also those which had a unique mode of failure. Included in their study is a summary of every bridge (66 in total) that was damaged during the San Fernando event. The one pertinent generalization drawn from their study was that it was the structural details which failed, precipitating most of the severe damage.

1.3 RESEARCH ON THE EARTHQUAKE RESPONSE OF HIGHWAY BRIDGES

1.3.1 Previous Analytical and Experimental Work

Immediately after the 1971 San Fernando earthquake, a comprehensive research program to study the seismic resistance of highway bridges was undertaken by the University of California, Berkeley. This program included both analytical and laboratory investigations on the seismic response of specific types of highway bridge structures. In the analytic phases, long-span, high, curved overcrossings as well as short, single-span bridges were investigated. In the laboratory phase, a scale model of a long-span overcrossing structure was subjected to simulated seismic excitations on a shaking table, and correlations between model and analytic results were made.

The conclusions and recommendations of the above program have been reported and no attempt will be made to discuss them here, other than to mention that current seismic design criteria for bridges reflect many of the recommendations of the research program (Gates, 1976; Mayes and Sharpe, 1981; AASHTO, 1977; Applied Technology Council, 1983). Complete discussions and bibliographies may be found in Iwasaki et al., (1972), Tseng and Penzien (1973), Chen and Penzien (1975), Kawashima and Penzien (1976), Williams and Godden (1976).

Other analytical research projects on bridges have been conducted as well. For example, Ghobarah and Tso (1974) analyzed the seismic response of a two-span skew highway bridge to the San Fernando earthquake, and Lisiecki (1982) has examined the response of the Meloland Overcrossing to the 1979 Imperial Valley earthquake. Gillies and Shepherd (1981) present an analysis technique for determining the response time-history of a bridge structure with allowance for inelastic member behavior.

Most early research on the response of bridges to earthquake motion has assumed uniform base excitation of the structure. Spatial variations in the seismic motions at a site may, however, cause the bridge foundations to be subjected to different amplitudes and phasing of excitation. For very short-span bridges and long seismic wavelengths these variations are expected to be negligible, but for long-span bridges the variations may be of appreciable magnitude.

One of the earliest studies of the effects of travelling seismic waves on bridge stuctures was conducted by Bogdanoff, et al., (1965) who examined the case of a seismic motion propagating along the length of a bridge foundation. The bridge responses were found to be noticeably different from those due to a uniform, rigid base excitation. Werner, et al., (1977) and Werner and Lee (1980), investigating the effects of travelling seismic waves on the response of a single-span bridge, report that both the type of seismic wave as well as the angle of approach may substantially influence a bridge's dynamic response. Abdel-Ghaffar (1977) has also studied the problem and reports similar results. For bridge structures more complex than a single span, differential support excitation significantly complicates the problem of dynamic response analysis.

To augment analytical and laboratory work in earthquake engineering, researchers have also performed tests on full-scale bridge structures. These experiments usually involve measurement of the dynamic response to ambient levels of excitation (e.g., wind or traffic), to controlled sinusoidal excitation, or to pull-back testing. In New Zealand, a series of sinusoidal excitation tests were conducted by Shepherd and Charleson (1971) at various stages of construction of a six-span bridge, and estimates were made of natural frequencies and damping values. Gates and Smith (1982) have published results of an ambient vibration survey on fifty-seven highway bridges in California and Nevada. Douglas and Reid (1982), and Douglas and Norris (1983) have analyzed vibration response data from pull-back tests on a Nevada

highway bridge where testing loads ranged from ambient forces to lateral loads 1.5 times the design loads.

While the observations of Douglas, et al., cover a number of points, the overall indication from their studies is that linear structural models with simple linear soil-structure interaction springs were found to work acceptably well for predicting seismic responses. At the Nevada test bridge, the overall rotation of pile foundations was found to be the major contributor to soil-structure interaction during large amplitude tests, rather than lateral pile stiffness (Douglas and Richardson, 1984).

A compilation of research and review papers, published by the Applied Technology Council (1979), covers many additional aspects of both analytical and experimental research on the earthquake response of highway bridges.

1.3.2 Strong-Motion Instrumentation of Bridges

For engineering purposes, the basic source of data on the earthquake response of structures is strong-motion accelerograms. Although many buildings are instrumented with strong-motion accelerographs, and many excellent records have been obtained from these installations, it was not until the mid-1970's that a program of strong-motion instrumentation of bridges and other transportation structures was initiated in California. The first sets of records were obtained in 1979 when two instrumented bridges in California were shaken by different earthquakes.

Currently, there are more than 567,000 highway bridges in the United States; approximately 23,150 of these being in the State of California. At present, only five California bridges are instrumented to record earthquake shaking. It is fortuitous that, since the beginning of the strong-motion instrumentation program for bridges, three of these five have yielded significant data, so that now there exists a limited supply of the accelerograms needed to examine the actual seismic response of highway bridges. A summary of the bridges which have been instrumented and the records obtained to date (May 1984) is given in Table 1.1.

In connection with the California Strong-Motion Instrumentation Program, Raggett and Rojahn (1978) have described some standard, general methods to aid in the interpretation of strong-motion records from highway bridges. Also, Rojahn and Raggett (1981) suggest guidelines for the strong-motion instrumentation of such bridges.

The work to be described in this thesis is the first investigation of the strong-motion records from the San Juan Bautista 156/101 Separation bridge. The overall objective in this study is to understand the seismic response of the bridge using the strong-motion data recorded during the 1979 Coyote Lake earthquake. It is desirable to extract from this data set as much information as possible, because of the limited data available from such structures.

TABLE 1.1

California Bridges with
Strong-Motion Instrumentation

Bridge Name and Location	Number of Transducers	Recorded Events
10-15E Interchange (San Bernardino)	1	None to date
San Juan Bautista 156/101 Separation (San Benito Co.)	12	8/6/79-Coyote Lake
Meloland Overcrossing (El Centro)	26	10/15/79-Imperial Valley 1980-81-several small events
101/Painter St. Overcrossing (Rio Dell; Humboldt Co.)	20	11/8/80-Trinidad Offshore 12/16/82-Rio Dell 8/24/83-Cape Mendocino Offshore
Vincent Thomas Suspension Bridge (Los Angeles)	26	None to date

1.4 OUTLINE OF PRESENT WORK

The research is presented in three chapters. Each chapter is more-or-less self-contained in a topical sense, but the results of each preceding chapter are used as a starting point for the analysis of the subsequent chapter. Relevant works of reference are listed at the end of each chapter.

In Chapter II, a detailed study is made of the earthquake ground motions recorded at two separate stations at the site of the San Juan Bautista bridge. The main objective in this chapter is to examine the

spatial variations in the ground motions occurring along the alignment of the bridge. The possibility of differential support motion induced by travelling body waves and surface waves is also investigated.

The third chapter contains an adaptation of an output-error method of system identification developed by Beck (1978), to the structural response records of the San Juan Bautista bridge. Estimates of modal frequencies and damping values are obtained for the dominant modes of bridge response, assuming time-invariant linear response. In addition, time variations in modal frequencies and damping values during the earthquake are investigated using a moving-window analysis.

Chapter IV is concerned with structural modeling of the bridge and the comparison of the computed dynamic characteristics of the structure with those observed during the earthquake. A linear finite element model, including linear soil springs at the foundations, is used to predict natural frequencies and mode shapes of the bridge. Common modeling assumptions for the dynamic behavior of the expansion joints are assessed in light of the measured responses during the earthquake.

Chapter V, the final chapter, summarizes the major findings of this study and presents conclusions on the seismic response of the San Juan Bautista bridge, as well as more general conclusions.

At this point the dimensional units employed in this dissertation should be mentioned. In keeping with common practice in that field, all dimensions in the seismological sections of this thesis are reported in metric units. This mainly involves Chapter II. In Chapter IV, which is mainly a structural engineering chapter, dimensions are presented in

feet and inches. These are the units in which the bridge was designed, and are the units of current engineering practice in the United States.

CHAPTER REFERENCES

Abdel-Ghaffar, A.M. (1977). "Studies on the Effect of Differential Motions of Two Foundations Upon the Response of the Superstructure of a Bridge," Earthquake Engineering Research Laboratory, EERL 77-02, California Institute of Technology, Pasadena, California.

American Association of State Highway and Transportation Officials (1977). "Standard Specifications for Highway Bridges," 12th edition (with revisions by Caltrans, Jan. 1983), Washington, D.C.

Applied Technology Council (1979). "Proceedings of a Workshop on Earthquake Resistance of Highway Bridges," Palo Alto, California.

Applied Technology Council (1983). "ATC-6-2 Seismic Retrofitting Guidelines for Highway Bridges," Palo Alto, California.

Bogdanoff, J.L., Goldberg, J.E. and Schiff, A.J. (1965). "The Effect of Ground Transmission Time on the Response of Long Structures," Bull. Seism. Soc. Am., Vol. 55, No. 3, June, pp. 627-640.

Beck, J.L. (1978). "Determining Models of Structures from Earthquake Records," Earthquake Engineering Research Laboratory, EERL 78-01, California Institute of Technology, Pasadena, California.

Chen, M-C. and Penzien, J. (1975). "Analytical Investigation of the Seismic Response of Short, Simple or Multiple-Span Highway Bridges," Earthquake Engineering Research Center, Report No. EERC 75-4, University of California, Berkeley, California.

Douglas, B.M. and Reid, W.H. (1982). "Dynamic Tests and System Identification of Bridges," Journal of the Structural Division, ASCE, Vol. 108, No. ST10, October, pp. 2295-2312.

Douglas, B.M. and Norris, G.M. (1983). "Bridge Dynamic Tests: Implications for Seismic Design," Journal of Technical Topics in Civil Engineering, ASCE, Vol. 109, No. 1, April, pp. 1-22.

Elliott, A.L. and Nagai, I. (1973). "Earthquake Damage to Freeway Bridges," in San Fernando, California, Earthquake of February 9, 1971, Vol. II, U.S. Dept. of Commerce, National Oceanic and Atmospheric Administration, Washington, D.C., pp. 201-233.

Douglas, B.M. and Richardson, J.A. (1984). "Maximum Amplitude Dynamic Tests of a Highway Bridge," to appear in Proceedings of the Eighth World Conference on Earthquake Engineering, San Francisco, California.

Gates, J.H. (1976). "California's Seismic Design Criteria for Bridges," Journal of the Structural Division, ASCE, Vol. 102, No. ST12, December, pp. 2301-2313.

Gates, J.H. and Smith, M.J. (1982). "Verification of Dynamic Modeling Methods by Prototype Excitation," California Dept. of Transportation, Report No. FHWA/CA/ST-82/07, Sacramento, California.

Ghobarah, A.A. and Tso, W.K. (1974). "Seismic Analysis of Skewed Highway Bridges with Intermediate Supports," International Journal of Earthquake Engineering and Structural Dynamics, Vol. 2, pp. 235-248.

Gillies, A.G. and Shepherd, R. (1981). "Dynamic Inelastic Analyses of a Bridge Structure," Bull. Seism. Soc. Am., Vol. 71, No. 2, April, pp. 517-530.

Iwasaki, T., Penzien, J. and Clough, R. (1972). "Literature Survey - Seismic Effect on Highway Bridges," Earthquake Engineering Research Center, Report No. EERC 72-11, University of California, Berkeley, California.

Jennings, P.C. and Wood, J.H. (1971). "Earthquake Damage to Freeway Structures," in Engineering Features of the San Fernando Earthquake, (P.C. Jennings, ed.), Earthquake Engineering Research Laboratory, EERL 71-02, California Institute of Technology, Pasadena, California.

Kawashima, K. and Penzien, J. (1976). "Correlative Investigations on Theoretical and Experimental Dynamic Behavior of a Model Bridge Structure," Earthquake Engineering Research Center Report No. EERC 76-26, University of California, Berkeley, California.

Lisiecki, L.C. (1982). "Analysis of the Meloland Overcrossing Response to the October 15, 1979 Imperial Valley Earthquake," M.S. Thesis, University of California, Irvine, California.

Mayes, R.L. and Sharpe, R.L. (1981). "Seismic Design Guidelines for Highway Bridges," U.S. Dept. of Transportation, Federal Highway Report FHWA/RD-81/081, Washington, D.C.

Raggett, J.D. and Rojahn, C. (1978). "Use and Interpretation of Strong-Motion Records from Highway Bridges," U.S. Dept. of Transportation, Federal Highway Report FHWA-RD-78-158, Washington, D.C.

Ragsdale, J. and Shakal, A. (1984). California Dept. of Transportation, Sacramento, California, personal communication.

Rojahn, C. and Raggett, J.D. (1981). "Guidelines for Strong-Motion Instrumentation of Highway Bridges," U.S. Dept. of Transportation, Federal Highway Report, FHWA/RD-82/016, Washington, D.C.

Shepherd, R. and Charleson, A.W. (1971). "Experimental Determination of the Dynamic Properties of a Bridge Substructure," Bull. Seism. Soc. Am., Vol. 61, No. 6, December, pp. 1529-1548.

Sturman, G.C. (1973). "The Alaska Highway System," in The Great Alaska Earthquake of 1964 - Engineering, National Academy of Sciences, Washington, D.C., pp. 987-1009.

Tseng, W-C. and Penzien, J. (1973). "Analytical Investigations of the Seismic Response of Long, Multiple-Span Highway Bridges," Earthquake Engineering Research Center, Report No. EERC 73-12, University of California, Berkeley, California.

Werner, S.D., Lee, L.C., Wong, H.L. and Trifunac, M.D. (1977). "An Evaluation of the Effects of Traveling Seismic Waves on the Three-Dimensional Response of Structures," Agbabian Associates, El Segundo, California.

Werner, S.D. and Lee, L.C. (1980). "The Three-Dimensional Response of a Bridge Structure Subjected to Traveling Rayleigh Waves, SV-Waves and P-Waves," Agbabian Associates, El Segundo, California.

Williams, D. and Godden, W.G. (1976). "Experimental Model Studies on the Seismic Response of High Curved Overcrossings," Earthquake Engineering Research Center, Report No. EERC 76-18, University of California, Berkeley, California.

CHAPTER II

ANALYSIS OF GROUND MOTION RECORDS

In this chapter, records of the ground motion for the San Juan Bautista bridge site are used to examine the nature of the seismic excitation to which the bridge was subjected during the 1979 Coyote Lake earthquake. By seismological and geophysical investigations of the strong-motion records, evidence is accumulated to show that surface wave effects are believed responsible for the presence of long-period components of ground motion observed at the site. There are indications that travelling wave effects may be responsible for a small amount of differential support motion along the 326-foot length of the bridge.

2.1 SEISMOLOGICAL CONSIDERATIONS

Seismic waves propagating in the earth can be conveniently classified into two major groups; body waves and surface waves, depending upon the type of path the waves take as they travel outwards from the source. The ground motion observed at a given site during an earthquake is normally a superposition of several types of body and surface waves, each of which has been influenced to some degree by factors such as geologic variations along the travel path, refraction and reflection at layer boundaries, dispersion, focussing, anelastic attenuation, and radiation patterns. The following paragraphs provide a highly condensed summary of some important aspects of seismic wave propagation in a homogeneous, elastic medium. The material is standard

in many texts on seismology (Richter, 1958) and mechanics (Fung, 1965). Some additional seismological aspects are also introduced in later sections of this chapter, where appropriate.

Body waves are represented by two main types of waves, depending upon the orientation of the particle motion with respect to the direction of wave propagation. Dilatational waves, or P waves (P for primary), with particle motions parallel to the direction of propagation are the first to arrive at a site from the earthquake hypocenter, and often arrive at nearly vertical angles of incidence. Most strong-motion accelerographs are designed to be activated at a threshold acceleration of approximately 0.01g in the vertical direction, in order that the first arrivals of vertical P waves will trigger the system. In a homogeneous elastic body, the P wave velocity α is given by

$$\alpha = \sqrt{\frac{\lambda + 2\mu}{\rho}} \tag{2.1}$$

where $\lambda = 2\mu\nu/(1-2\nu)$ is Lame's constant (ν = Poisson's ratio), μ is the shear modulus and ρ is the density. For many seismological applications ν may be taken as $\frac{1}{4}$, hence $\lambda = \mu$ and

$$\alpha = \sqrt{\frac{3\mu}{\rho}} \tag{2.2}$$

Shear waves, or S waves (S for secondary) normally arrive a few seconds to many seconds after the first P arrival, depending on the distance to the source and the wave speeds. The particle motion of an S wave is on a plane perpendicular to the direction of propagation (a shearing action in the medium) and the velocity of propagation is given

by

$$\beta = \sqrt{\frac{\mu}{\rho}} \tag{2.3}$$

For geophysical applications $\alpha = \sqrt{3}\,\beta$ is often a suitable approximation. When the particle motion is oriented parallel to a material boundary (say the surface), the motion is termed SH, and when it is on the plane perpendicular to the boundary the waves are called SV.

In an elastic medium bounded by a plane surface, an SV wave incident at the surface will cause both P and SV waves to be reflected back into the medium when the SV angle of incidence i, measured with respect to the vertical, is less than the critical angle $i_c = \sin^{-1}(\beta/\alpha)$. When $i > i_c$, however, no P wave will be reflected and part of the incident wave energy will be trapped along the surface. The result is a coupling of P waves and SV waves at the surface which produces a Rayleigh surface wave. It can be shown (Fung, 1965) that when $\nu = 1/4$ the propagation velocity c_R, of a Rayleigh wave in a homogeneous elastic medium is

$$c_R = 0.92\beta \tag{2.4}$$

The particle motion at the surface for a Rayleigh wave is retrograde elliptical in the plane of propagation. In a heterogeneous medium (e.g., the earth) the wave propagation is dispersive since c_R is a function of the wavelength, with larger values of c_R being associated with the longer wavelengths.

With a seismological understanding of the ways in which various types of seismic waves combine to create the total earthquake ground motion, and with the increase in information on the spatial variability of ground motion as a result of deployment of closely-spaced arrays of accelerographs, it becomes increasingly significant that this information be used in a productive way. One such application is in earthquake engineering studies of structures which may be particularly influenced by spatial variations in ground motions and travelling wave effects. The remainder of this chapter is devoted to such a study for the ground motions recorded at the San Juan Bautista Separation Bridge during the 1979 Coyote Lake earthquake.

2.2 THE SAN JUAN BAUTISTA 156/101 SEPARATION BRIDGE

The purpose of this section is to provide a general description of the San Juan Bautista 156/101 Separation Bridge and a discussion of the strong motion instrumentation system deployed on the bridge. The availability of strong ground motion records at two separate stations at the bridge site provides the basis for subsequent analyses in this chapter.

2.2.1 Description of the Bridge

The San Juan Bautista 156/101 Separation Bridge is located approximately 3.2 kilometers (2 miles) north-west of the town of San Juan Bautista in San Benito County, California (see Fig. 2.1). This two-lane bridge, constructed in 1959 and owned by the California

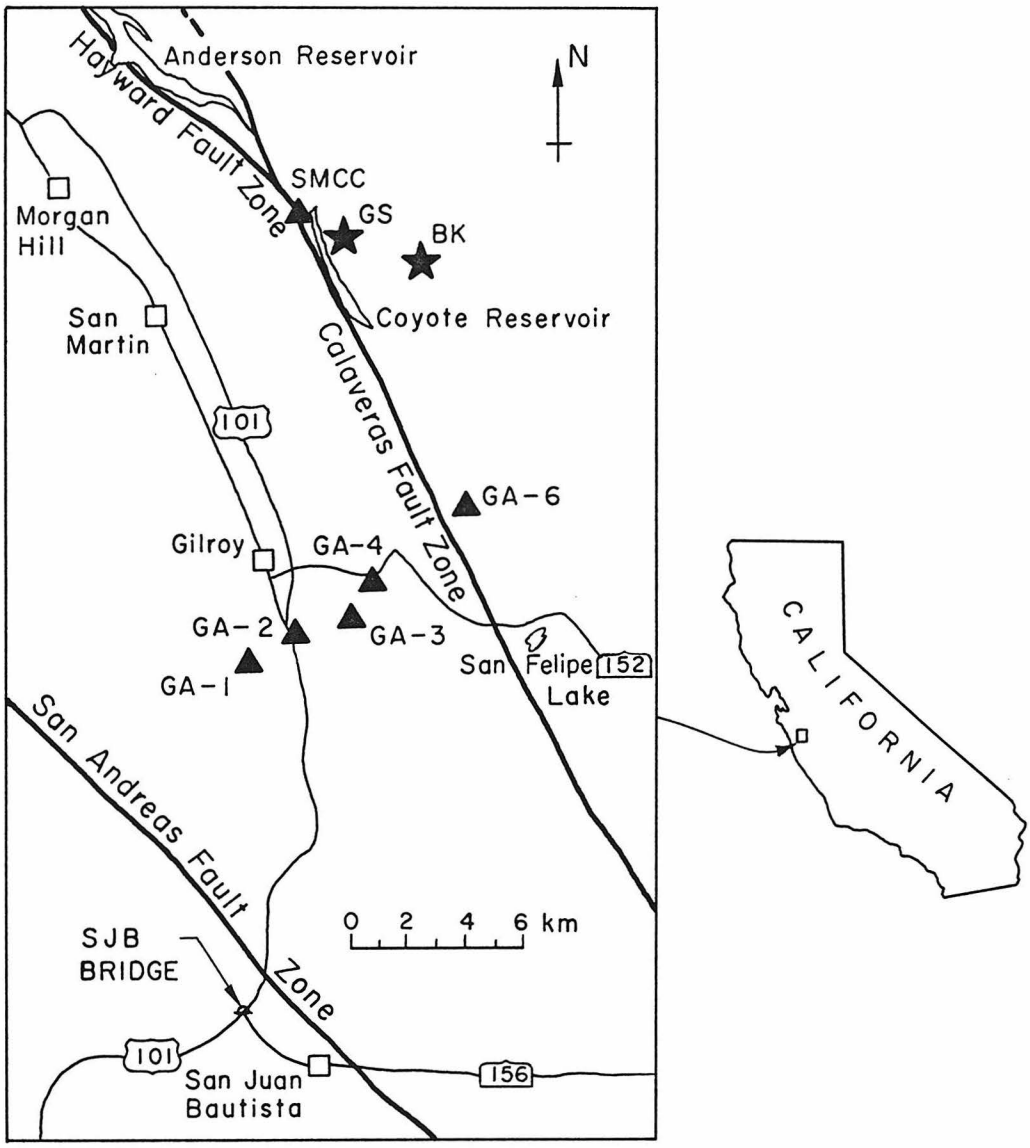

Figure 2.1 Location of the San Juan Bautista Separation Bridge and Epicenter of the 1979 Coyote Lake Earthquake (after Liu and Helmberger, 1983)

Department of Transportation (Caltrans), carries a moderate amount of automobile and truck traffic on California State Highway 156 over U.S. Highway 101, and is typical of the late 1950's - early 1960's style of highway bridge design in the United States. Only a minimal amount of seismic resistance was designed into bridge structures in the late 1950's, and for practical purposes, all loadings arose from service conditions.

The San Juan Bautista bridge consists of six simple spans of steel girders composite with a reinforced concrete deck. Between each span is a small gap (1 inch), filled with an expansion joint material, to allow for thermal expansion and contraction of the road deck. The spans are simply-supported on two-column, reinforced concrete bents with a fixed bearing at one end of each span (the left-hand end of each span in Fig. 2.2) and an expansion bearing at the other end. The design and orientation of the bearings is such as to allow for longitudinal movement (in a direction parallel to the centerline of the roadway) across the expansion bearings. Detailed views of the bridge are shown in Figs. 2.2 and 2.3; these include some of the major overall dimensions. Cross-sectional dimensions of deck members are the same throughout the 326-foot length of the bridge, with the exception of a slight change in section size of the steel girders on the two longest spans. A detailed summary of the material and geometric properties is given in section 4.1.1 of this dissertation.

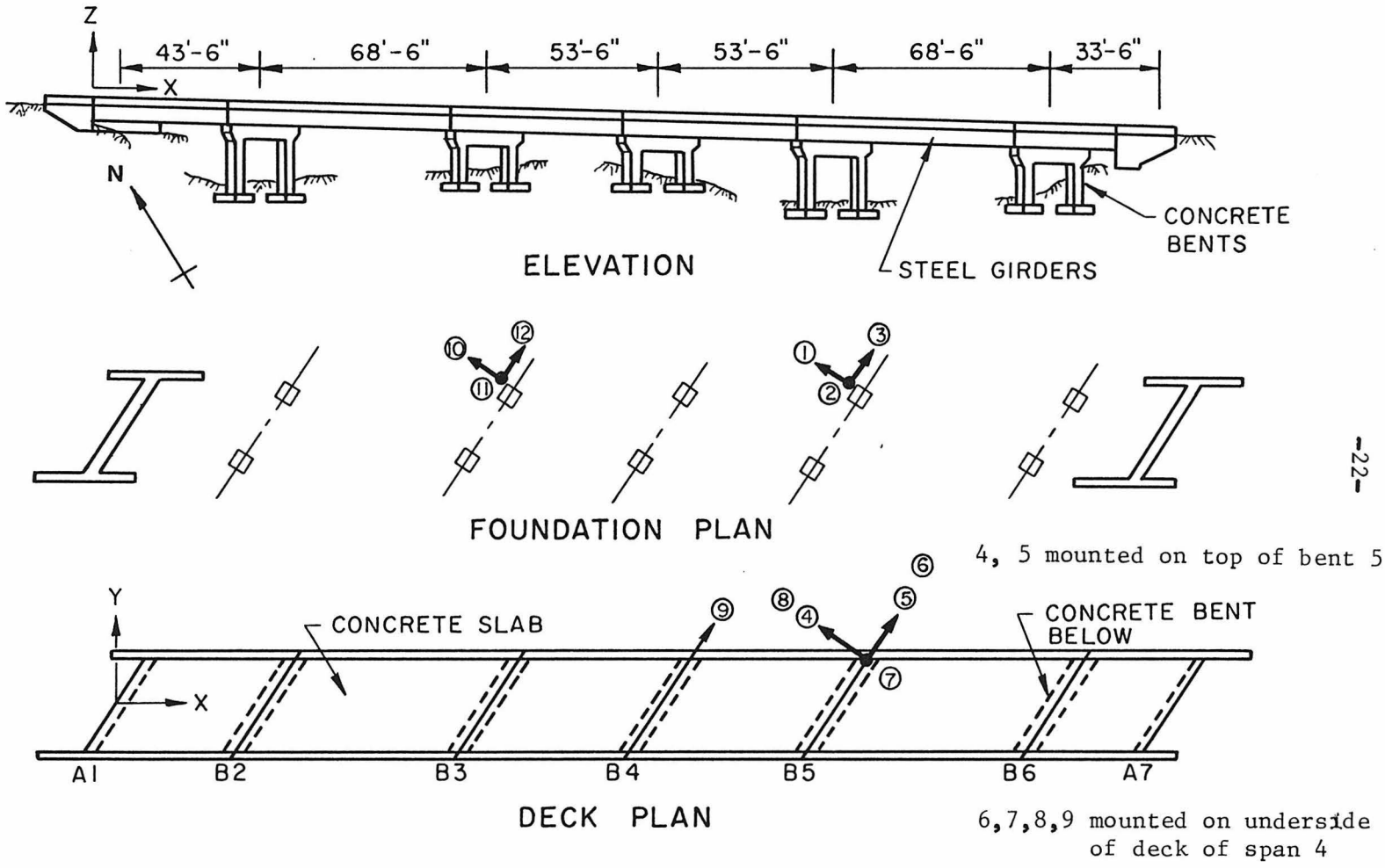

Figure 2.2 The San Juan Bautista 156/101 Separation Bridge and Strong-Motion Instrumentation

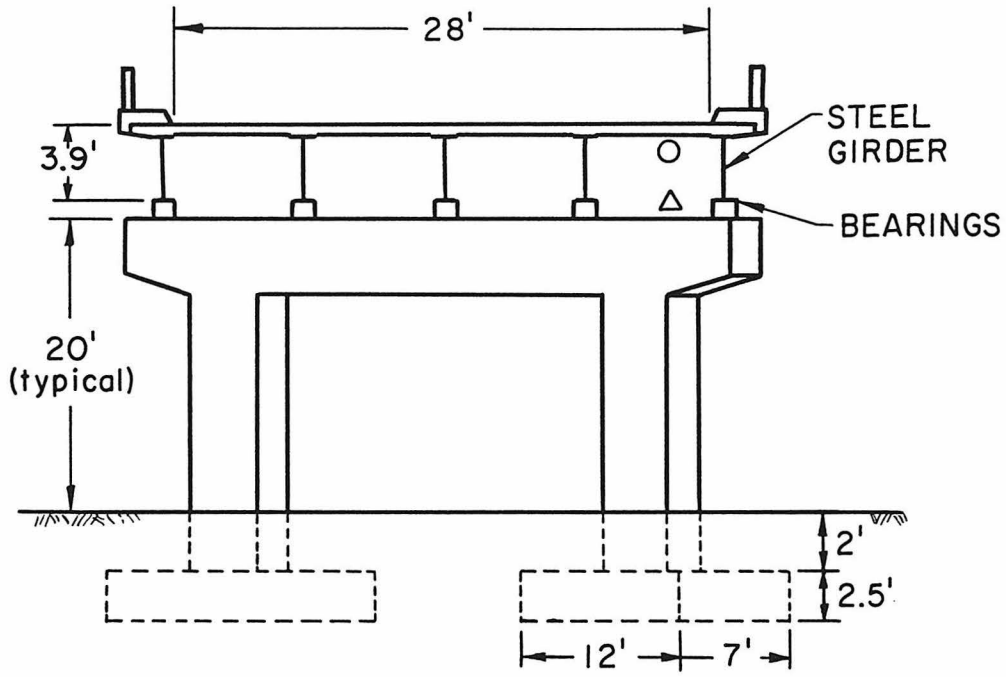

Figure 2.3 The San Juan Bautista 156/101 Separation Bridge

Foundation support for the bridge consists of a 7 × 12 × 2.5-foot spread footing at the base of each column (2 per bent). These footings bear directly on horizontal beds of Pliocene alluvial deposits estimated to be approximately fifty feet in thickness, which in turn overlie granitic basement rock (Porter, et al., 1983). Soil tests at the bridge site prior to construction gave Standard Penetration Test (SPT) values of N of approximately 50. Values of N this high indicate a very dense soil (Scott, 1981).

The left abutment, denoted as A1 on Fig. 2.2, was constructed on a naturally occurring rise of the ground surface while the right abutment (A7 on Fig. 2.2) was constructed on fill material. The deck-to-abutment connections also include an allowance for expansion. The abutments and bents are skewed at 34.8° with respect to the bridge deck. For later discussions, a global X-Y-Z coordinate system is defined such that the X axis points in the longitudinal direction (parallel to the centerline of the road), the Y axis points in a transverse direction, and the Z axis is vertical. These coordinate directions are shown on Fig. 2.2.

2.2.2 Strong-Motion Instrumentation of the Bridge

In May 1977 the San Juan Bautista bridge was instrumented by the Office of Strong Motion Studies of the California Division of Mines and Geology with twelve channels of strong-motion instrumentation, all linked to a central recording system having a common trigger and time signal. The strong-motion transducers were force balance accelerometers (Kinemetrics FBA-1 and FBA-3 models) which were connected to a CRA-1

central recording system. Some relevant specifications of the accelerometers and recording system, all of which were supplied by Kinemetrics Incorporated, are given in Appendix 2A at the end of this chapter. Six transducers were placed at ground level to measure the input motions to the structure, three at bent 3 (B3) and three at bent 5 (B5). The remaining six transducers were placed at various locations on the superstructure as shown in the instrumentation plan in Fig. 2.2.

The main shock of the August 6, 1979 Coyote Lake earthquake (M_L = 5.9) triggered the system and resulted in the recording of approximately 27 seconds of acceleration on each of the twelve channels. The peak recorded ground acceleration (channel 1) was 0.12g and the peak recorded structural response (on channel 8) was 0.27g (corrected absolute values) with the duration of strong motion lasting about 10 seconds.

The instrumentation system was designed to measure the motion of a single bay and supporting bents. As a result, the lack of instruments at the abutments and at free-field locations was a limitation in determining the global response of the bridge-soil system. However, the deck level instruments provide an opportunity to study certain aspects of the superstructure response, and the two sets of triaxial instruments at the base of bents 3 and 5 allow base input motions to be studied. Plots of corrected absolute accelerations for each data channel are shown in Fig. 2.4. In some of the later analyses it will prove useful to rotate the horizontal components into the global X-Y coordinate directions of the bridge, as previously defined.

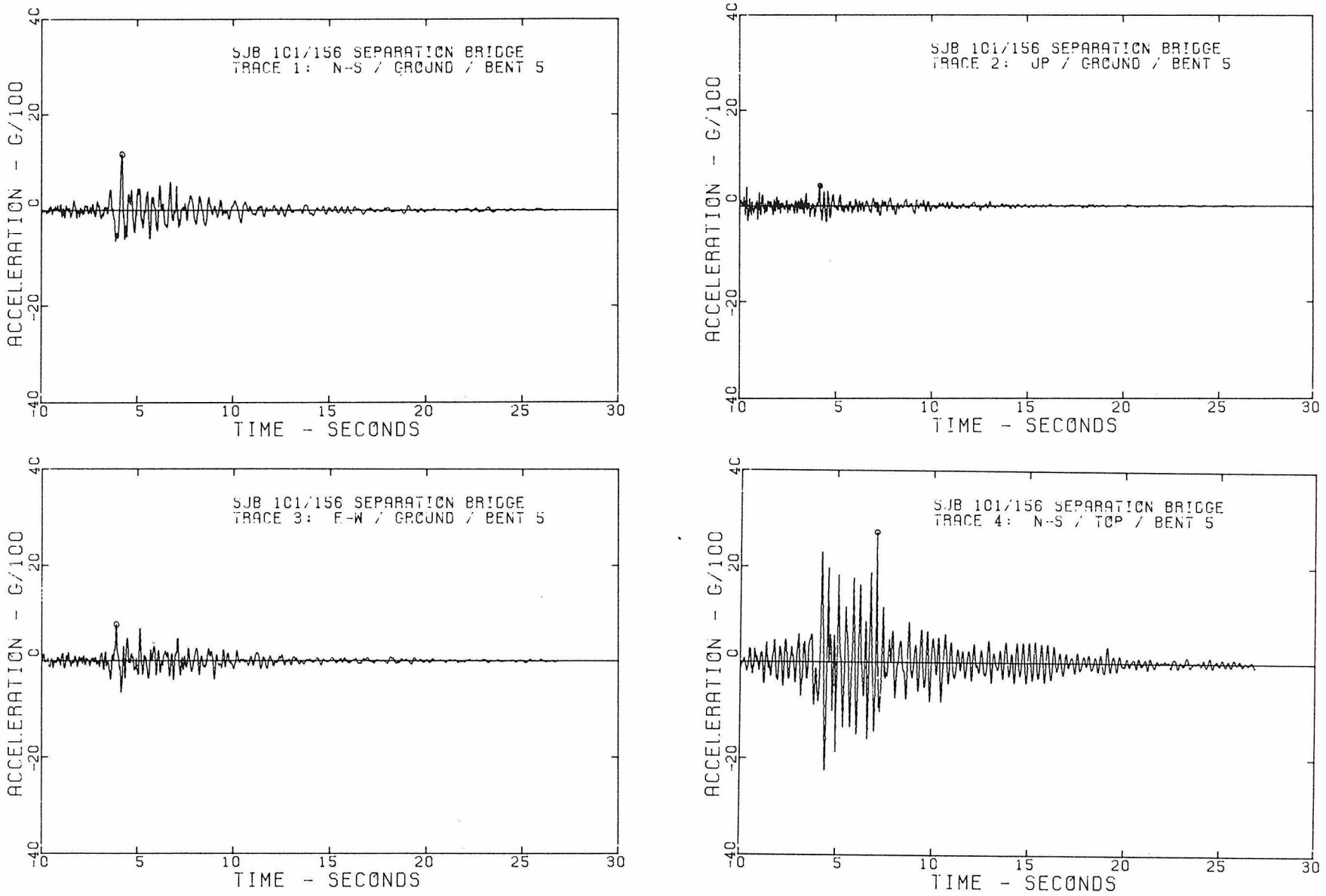

Figure 2.4 Accelerograms from the San Juan Bautista Bridge

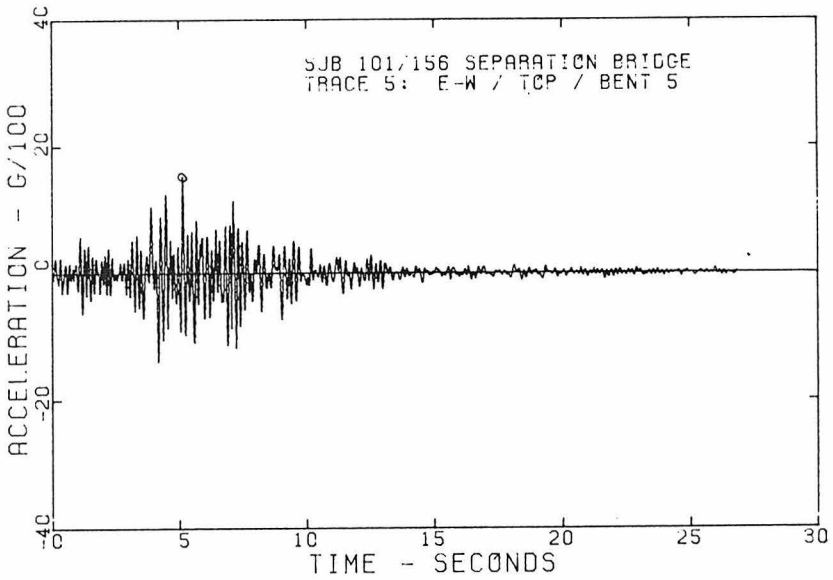

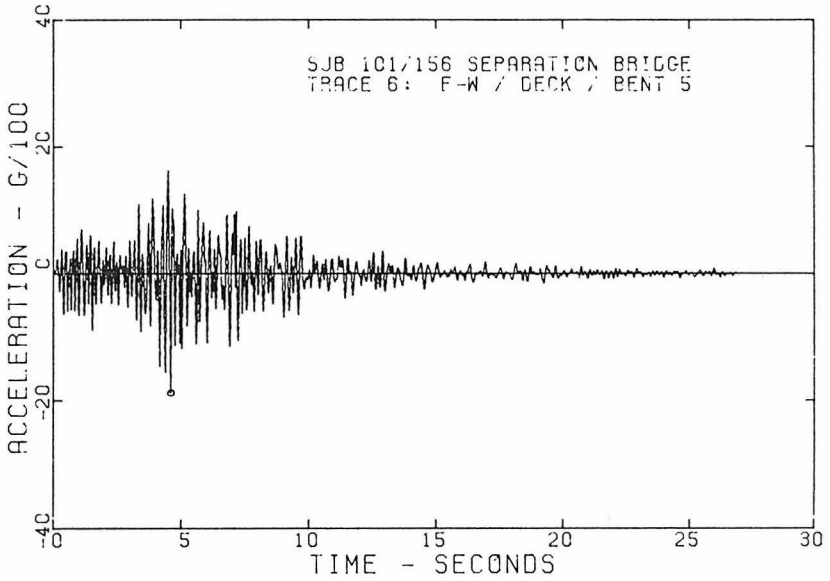

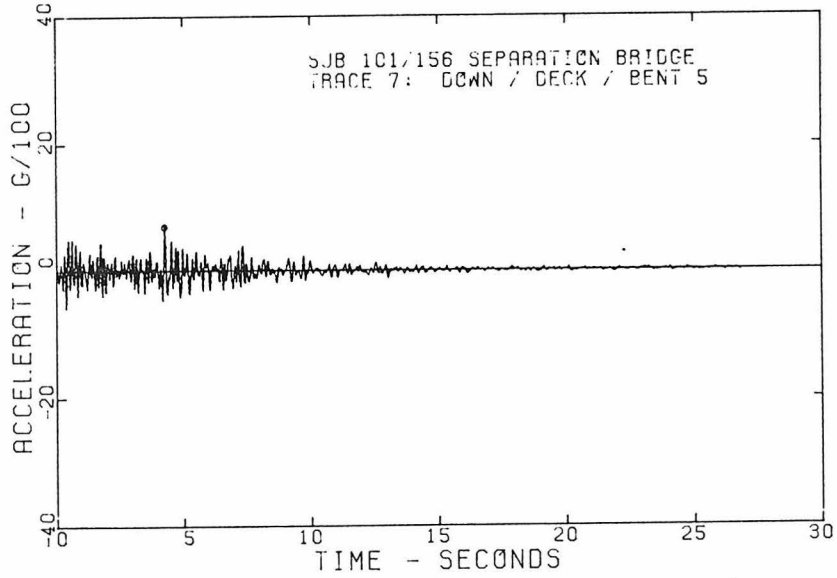

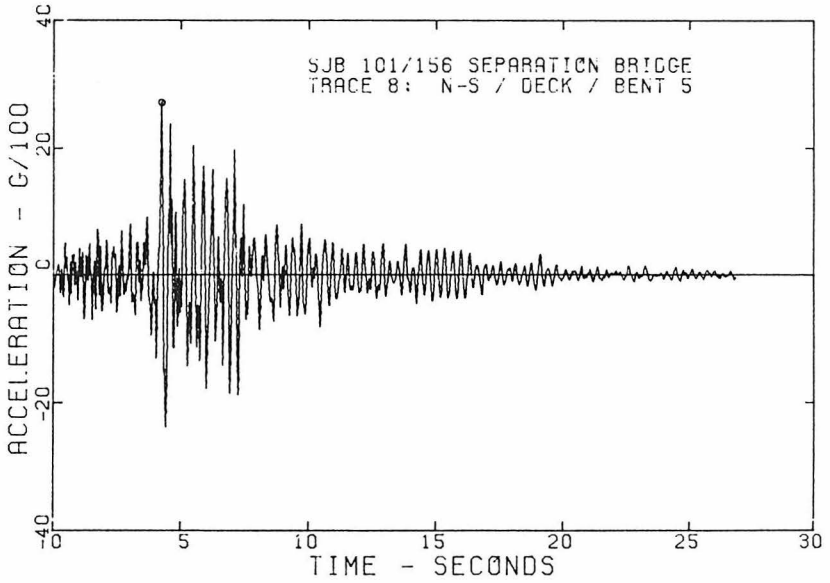

Figure 2.4 (cont'd)

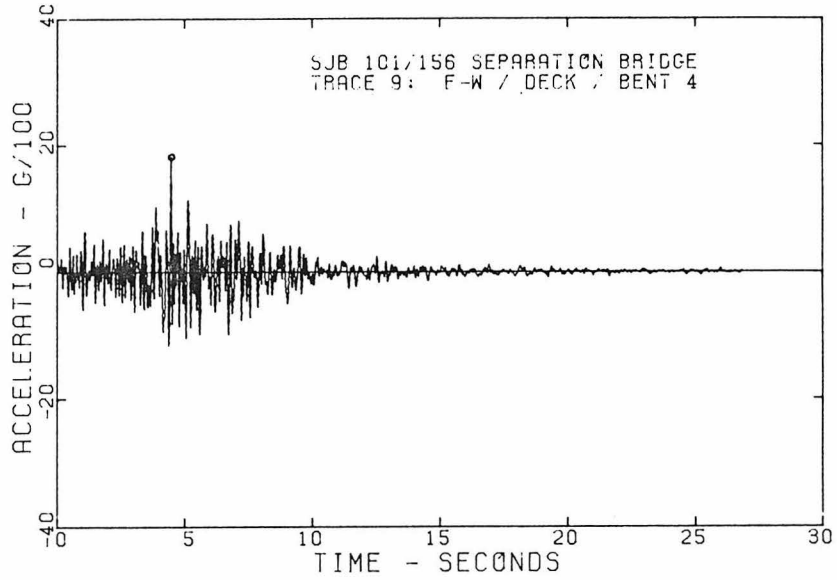

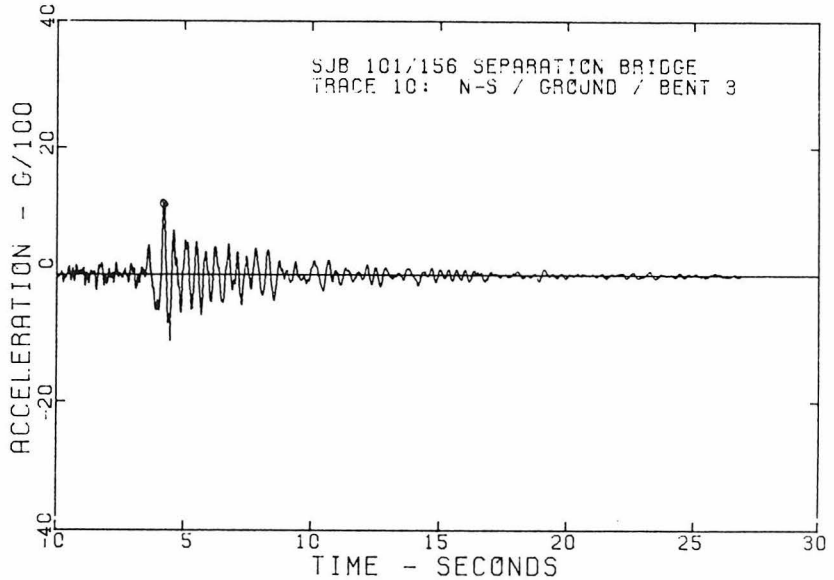

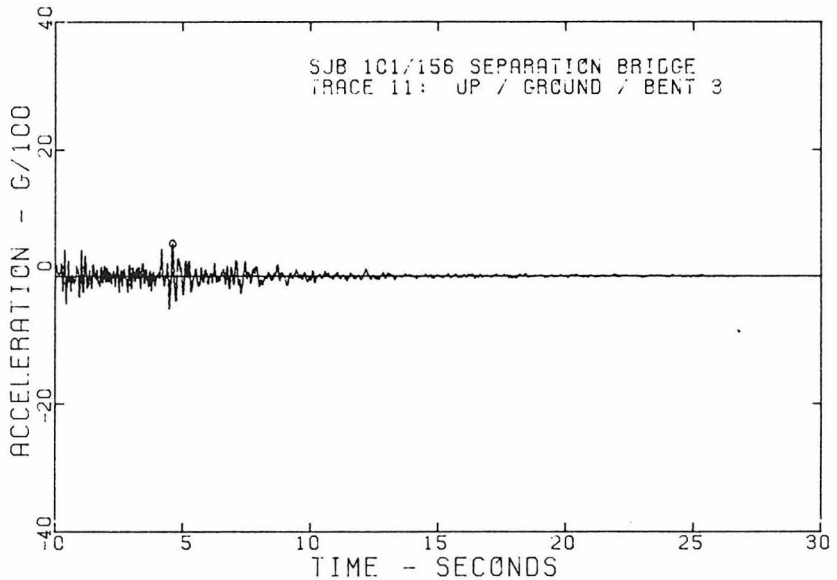

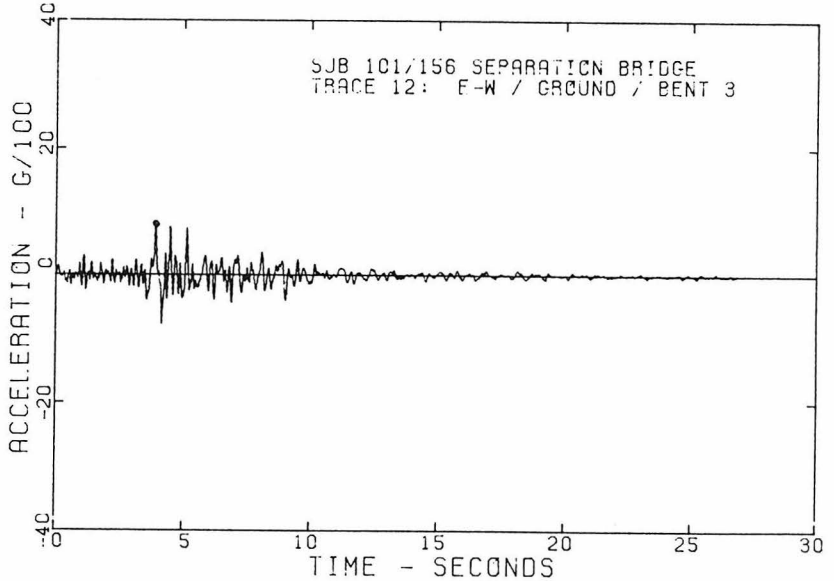

Figure 2.4 (cont'd)

In addition to the bridge site, several other strong motion accelerographs were deployed throughout the region. A linear array of five triaxial instruments spanned the Calaveras fault zone in the vicinity of Gilroy, about 20 km north of the bridge. Also, there was an instrument installed in the town of San Juan Bautista, about 3 km east of the bridge. The locations of these instruments are also indicated on the map in Fig. 2.1. With the availability of a significant number of near-source strong ground motion records and also world-wide teleseismic data, the Coyote Lake earthquake has been well researched (Joyner, et al., 1981; Liu and Helmberger, 1983; Uhrhammer, 1980). Compilations of strong-motion records recovered from the earthquake are given by Porcella, et al., (1979), and processed data from the San Juan Bautista bridge and the station in the town of San Juan Bautista are given by Porter, et al., (1983). Liu and Helmberger (1983) report that the earthquake was nearly a pure strike-slip mechanism with strike ($N24^{o}W$) parallel to the Calaveras fault. They indicate that faulting initiated at a depth of 8 km and ruptured towards the south-east. The epicenter of the earthquake located by the University of California, Berkeley (BK) and the location given by U.S. Geological Survey (GS) are also indicated on Fig. 2.1. They are about 3 km apart.

2.3 SPATIAL VARIATIONS IN GROUND MOTION

2.3.1 Introduction

Most commonly, the seismic response of a structure is calculated with the assumption that the base of the structure is excited everywhere by the same ground motion. That is, the amplitude and phase characteristics of the ground motion are identical at all points where the structure is attached to the ground. This assumes that the ground motion is a result of spatially uniform, vertically propagating shear waves (for horizontal excitation), or, that the wavelength of the ground motions are long with respect to the dimensions of the structure. For structures of large spatial extent, such as bridges, dams and pipelines, the variations in ground motion over the length of support of the structure may be great enough to make the assumption of uniform ground motion inappropriate. In this case, the different ground motions occurring at each support must be accounted for in what is often called the problem of "multiple-support excitation."

The formulation of the equations of motion for a lumped-mass multi-degree-of-freedom (MDOF) system subjected to multiple-support excitation is somewhat different than the formulation for a single input rigid base excitation. One approach is based on the concept that the total response of the structure can be found by superposition of the responses due to each independent support motion. This approach has been presented by Clough and Penzien (1975) and only a brief explanation is given here, mainly to introduce the terminology.

When a single support is subjected to a movement while all other supports are held fixed, the total structural displacement $\underline{y}^t$ may be expressed as the sum of a pseudostatic displacement $\underline{y}^s$ and a relative displacement $\underline{y}$

$$\underline{y}^t = \underline{y}^s + \underline{y} \tag{2.5}$$

The pseudostatic displacement is that which occurs when the individual support is displaced by an amount v_g with respect to the remaining fixed supports. The relative displacement $\underline{y}$ is the dynamic displacement of the structure induced by the motion of the one support, and is measured relative to the pseudostatic displacement position of the structure. The pseudostatic displacements can be expressed by an influence coefficient vector $\underline{r}$ such that

$$\underline{y}^s = \underline{r} v_g \tag{2.6}$$

where, once again, v_g is the displacement of one of the supports in a given coordinate direction while all other supports are held fixed. For a lumped-mass system then, the equation of motion when a single support is given a motion v_g and all other supports are held fixed is given by

$$[M]\ddot{\underline{y}} + [C]\dot{\underline{y}} + [K]\underline{y} = -[M]\underline{r}\,\ddot{v}_g \tag{2.7}$$

where [M],[C],[K] are the mass, damping and stiffness matrices, respectively. When $\underline{r} = \{1\}$, Eq. 2.7 becomes the well-known equation for the response of a MDOF system to a uni-directional rigid base excitation $\ddot{v}_g$. The complete response of the MDOF system to multiple-support

inputs is expressed by changing the $\underset{\sim}{r}$ vector to a matrix of pseudostatic influence coefficients [r], and the scalar $\ddot{v}_g$ to a vector of support motions $\ddot{\underset{\sim}{y}}_g$. Hence, the complete matrix formulation of the equations of motion becomes

$$[M]\ddot{\underset{\sim}{y}} + [C]\dot{\underset{\sim}{y}} + [K]\underset{\sim}{y} = -[M][r]\ddot{\underset{\sim}{y}}_g \tag{2.8}$$

It is clear from the above discussion that vector $\underset{\sim}{r}$ (or matrix [r]) will be unique for a given structure and must be evaluated prior to the dynamic analysis.

2.3.2 Analysis of Long-Period Errors in Strong-Motion Data

A large amount of the strong-motion accelerograph data currently available to researchers and engineers is a result of an extensive program of data processing initiated by the Earthquake Engineering Research Laboratory at the California Institute of Technology in the early 1970's. This program resulted in the issue of several volumes of uncorrected accelerograms as well as corrected acceleration, and integrated velocity and displacement curves (Hudson, et al., 1972). The majority of records processed under this program were obtained during the 1971 San Fernando earthquake.

As a significant aspect of this data processing program, detailed studies were undertaken to determine optimum procedures for processing the accelerograms so that the corrected digitized accelerograms would provide an accurate representation of the actual ground motions over the widest possible frequency band. As part of this effort, Trifunac,

et al., (1973) have presented an analysis of the errors which might reasonably be expected to be present in data from the Strong-Motion Accelerograph processing program. The processing techniques currently being used (1984) are an outgrowth of the earlier methods, with modifications having been made through experience and through advances in technologies associated with the processing procedures.

In view of some of the analyses which follow, it is important that an examination be made of the possible errors present in the digitized accelerograms, and in the displacement curves obtained by double integration of the accelerations. Since the accuracy of the data in this investigation only becomes a problem for low-frequency signals, the following discussions will be restricted to the long-period components.

(a) Typical Processing Conditions

The routine data processing of earthquake accelerograms as performed on the San Fernando data is described by Hudson (1979). Accelerograms typically written on 70 mm film (by instruments with sensitivity of 1.9 cm/g, for the SMA-1 accelerograph), were photographically enlarged four times prior to digitization to give an effective sensitivity of 7.6 cm/g. The photographic enlargements were then digitized on a semi-automatic digitizing table which required that a human operator use a set of cross-hairs placed on the center of the trace to follow the accelerogram. Trifunac (1973) reports that of possible errors resulting from (1) acceleration line thickness, (2) human reading error, (3) digitizer truncation error, and (4) digitizer discretization, the human reading error is the main

contributing factor to the variance of error in digitizing an accelerogram. Random digitization errors of acceleration from all sources were found to be normally distributed with zero mean and standard deviation of 1/312 cm (the resolution capability of the digitizer). For integrated displacement curves, the results of Trifunac (1973) suggest that errors at periods of about 8 seconds may be near 1 cm when an effective sensitivity of 7.6 cm/g is considered.

Hanks (1975) performed an empirical evaluation of the accuracy of ground displacement records using 234 components from the San Fernando earthquake. The basic premise behind his investigation is that ground displacements at closely spaced stations should show little distortion in the long-period, long-wavelength signals crossing the array. Any difference in the long-period amplitudes observed on doubly-integrated accelerograms, he claims, must be attributed to either instrument or processing errors. Hanks reports that, for an effective digitization sensitivity of 7.6 cm/g, displacement uncertainties are approximately 0.5 to 1 cm in the period range 5 to 8 seconds, and 1 to 2 cm in the range 8 to 10 seconds. Subsequent processing using a high-pass filter (f_{LC} = 0.125 Hz) results in ground displacements which are considered to have a noise level of no more than 1 cm amplitude at periods of 8 seconds. Both Trifunac (1973) and Hanks (1975) indicate that this uncertainty decreases dramatically for shorter period components in the record. Basili and Brady (1979) have used the work of Hanks (1975) to

establish an empirical criteria for the low frequency cut-off (f_{LC}) of a high-pass Ormsby filter and suggest that uncertainties in displacements may be ± 0.25 cm when f_{LC} = 0.25 Hz.

(b) Processing of the Coyote Lake Earthquake Data

The Coyote Lake data, processed by the California Division of Mines and Geology (CDMG), was handled in a somewhat different way than the San Fernando data. Details are provided by Porter, et al., (1983) and similar processing used by Fletcher, et al., (1980) for Oroville aftershocks provide additional insights into the techniques. The basic difference between the CDMG procedure and the earlier San Fernando procedures is in the method of digitization. For the Coyote Lake event, the accelerograms have been digitized from contact prints of the original film traces using a trace-following laser scan device. The original film traces for the San Juan Bautista bridge data were recorded at a sensitivity of approximately 1.9 cm/g. The laser scanner's least count (ultimate resolution) is reported to be 1 micron (10^{-6} m) and its random error in digitizing a straight line of similar photographic quality to the accelerogram traces is claimed to be 10 microns (Porter, et al., 1983).

The potential resolution of the laser scan device can be used to estimate the random noise level in the doubly integrated displacement signal. A random digitization error of 10μm on a trace with sensitivity of 1.9 cm/g corresponds to 5.26×10^{-4}g. Hence, uncertainties in displacements for various periods are estimated to be 0.1 mm at 1 second, 1 mm at 3 seconds, and 8 mm at 8 seconds. Since the Coyote Lake data

was band-pass filtered with filter frequencies $f_{LT} = 0.05$, $f_{LC} = 0.25$ and $f_{HC} = 23$, $f_{HT} = 25$ Hz, the computed displacements may be expected to have an uncertainty of about 1 mm at periods of 3 seconds.

In the next section the uncertainties in computed displacements are used in an examination of differences in motions at the ground level stations at the San Juan Bautista bridge. The results will show that, while the differences in computed displacements at the two stations are of the same magnitude as the expected level of random digitization noise, several features of the data suggest that the differences are mainly due to differential motion of the supports.

2.3.3 Differential Support Motion

The instrumentation layout for the San Juan Bautista bridge includes two sets of triaxial transducers mounted at the base of bents 3 and 5. Records taken at these locations during the 1979 Coyote Lake earthquake provide a possibility to study the differences in ground motion occurring at two separate supports of the bridge. This marks one of the first instances where recorded strong ground motion and the associated structural responses might be used to examine the problem of multiple-support excitation of a bridge.

The X, Y and Z displacement components of ground motion at B3 and B5, obtained from double integration of the recorded ground accelerations, are shown in Fig. 2.5, and appear to be well correlated for their respective directions. This correlation is to be expected because of the close proximity of the two stations. However, subtraction of the X,

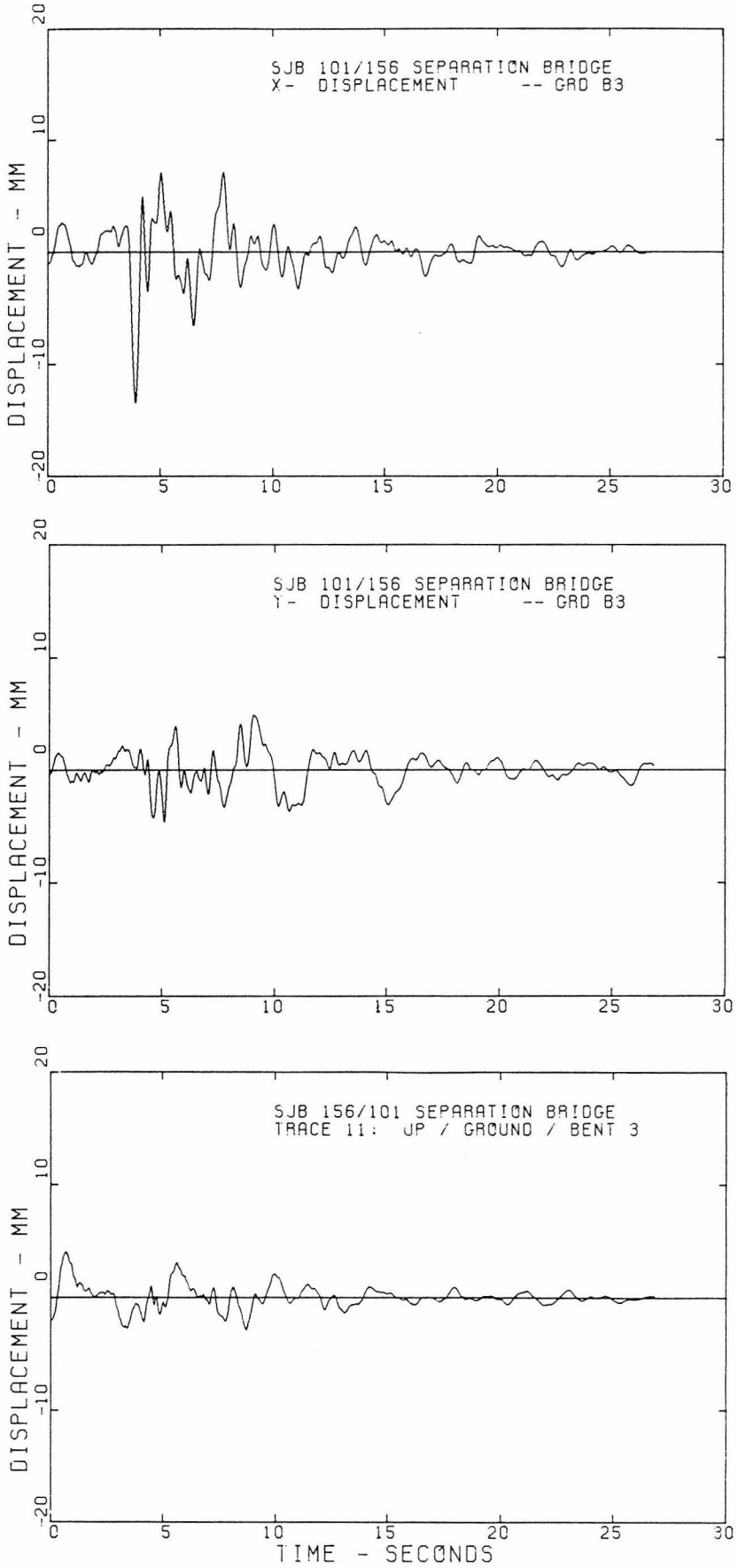

Figure 2.5 Absolute Ground Displacements at Bents 3 and 5

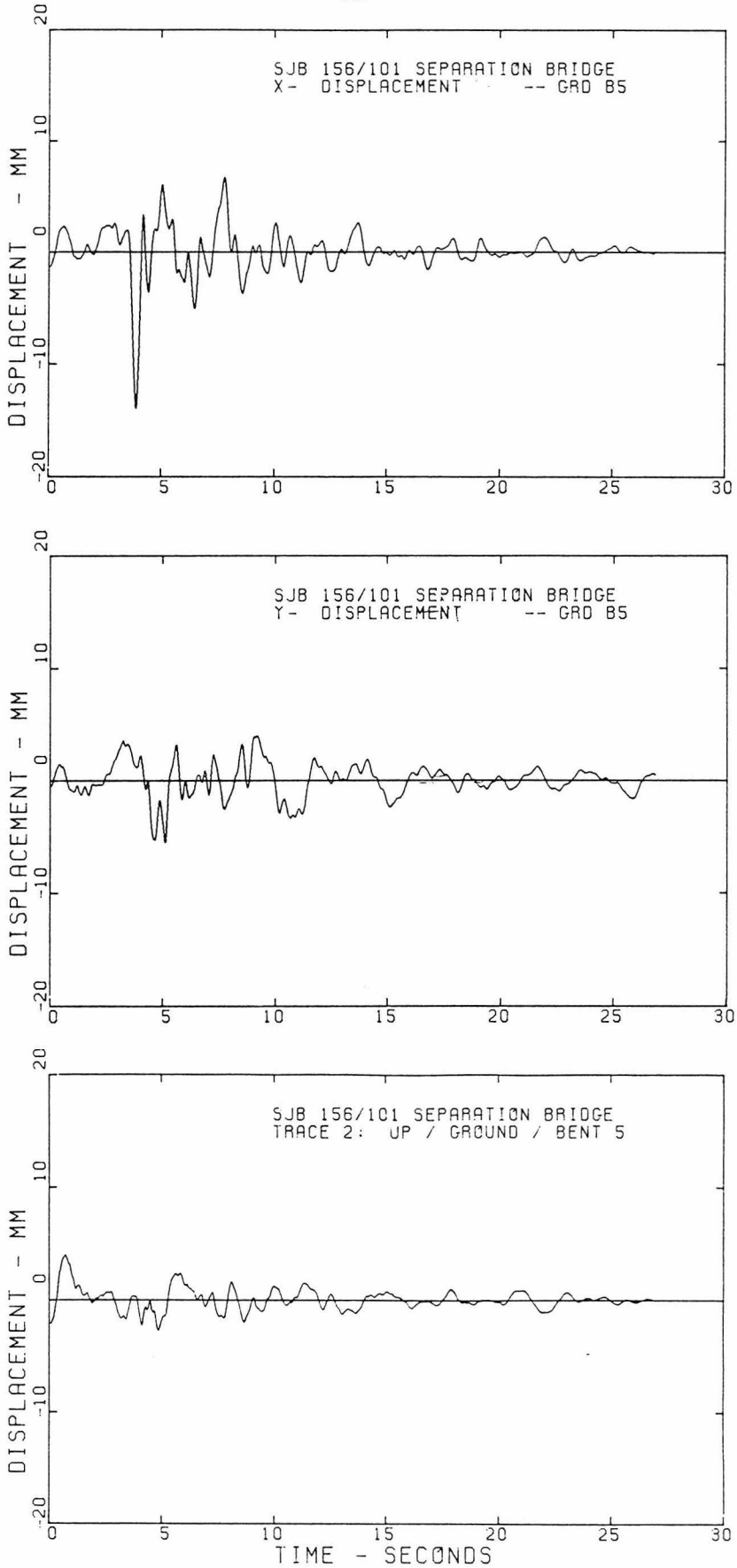

Figure 2.5 (cont'd)

Y and Z-pairs, as shown in Fig. 2.6, reveals what appears to be a differential displacement occurring between B3 and B5 with a period of about 3 seconds. Superimposed on the early part of this signal are some small amplitude, higher frequency components but most of the differential amplitude is a result of the long-period component. If the doubly-integrated accelerograms at the two locations had been identical in amplitude and phase, subtraction of the pairs of records (as in Fig. 2.6) would have yielded zero.

In examining the differential motions, it was initially thought that the long-period component may have been simply an error introduced during the accelerogram processing, as discussed in the previous section. The amplitudes of the differential displacements border on the amplitudes predicted for random noise in processing, but the following analyses support fairly strongly that they may, instead, be caused by passage of seismic waves.

In a seismological context, the presence of the 3-second component in the differential displacements may be partially explained as being a consequence of a phase delay in a long-period wave propagating across the bridge site. If one considers a sinusoidal wave propagating in a radial direction (with respect to the epicenter) across the site with wave speed c, then for radial motions at B3 and B5 the displacements are given by

$$y_3(t) = A \cos \omega(t - \frac{x_3}{c}) \qquad (2.9a)$$

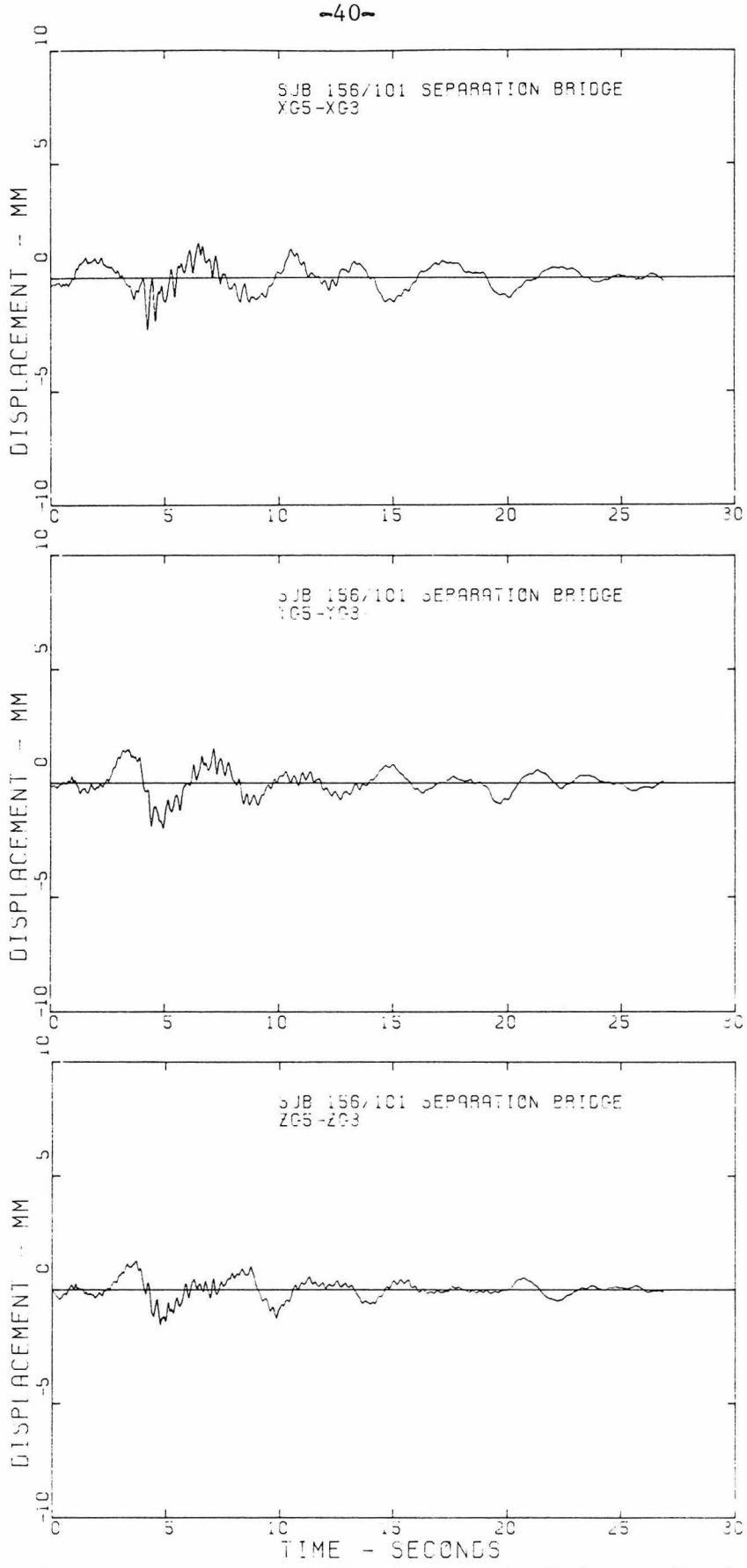

Figure 2.6 Relative Ground Displacements Between Bents 3 and 5

$$y_5(t) = A \cos \omega(t - \frac{x_5}{c}) \tag{2.9b}$$

Choosing station B3 as a reference ($x_3 = 0$) then

$$\Delta y(t) = y_5(t) - y_3(t)$$

$$\Delta y(t) = A \cos \omega t \cos \frac{\omega \Delta x}{c} - A \sin \omega t \sin \frac{\omega \Delta x}{c} - A \cos \omega t$$

But $\frac{\omega \Delta x}{c} << 1$ for closely spaced stations

$$\text{hence} \qquad \Delta y(t) \simeq - \Delta A \sin \omega t \tag{2.10}$$

$$\text{where} \qquad \Delta A = \frac{A \omega \Delta x}{c} \tag{2.11}$$

From the displacement records, the 3-second motion appears to have a maximum amplitude of approximately 5 mm, Δx from the site geometry is about 13 m and a reasonable value for a surface wave velocity in the low-velocity surficial soil layer might be 300 to 400 m/sec. These values, substituted into Eq. 2.11 give $\Delta A \simeq 0.3$ to 0.5 mm. The estimated value for ΔA from this simplified analysis is a factor of two to four less than seen in Fig. 2.6, but it does suggest further examination. The observation of surface waves at about 3-second period in a low-velocity ($c_R \sim 300$ m/sec) surface layer has been noted by Okamoto (p. 509; 1973) in data obtained from a linear array of instruments in Japan. In the case of the San Juan Bautista bridge however, such differences in amplitudes are, unfortunately, of the order of the amplitudes expected from the random digitization noise. If the recording stations had been placed at the abutments, the estimated

difference in amplitudes would have been on the order of 1 to 1.5 mm. Furthermore, a more favorable orientation of the bridge with respect to the epicenter would have increased the time delay of signals propagating from one station to the next, thereby creating a more discernible phase shift.

Some stronger evidence that the three-second component is, in part, due to differential support motion is seen by examining the response of the bridge superstructure. The relative displacements of the top of bent 5 with respect to the base of bent 5 are shown in Fig. 2.7. In each case (X and Y directions) it is apparent that there exists a three-second component with an amplitude of 2 to 3 mm. The nature of the differential motion on the superstructure is very similar to that of the bases of the two bents. This similarity is consistent with differential motion of the supports as well as systematic errors in data processing, but it is not expected from random errors in data processing. The three-second component, if present in the structural response as a result of the differential motion occurring along the line of supports, is viewed by the bridge as a pseudostatic component of the excitation since the natural periods of bridge response are much shorter than three seconds.

To complete this discussion, Fourier amplitude spectra of X and Y ground accelerations at bent 3 and bent 5 are shown in Fig. 2.8. It is evident that even over the distance of 32.6 m (107 feet) between B3 and B5 some differences appear in the frequency content of the ground accelerations. This occurs mostly in the frequency band of 3 to 8 Hz.

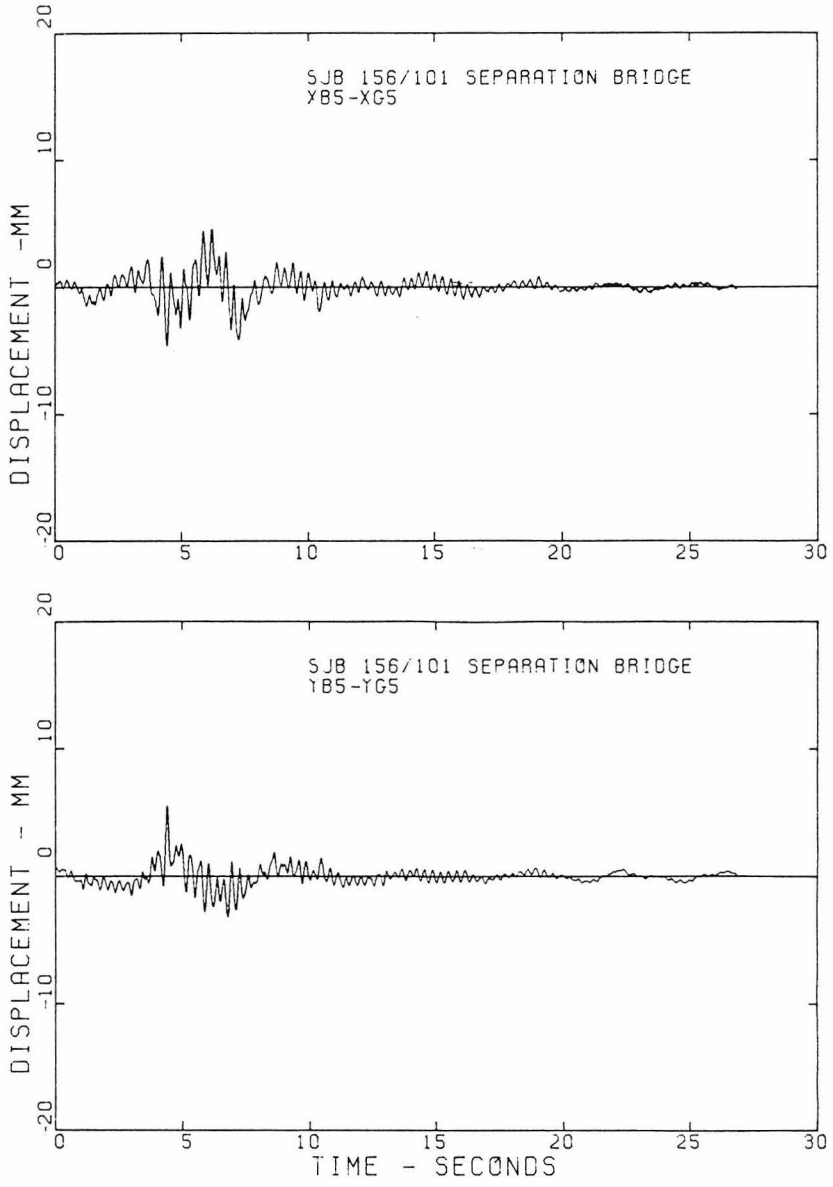

Figure 2.7 Displacements at Top of Bent 5 Relative to Ground at Bent 5

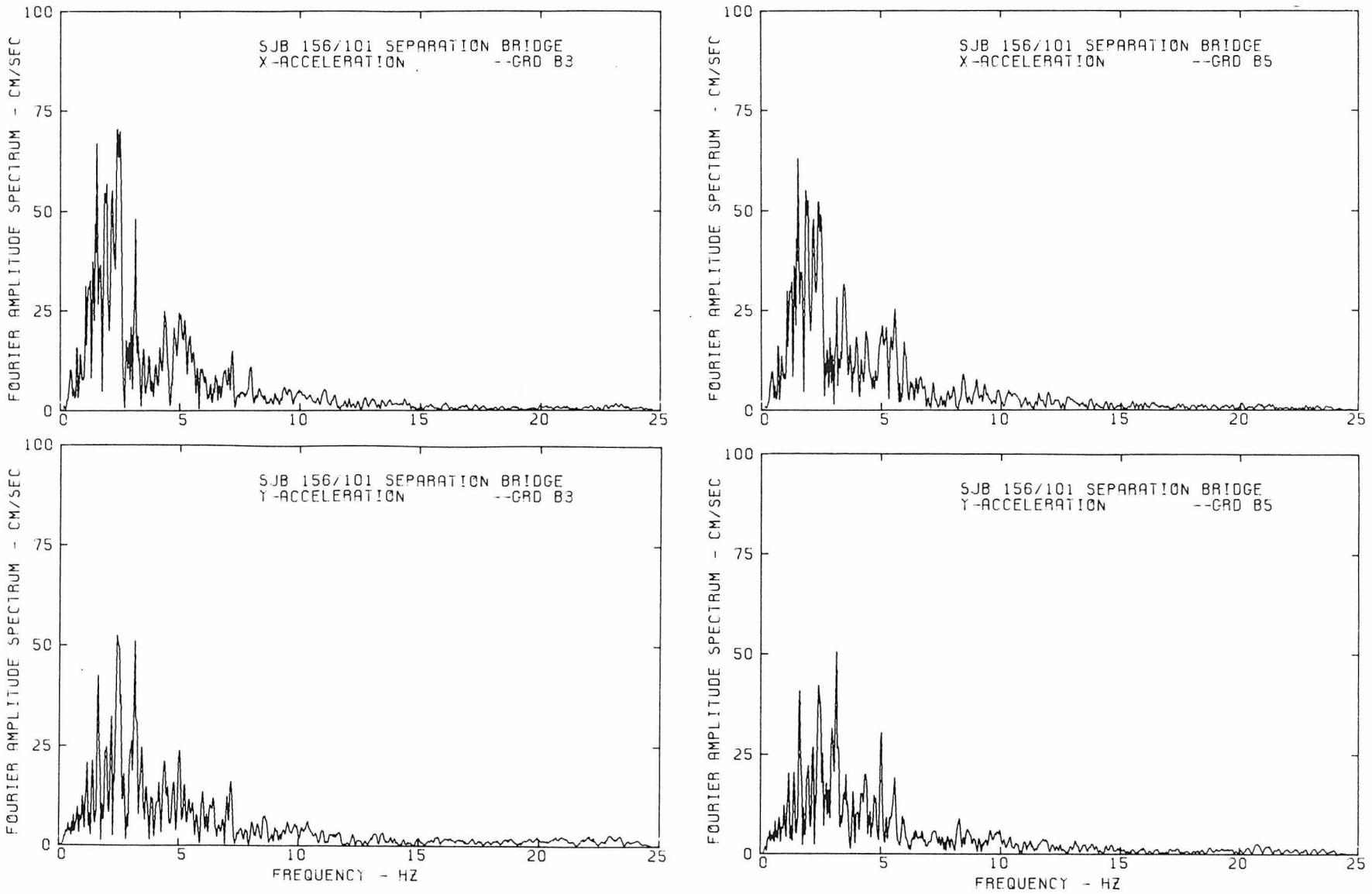

Figure 2.8 Fourier Spectra of Absolute Ground Accelerations at Bents 3 and 5

As discussed in later sections, this is the same frequency range within which most of the bridge's dynamic response occurs, and in some instances the frequency components measured at the base of the bents probably owe some of their amplitude to feedback from the bridge response.

To study the soil-structure interaction problem in detail, and to know precisely what the free-field ground motion is at a given bridge site, it is important to have available a triaxial free-field record taken close to the bridge, but far enough away so as not to be significantly influenced by the localized effects of soil-structure interaction.

The San Juan Bautista bridge was instrumented to record ground accelerations only at the base of B3 and B5, with no provisions made for a free-field station near the bridge. The closest available station is in the town of San Juan Bautista, about 3 km to the south-east of the bridge, and is referred to as the San Juan Bautista "free-field" site in data reports (Porter, et al., 1983). This record is too far away to be representative of the free-field motions at the bridge site.

2.3.4 Rayleigh Waves

The observations and qualitative descriptions of long-period displacements presented in the previous section point to an interesting phenomenon which is not present in strong-motion records from typical buildings. Assuming long-period processing errors are not large, components of ground motion at periods significantly longer than the

fundamental period of the structure would appear identically in all accelerograph records for a given direction in a building owing to the fact that all floor levels respond identically to a pseudostatic base motion. In a mathematical context, the pseudostatic influence coefficient vector $\underline{r}$ in Eq. 2.7 is a column vector of ones. For a bridge, the problem is different since $\underline{r}$ is no longer a unit vector and thus components of differential ground motion may have a noticeable effect on the structural response. It is therefore of considerable interest for bridge response to explore the nature of the long-period components of ground motion in greater detail.

The long-period component having a period of about 3 seconds appears in displacement time-histories of both ground motions and superstructure responses. Since the body wave phases (P waves and S waves) are clearly evident on the ground motion accelerograms at relatively high frequencies it was conjectured that the long-period components observed in the displacements might be due to lower frequency surface waves propagating across the bridge site. The presence of surface waves in recorded strong ground motions has been investigated by several researchers (Anderson, 1974; Hanks, 1975; Liu and Heaton, 1983) who report that a substantial contribution to amplitudes of ground motion can be made by surface waves.

To investigate the presence of surface waves at the San Juan Bautista bridge site, the horizontal components of ground motion recorded at B5 were rotated into radial and transverse components

defined relative to the epicenter BK, on Fig. 2.1. These components, as well as the vertical component, are shown in Fig. 2.9. A long-period 3-second component is visible in the radial direction, particularly in the time interval between 4 and 10 seconds. In the transverse direction it is more difficult to assess the contributions from long-period components. The fact that the 3-second motion is primarily confined to the radial-vertical plane is a strong indication that it is mainly a Rayleigh wave.

A Rayleigh wave, propagating in the +x direction along the surface of a homogeneous, elastic half-space with (nondispersive) wave velocity c_R will have horizontal and vertical displacement components, u(x,t) and w(x,t) respectively, given by

$$u(x,t) = A_H \cos \omega\left(t - \frac{x}{c_R}\right) \qquad (2.12a)$$

$$w(x,t) = A_V \sin \omega\left(t - \frac{x}{c_R}\right) \qquad (2.12b)$$

When Poisson's ratio equals 0.25, the wave velocity c_R will be 92% of the shear wave velocity for the medium, as previously stated by Eq. 2.4. Also, in a homogeneous, elastic half-space $A_V = 1.48A_H$. Thus, Eqs. 2.12a and 2.12b show that the particle motion is retrograde elliptic for a Rayleigh wave propagating in the positive x direction.

In Fig. 2.10 the vertical displacements are plotted as a function of the radial displacements for the station at B5, with time as a parameter. For clarity the plots are shown in four second segments, except for the last plot which is a six second segment. To produce these

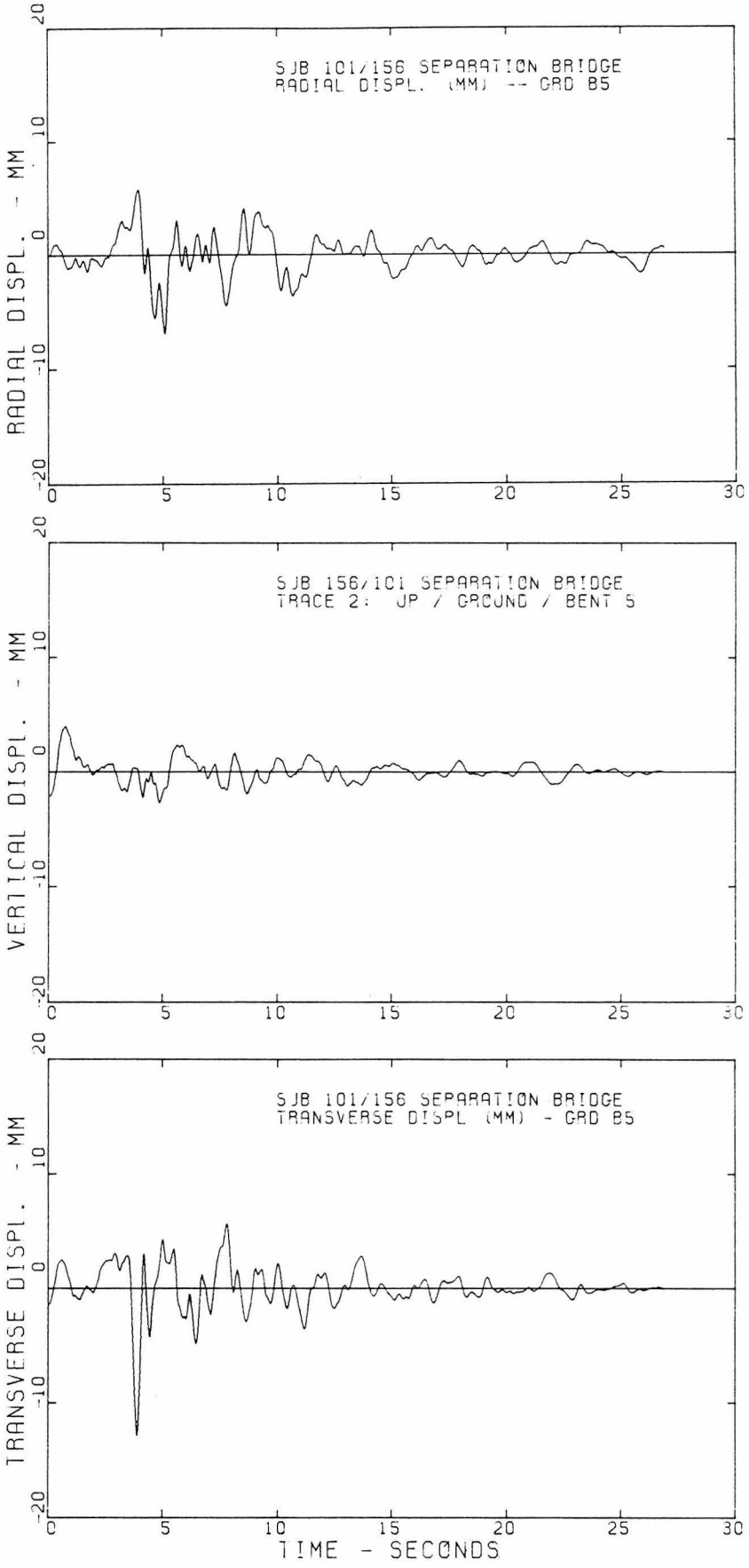

Figure 2.9 Ground Displacements at Bent 5

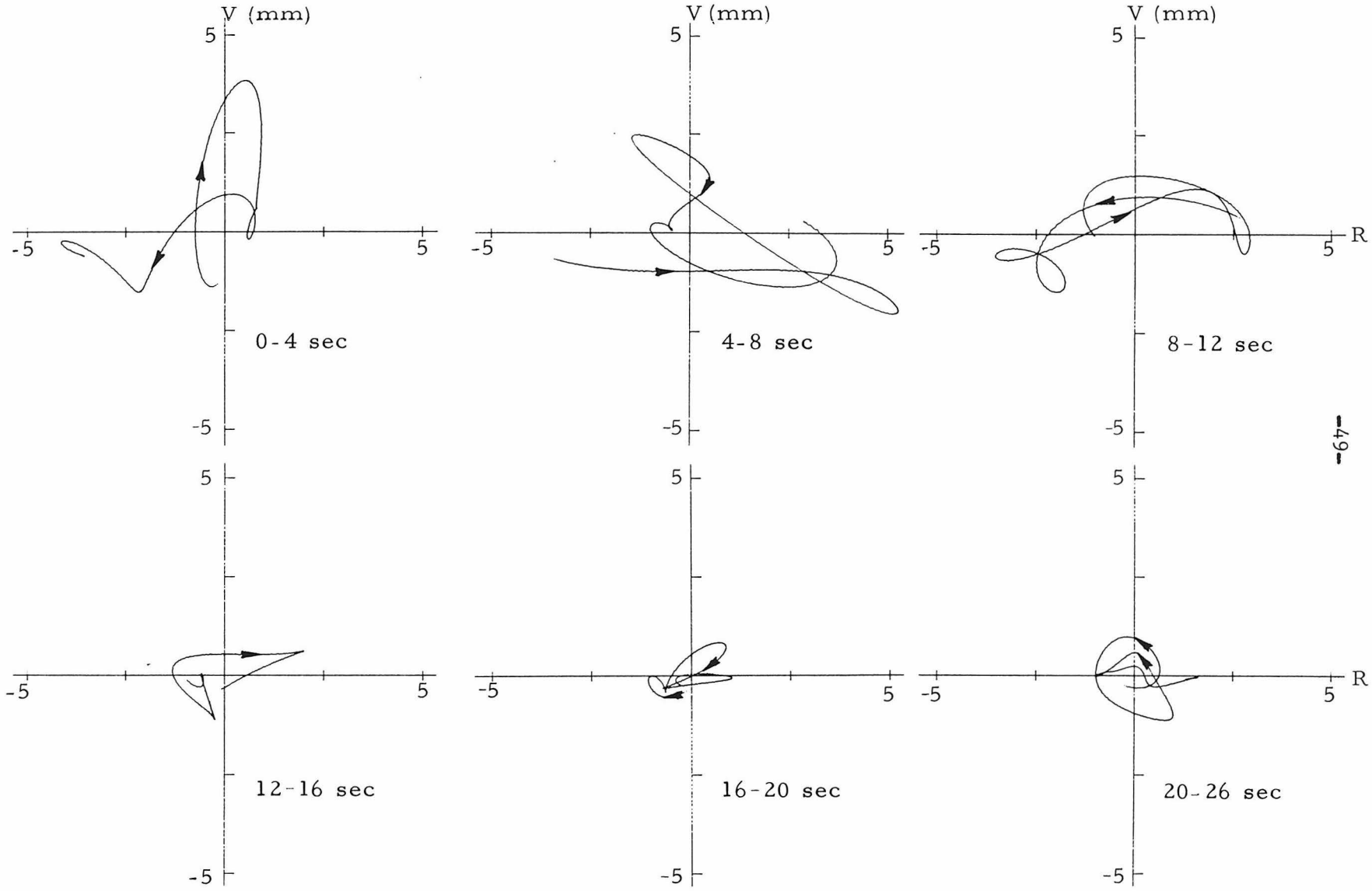

Figure 2.10 Particle Motions of Absolute Ground Displacements at Bent 5 (V=vertical; R=radial)

plots, the radial and vertical displacements shown in Fig. 2.9 were low-pass filtered to remove all frequency components above 1.25 Hz. This was necessary so that higher frequency displacements, resulting from other sources, would not confuse the trace of the long-period motion. The direction of increasing time, and hence the particle motion trajectory, is indicated on each plot. To a large extent, the particle motions are retrograde within the time interval of 6 to 26 seconds (26 seconds is nearly the end of record), the exception being an interval between 14 and 18 seconds when the motion is prograde.

The motion is not always in a well-defined elliptical path, but this is likely attributable to the fact that at an epicentral distance of approximately 30 km, the Rayleigh waves are not yet fully developed. In a study of San Fernando data, Liu and Heaton (1983), found that surface waves started to develop rapidly at epicentral distances of approximately 30 km and dominated records beyond 40 km, so it seems reasonable to view the San Juan Bautista bridge site as being in a transition zone where rapidly developing surface waves are challenging the body waves for a dominant place in the records. The retrograde elliptical motion at the B5 station is very clear in the time intervals of 6 to 10 seconds and 18 to 24 seconds, indicating a few cycles of well-developed Rayleigh wave motion are occurring, interspersed with some less well-developed elliptical motions. The elongation of trajectories in the radial direction is caused by surface layers which have a low

wave velocity relative to the wave velocity of layers beneath. This elongation phenomenon was also found by Hanks (1975) for Rayleigh waves from the San Fernando earthquake.

The arrival time of a Rayleigh wave at the bridge site may be estimated using an adaptation of the S wave minus trigger time approach used for calculating the distance d to the earthquake. The distance d may be expressed as

$$d = \alpha t_p = \beta t_s = c_R t_R \tag{2.13}$$

where α is the P wave velocity and t_p is the arrival time of the P wave. Similarly, s and R denote S wave and Rayleigh wave parameters. Rearranging Eq. 2.13 in terms of the S-P time (Hudson, 1979) which can be read from the accelerogram gives

$$d = \frac{(t_s - t_p)\beta\alpha}{\alpha - \beta} = \frac{(t_R - t_p)c_R\alpha}{\alpha - c_R} \tag{2.14}$$

At the San Juan Bautista bridge site, $t_s - t_p \simeq 4$ seconds, and using typical regional geophysical values of $\alpha = 5.5$ km/sec, $\beta = 3.0$ km/sec gives an arrival time for the Rayleigh wave of $t_R - t_p \simeq 5$ seconds. This simplified calculation does not consider the dispersive nature of surface waves, nor does it account for the possibility of velocity gradients along the travel path. However, it does agree closely with the time when retrograde particle motion commences.

The radial polarization of the 3-second wave, the delayed onset of retrograde particle motion, and the radial elongation of elliptical

particle trajectories all provide evidence to indicate that the 3-second wave component is a Rayleigh wave, likely still in a developmental stage owing to the moderate epicentral distance. At greater epicentral distances the significance of the Rayleigh waves as compared to the body waves would be expected to be greater. With the preponderance of the evidence indicating that the 3-second component in the displacement is actual ground motion rather than noise, its appearance in the differential support motions and in the structural deflections seems very likely real as well, and not simply an accident of the data processing.

2.4 CORRELATION ANALYSIS OF VERTICAL GROUND ACCELERATIONS

The seismic waves first arriving at a site are the P waves, often arriving at a nearly vertical angle of incidence to the ground surface if the source is not too close. The first few seconds of motion at a site are generally composed of simpler wave forms than later arriving signals since refraction, reflection and modal conversions, although they occur, are not yet complicated by the contributions of S waves and other phases from the source. It is conjectured therefore, that the vertical motion between the first P wave arrival and the S wave provides one of the better segments of record to use in a correlation analysis to determine whether any observable differences in accelerations at the two points could be attributed to coherently propagating seismic waves.

The first 4 seconds of vertical accelerations (P waves) at B3 and B5 (see Fig. 2.11), digitized at 100 points per second, were used to compute cross-correlation coefficients (normalized cross-covariances)

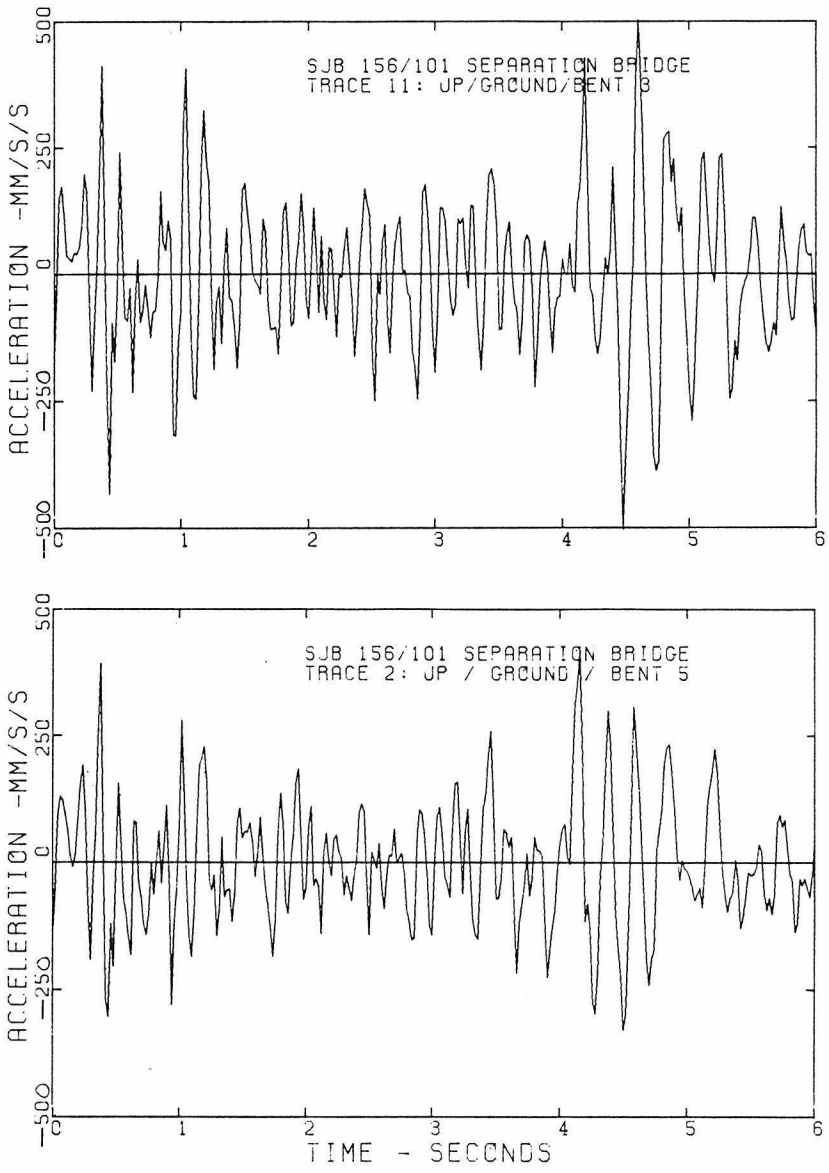

Figure 2.11 First Vertical P Wave Accelerations at Bents 3 and 5

for various time shifts τ, between the two records. The record at B5 was taken as a reference and the record at B3 was shifted by $\pm\tau$ with respect to B5. A similar type of analysis has been used by Smith, et al., (1982) in examining data from an array of strong-motion accelerographs near El Centro, California.

The cross-correlation between two time signals x(t), y(t) is given by

$$\rho_{xy}(\tau) = \frac{R_{xy}(\tau)}{R_{xx}(0)R_{yy}(0)} \tag{2.15}$$

where

$$R_{xy}(\tau) = \frac{1}{N-r}\sum_{i=1}^{N-r} x(t_i)y(t_{i+r}) \tag{2.16}$$

and

$$R_{xx}(0) = \frac{1}{N}\sum_{i=1}^{N} x^2(t_i) \tag{2.17}$$

$$R_{yy}(0) = \frac{1}{N}\sum_{i=1}^{N} y^2(t_i) \tag{2.18}$$

and $\tau = r\Delta t$; $r = 0,1,\ldots,m$; $\Delta t = 0.01$ seconds.

The resulting cross-correlation coefficients $\rho_{xy}(\tau)$, plotted in Fig. 2.12, show that the time shift which maximizes $\rho_{xy}(\tau)$ is near 0.007 seconds. This means the maximum correlation between the first four seconds of vertical excitation occurs when the record of B3 (channel 11) leads the record at B5 (channel 2) by approximately 0.007 seconds. This indicates that the seismic P wave propagating from the source reaches B3 slightly before it reaches B5, an observation that is consistent with

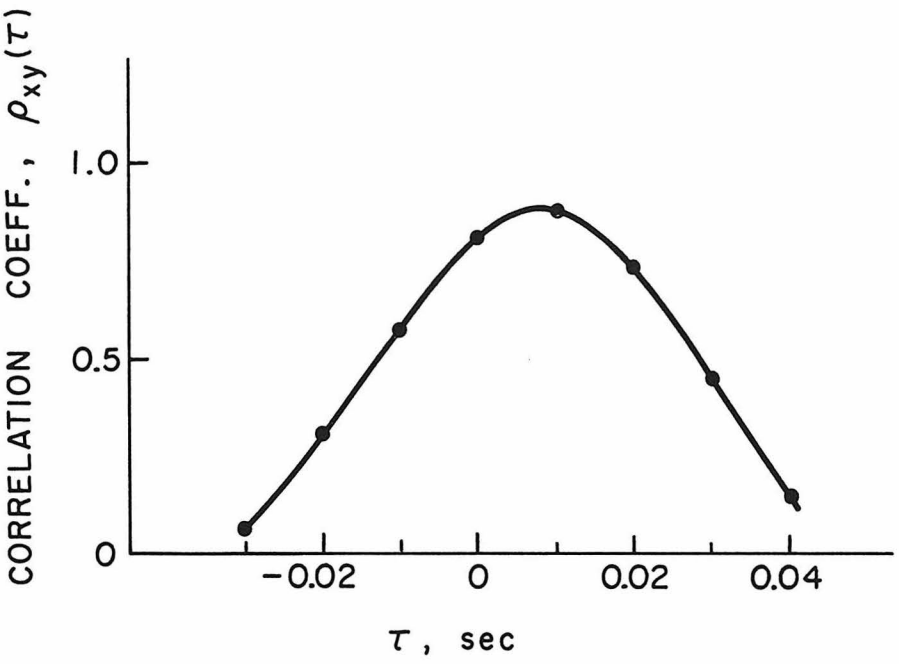

Figure 2.12 Cross-Correlation of First Four Seconds of Vertical P Wave Motion

the orientation of the bridge with respect to the epicenter (see Figs. 2.1 and 2.2).

An approximation to the apparent P wave velocity at the bridge site (the transit velocity across the site) can be made using the time delay found above and calculating the additional distance the P wave must travel to reach bent 5 along an azimuthal angle of approach from the epicenter of about 12°. This yields an apparent P wave velocity at the bridge site of 1800 meters per second. This value, however, does not provide a complete picture of the P wave arrivals at the bridge site because the first arrivals of P waves are those which travel through the deeper, higher velocity layers and then propagate upwards to the surface. If the angle of incidence of P waves at the surface were zero, i.e., the direction of propagation were vertical, all support points of the bridge would be subjected to in-phase (correlated) motions. However, this is not the case for the San Juan Bautista bridge. The time lag between P wave arrivals at B3 and B5 indicates that the P waves are arriving at an oblique angle of incidence to the ground surface, thereby subjecting the bridge to multiple-support excitation.

An estimate of the angle of incidence can be made by using the time lag of approximately 0.007 seconds computed from the correlation analysis, and a reasonable value for the P wave velocity of the soil in the vicinity of the footings. In a more detailed discussion of the site soil conditions presented in section 4.1.2, a shear wave velocity of 460 m/sec is considered to be appropriate for the bridge's foundation soil. Using relations for the propagation of a planar wave in a homogeneous

elastic medium (Eqs. 2.2 and 2.3) the P wave velocity is taken to be 800 m/sec. The angle of wave emergence θ, with respect to the ground surface as shown in Fig. 2.13, can then be found using

$$\alpha_a = \frac{\alpha}{\cos \theta} \tag{2.19}$$

which expresses the relationship between the P wave velocity in the foundation soil α, and the apparent P wave velocity on the surface, α_a, as a function of the angle of θ. Using α = 800 m/sec and α_a = 1800 m/sec, the angle of wave emergence is found to be 63.6^o. (The angle of incidence is, therefore, $90^o - 63.6^o = 26.4^o$).

The foregoing analysis has used as a starting po3nt the time delay between B3 and B5 predicted by correlation of the P wave motion. Since the accelerograms were digitized at 100 points per second, it is difficult to determine accurate time delays of less than one interval of digitization (0.01 second). A different approach is possible however, wherein the geophysical velocity structure of the region is used to examine P wave arrivals at the bridge site. The method, explained in greater detail in Appendix 2B, uses the velocity structure for the region given in Table 2.1 and assumes that wave propagation paths can be described by rays. At layer boundaries Snell's law is used to find the change in direction of the ray.

Using the velocity structure in Table 2.1 and the ray path computed in Appendix 2B, the angle of emergence θ, of P waves at the ground surface is found to be 59^o, in good agreement with the value from the correlation analysis. However, the corresponding apparent P wave

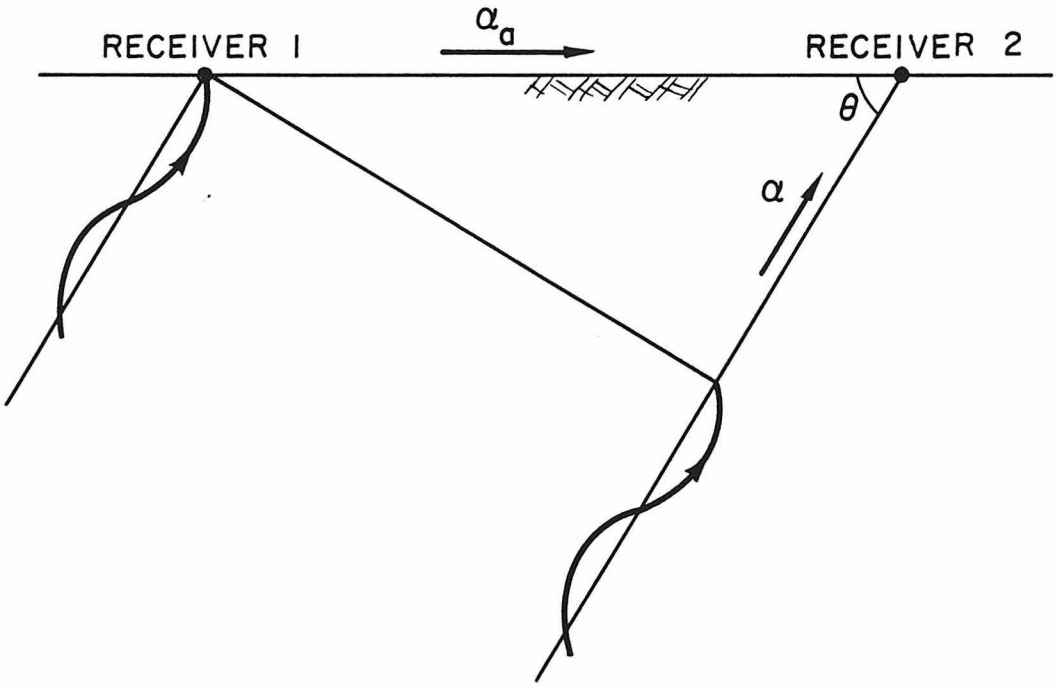

Figure 2.13 True (α) and Apparent (α_a) Wave Velocities

velocity at the bridge site is found to be 5825 m/sec (using α for the 0.5 km layer) which is obviously much too large. This error arises because the ray approach considers only the gross geologic structure of the region and demonstrates that

TABLE 2.1

Velocity Structure for the Coyote Lake - San Juan Bautista Region

Thickness (km)	P Velocity α (km/sec)	S Velocity β (km/sec)
0.5	3.0	1.5
2.5	5.0	2.8
9.0	5.7	3.3

(after Liu and Helmberger, 1983)

wave signals, as recorded at the bridge, must be influenced by the local site soil conditions. The low-velocity surface layer of soil at the bridge site, not included in the ray model, slows down the P waves arriving from below and turns the wave front (ray) more towards the vertical as the wave crosses into the surface layer soil.

A further look at the problem using ray theory involves taking into consideration the surface soil layer with $\alpha = \alpha_o = 800$ m/sec and the angle of emergence of 59^o, as computed in Appendix 2B. The angle at the ground surface θ, is found by applying Snell's law

$$\theta = 90^{o} - i_{o} \quad .$$

where $$i_{o} = \sin^{-1} \left[\frac{\alpha}{\alpha_{I}} \sin 31^{o} \right]$$

which gives $\theta = 82^{o}$. This value is greater than the 63.6^{o} computed from the correlation analysis.

The previous analyses (correlation and ray theory) indicate that the ray approach, while providing an informative picture of the overall paths of wave travel is not sufficiently detailed to account for the local soil effects in the vicinity of the foundation. Its usefulness seems to be more suited to describing the regional features of seismic wave propagation.

The first approach, using the correlation of strong motion data recorded at two stations may be somewhat inaccurate, but it is believed to provide the better estimate of wave arrivals at the bridge site. In further discussion, the value of 0.007 seconds will be used as the time delay in P wave arrivals between B3 and B5.

An estimate of the phase difference between motions occurring at the two abutments due to the travelling P wave may be made using the predominant frequency f_{p}, of the P wave and relating this to the P wavelength λ_{p}, via $\lambda_{p} = \alpha/f_{p}$. Examining the first four seconds of the vertical acceleration records at B3 and B5, it is seen that the predominant P wave frequency is about 9 Hz. Using a surface layer P phase velocity of 800 m/sec gives a P wavelength of approximately 89 m (290 feet). If it is assumed that the delay of 0.007 seconds between B3

and B5 occurs uniformly over the length of the bridge, then a P wave will arrive at A7 0.021 seconds after its arrival at A1. Thus, the maximum anticipated phase difference between abutments due to the observed non-vertically incident P wave is approximately 0.38π, or about 68^{o}.

Werner and Lee (1980) have performed a parametric study on the response of a single span bridge structure subjected to excitation by various types of seismic waves. Their findings, although not directly applicable to the structural configuration of the San Juan Bautista bridge, do provide interesting observations on the response of a simpler bridge system to spatially varying excitations. A significant finding of their work is that non-vertically incident waves propagating obliquely to the bridge span (as is the case for P waves at the San Juan Bautista bridge) can induce torsional deformations in various elements of the bridge. For the San Juan Bautista bridge these torsional deformations may possibly be induced in the deck as a result of differences in the rocking displacements of adjacent bents. The rocking of the bents may, in turn, be induced by both the oblique angle of approach of the P waves and by the non-vertical angle of incidence. Thus, the two footings at each bent may be subjected to phased inputs having both horizontal and vertical components.

The Fourier spectra of vertical motions (Fig. 2.8) indicate that 9 Hz is about equal to the maximum frequency component which has a significant Fourier amplitude. Lower frequency P waves will have longer wavelengths, which will result in smaller phase differences between

abutments than the previously estimated 68^{o}. This gives an indication that vertical differential support motion of the San Juan Bautista bridge due to travelling P waves is likely to be minimal for the 1979 Coyote Lake event. Furthermore, as will be pointed out later, the vertical response of the bridge is uncoupled from the horizontal response due to the simply-supported spans, and consequently any effects of multiple-support excitation in the vertical direction would be confined to the vertical or torsional response of the individual spans.

2.5 SUMMARY

The presence of long-period components in the ground displacement records at the San Juan Bautista bridge site may be the result of one or more of the following sources: long-period seismic waves, systematic data processing errors; and random data processing errors. While systematic data processing errors cannot be completely ruled out by the writer, the evidence suggests that the three-second component observed in the ground displacement records are caused by a Rayleigh wave travelling across the bridge site. Radial polarization of the three-second component and retrograde elliptical particle motions are strong indications to support the Rayleigh wave hypothesis.

Although random digitization noise might be of the same general amplitude as the observed displacements, the fact that the three-second displacement components are correlated at the two ground sites and in the superstructure records, seems to rule out the presence of any significant amount of random processing error at a three second-period.

In the vertical direction, a very small time delay was detected between the arrival of P waves at bent 3 and bent 5. At least in this case, the influence of differential support motion induced by body waves in the vertical direction appears to be much less noticeable than the differential motion induced by long-period surface waves.

Although the consequences of differential support motion were not serious for the San Juan Bautista bridge in this earthquake, they did complicate the analysis of the response and they could be of much more importance for more extended structures with longer natural periods.

APPENDIX 2A

SPECIFICATIONS ON RECORDING INSTRUMENTATION AT THE SAN JUAN BAUTISTA BRIDGE

I. Central Recording Acceleration System*: CRA-1

- a multi-channel, photographic recording system.
- 12 channels of acceleration data on 7" wide film.
- film speed: 1 cm/sec.
- start up: full operation within 0.1 second.
- timing: 0.5 second marks.
- references: 6 fixed traces.
- transducers: force balance accelerometers.

II. Force Balance Accelerometers*: FBA-1 and FBA-3

- range: ±1g (approximately 1.9 cm/g on film)
- damping: 70% critical.
- natural frequency: 50 Hz.

* manufactured by Kinemetrics, Inc., Pasadena, California

APPENDIX 2B

SEISMIC WAVE PROPAGATION ALONG RAY PATHS

The propagation of a seismic body wave from the earthquake focus to a surface receiver can be described by ray paths when the layers through which the wave passes are each assumed to have constant wave speed. Figure 2B.1 illustrates the case where the focus is located in the third layer. Snell's law is assumed to hold at layer boundaries and also it is assumed that the wave velocities v in the three layers are such that $v_3 > v_2 > v_1$.

Let the initial take-off angle of a wave front from the focus be i_3, as shown in Fig. 2B.1. Hence, the angle of incidence of the ray (describing the direction of motion of the wave front) at the 3-2 boundary is also i_3. By Snell's law

$$\frac{\sin i_3}{v_3} = \frac{\sin i_2}{v_2} = \frac{\sin i_1}{v_1} \qquad (2B.1)$$

and from Fig. 2B.1 the epicentral distance is

$$e = \sum_{k=1}^{3} d_k \tan i_k \qquad (2B.2)$$

Also, from the geometry of the problem

$$\ell_k = \frac{d_k}{\cos i_k} \qquad k=1,2,3 \qquad (2B.3)$$

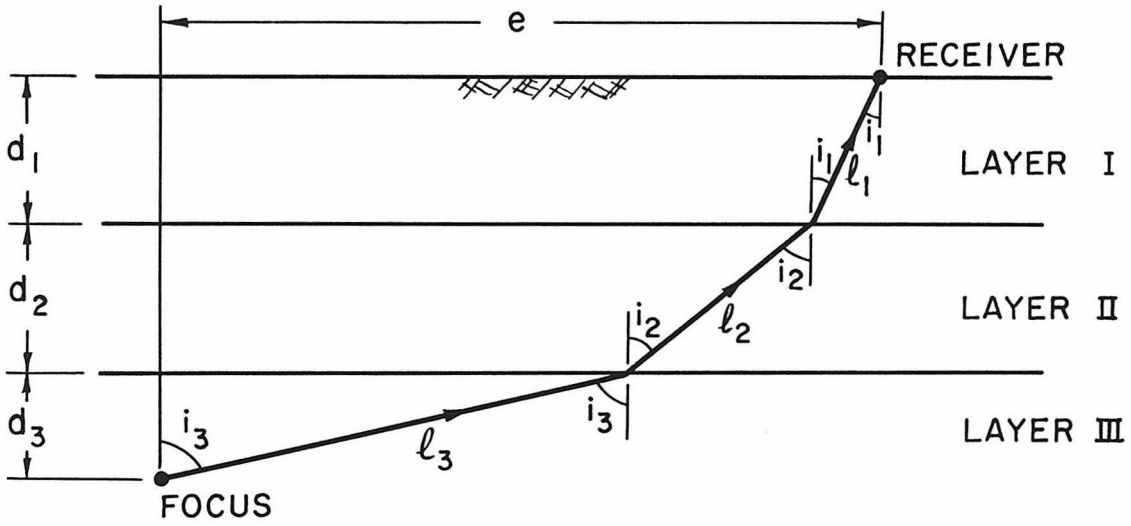

Figure 2B.1 Ray Paths in a Layered Medium

The solution of the problem to find travel times and angles of incidence involves an iterative procedure as follows:

Solution Iteration:

1) Assume an initial take-off angle i_3.

2) Calculate i_2 and i_1 using Eq. 2B.1.

3) Calculate $\tilde{e}$ (an estimate of e) using Eq. 2B.2.

4) If $\frac{|\tilde{e}-e|}{e} \leq \varepsilon$, where ε is a prescribed tolerance (say 1%) then stop. Otherwise, assume a new i_3 and repeat steps 2 and 3.

5) Calculate travel distance $\ell_{TOT} = \sum_{k=1}^{3} \ell_k$ using Eq. 2B.3.

6) Calculate total travel time $T = \sum_{k=1}^{3} \frac{\ell_k}{v_k}$.

The above procedure, when applied to the San Juan Bautista bridge site using e = 26.87 km, d_1 = 0.5 km, d_2 = 2.5 km, d_3 = 5.0 km gives the following results:

ℓ_1 = .583 km $i_1 = 30.907^{o}$

ℓ_2 = 4.837 km $i_2 = 58.878^{o}$

ℓ_3 = 22.921 km $i_3 = 77.400^{o}$

ℓ_{TOT} = 28.341 km

T = 5.183 seconds (for a P wave).

CHAPTER REFERENCES

Anderson, J. (1974). "A Dislocation Model for the Parkfield Earthquake," Bull. Seism. Soc. Am., Vol. 64, No. 3, June, pp. 671-686.

Basili, M. and Brady, G. (1978). "Low Frequency Filtering and the Selection of Limits for Accelerogram Corrections," Proceedings of the 6th European Conference on Earthquake Engineering.

Clough, R.W. and Penzien, J. (1975). Dynamics of Structures, McGraw-Hill, Inc., New York.

Fletcher, J.B., Brady, A.G., and Hanks, T.C. (1980). "Strong-Motion Accelerograms of the Oroville, California, Aftershocks: Data Processing and the Aftershock of 0350 August 6, 1975," Bull. Seism. Soc. Am. Soc. Am., Vol. 70, No. 1, February, pp. 243-267.

Fung, Y.C. (1965). Foundations of Solid Mechanics, Prentice-Hall, Inc., New York.

Hanks, T.C. (1975). "Strong Ground Motion of the San Fernando, California, Earthquake: Ground Displacements," Bull. Seism. Soc. Am., Vol. 65, No. 1, February, pp. 193-225.

Hudson, D.E., Trifunac, M.D., Brady, A.G. and Vijayaraghavan, A. (1972). "Strong-Motion Earthquake Accelerograms, Vol. IIA, Corrected Accelerograms and Integrated Velocity and Displacement Curves," Earthquake Engineering Research Laboratory, EERL 72-50, California Institute of Technology, Pasadena, California.

Hudson, D.E. (1979). Reading and Interpreting Strong Motion Accelerograms, Earthquake Engineering Research Institute, Berkeley, California.

Joyner, W.B., Warrick, R.E. and Fumal, T.E. (1981). "The Effect of Quaternary Alluvium on Strong Ground Motion in the Coyote Lake, California, Earthquake of 1979," Bull. Seism. Soc. Am., Vol. 71, No. 4, August, pp. 1333-1349.

Liu, H-L, and Helmberger, D.V. (1983). "The Near-Source Ground Motion of the 6 August 1979 Coyote Lake, California, Earthquake," Bull. Seism. Soc. Am., Vol. 73, No. 1, February, pp. 201-218.

Liu, H-L, and Heaton, T. (1983). "Array Analysis of the Ground Velocities and Accelerations from the 1971 San Fernando, California Earthquake," submitted to the Bull. Seism. Soc. Am.

Okamoto, S. (1973). Introduction to Earthquake Engineering, John Wiley and Sons, Inc., New York.

Porcella, R.L., Matthiesen, R.B., McJunkin, R.D. and Ragsdale, J.T. (1979). "Compilation of Strong-Motion Records Recovered from the Coyote Lake Earthquake of 6 August 1979," California Division of Mines and Geology Preliminary Report 25, and U.S. Geological Survey Open-File Report 79-385.

Porter, L.D., Brady, A.G., Mork, P.N. and Perez, V. (1983). "Processed Data from the San Juan Bautista 101/156 Separation Bridge and the San Juan Bautista Freefield Records, Coyote Lake Earthquake, 6 August 1979," U.S. Geological Survey, Special Publication 64.

Richter, C.F. (1958). Elementary Seismology, W.H. Freeman and Co., Inc., San Francisco.

Scott, R.F. (1981). Foundation Analysis, Prentice-Hall, Inc., New Jersey.

Smith, S.W., Ehrenberg, J.E. and Hernandez, E.N. (1982). "Analysis of the El Centro Differential Array for the 1979 Imperial Valley Earthquake," Bull. Seism. Soc. Am., Vol. 72, No. 1, February, pp. 237-258.

Trifunac, M.D. (1970). "Low-Frequency Digitization Errors and a New Method for Zero Base-Line Correction of Strong-Motion Accelerograms," Earthquake Engineering Research Laboratory, EERL 70-07, California Institute of Technology, Pasadena, California.

Trifunac, M.D., Udwadia, F.E. and Brady, A.G. (1973). "Analysis of Errors in Digitized Strong-Motion Accelerograms," Bull. Seism. Soc. Am., Vol. 63, No. 1, February, pp. 157-187.

Uhrhammer, R. (1980). "Observations of the Coyote Lake, California Earthquake Sequence of August 6, 1979," Bull. Seism. Soc. Am., Vol. 70, No. 2, April, pp. 559-570.

Werner, S.D. and Lee, L.C. (1980). "The Three-Dimensional Response of a Bridge Structure Subjected to Travelling Rayleigh Waves, SV-Waves and P-Waves," Agbabian Associates, El Segundo, California.

CHAPTER III

SYSTEMATIC IDENTIFICATION OF BRIDGE DYNAMIC PROPERTIES

A time-domain technique of system identification developed by Beck (1978, 1982) and Beck and Jennings (1980) for analysis of strong-motion records from buildings is reviewed in the first part of this chapter. Next, the technique is applied to the earthquake records obtained from the San Juan Bautista Separation bridge during the 1979 Coyote Lake earthquake to find optimal estimates of the modal parameters for the response of the bridge. Initial difficulties encountered in obtaining reliable and stable parameter estimates were resolved by a series of preliminary data processing steps applied before performing the system identifications. These operations resulted in reliable optimal parameter estimates for the first two modes of bridge response and also permitted an examination of the time variation of modal properties during the earthquake.

3.1 A SYSTEM IDENTIFICATION TECHNIQUE FOR EARTHQUAKE ENGINEERING

Recent advances in application of the theory of system identification to problems in structural dynamics have led to the development of techniques which are particularly well-suited to earthquake engineering. A time-domain approach developed by Beck (1978) is reviewed in preparation for later applications to bridge response records. An analogous procedure in the frequency domain has been developed by McVerry (1979).

3.1.1 Output-Error, Identifiability and Measurement Noise

Beck's technique is based upon a general system identification formulation called an output-error approach. The output-error $\underset{\sim}{v}$ is defined as

$$\underset{\sim}{v}(t,\underline{a}) = \underset{\sim}{y}(t) - \underset{\sim}{m}(t,\underline{a},\underline{z}) \tag{3.1}$$

where $\underset{\sim}{v}$ is a function of both time t and model parameters $\underline{a}$. In Eq. 3.1 $\underset{\sim}{y}$ is the measured output (displacement, velocity or acceleration) of the real system and $\underset{\sim}{m}$ is the model output which also has a dependence upon the input $\underline{z}$. In the output-error approach, optimal estimates $\hat{\underline{a}}$ of the parameters $\underline{a}$ of a linear structural model are obtained by systematically varying the parameters until a selected measure-of-fit between the recorded response of the structure $\underset{\sim}{y}$ and the calculated response of the model $\underset{\sim}{m}$ has been minimized. Both the model and the real system are assumed to be subjected to the same input excitation $\underline{z}$. In the approach proposed by Beck, the measure-of-fit, denoted by J, is chosen to be an integral mean-square evaluation of the output-error $\underset{\sim}{v}$ in Eq. 3.1.

In the course of developing a system identification procedure for application to strong-motion studies, two important questions must be addressed: (1) Is the model, as described by optimal parameter estimates $\hat{\underline{a}}$ unique? and, (2) What are the effects of model error and measurement noise on the accuracy of the estimates of the model properties? Both of

these questions have been studied in detail by Beck (1978) for the output-error method of system identification. For a general class* of linear structural models with N degrees of freedom which possess classical normal modes and for which the mass matrix is known, Beck has shown that it is necessary to measure the response at no less than ½N of the degrees of freedom in order to uniquely define the stiffness matrix [K] and the damping matrix [C]. This assumes that the optimal [K] and [C] can be selected from a finite number of possible choices. If this is not the case, then a unique solution can be found only if the response is measured at all N degrees-of-freedom. This restriction is a severe problem for the identification of structural models from earthquake records because the seismic response of most structures is measured for only a very few degrees-of-freedom. In many buildings, instrumentation is installed only at the ground level and the roof, and possibly also at the mid-height. In some cases, such as the Imperial County Services Building (Pardoen, et al., 1981) there may be as many as 12 or 13 transducers in a building, but this is still a small number compared to the degrees-of-freedom of the system.

To overcome the very restrictive nature of the problem of identifying [K] and [C] another approach was adopted. Beck showed that if the base input and the response at a particular degree-of-freedom are known, then, regardless of the total number of degrees-of-freedom in the model,

---

* A class of models is defined by the theoretical model chosen to represent the system, together with an output equation. A particular model within the class is specified by assigning values to the parameters of the theoretical model.

the modal frequency f_r, modal damping ζ_r, and effective modal participation factor p_r, at each point of measurement (for mode r) can be uniquely determined for the general class of linear models. Because of practical limitations on the number of measurements usually taken, it is nearly always preferable to attempt identification of modal parameters f_r, ζ_r, p_r rather than elements of [K] and [C] when using earthquake response data.

The presence of measurement noise also affects the ability to determine complete structural models from earthquake data. This becomes especially significant at higher frequencies where the recorded signal-to-noise ratio decreases and for this reason, estimation of the parameters of higher modes becomes unreliable. In a modal approach, identification should be restricted to estimating parameters only for the first few dominant modes of response. The limited capability to resolve all the modal parameters in the presence of noise once again indicates that the stiffness and damping matrices normally cannot be found with sufficient accuracy to provide a good structural model.

The output-error technique and the associated developments by Beck to identify linear models of structures from earthquake response data are based upon using a single input (ground acceleration) and a single output (structural response at a specified location), although the method can be extended to handle multiple inputs and multiple outputs (Beck, 1978; McVerry, 1979). By allowing only a single input-single output situation the identifiable models are restricted to the subset of planar linear models within the broader class of linear models. While

the restriction of planar modeling has obvious drawbacks in application to bridge response records where coupled two- and three-dimensional responses often occur, the use of systematic computer-based identification techniques, even on a single input-single output basis, offers many advantages and improvements over other less systematic approaches such as trial-and-error modeling, or transfer function estimations.

System identification in structural dynamics and earthquake engineering is still in early developmental and experimental stages. Its implementation, refinement and use as an effective research and investigative tool can be expected to increase as more experience and greater confidence is obtained in applying it in a variety of situations.

3.1.2 Optimal Models: Modal Minimization Method

An output-error approach to finding optimal estimates of modal parameters from earthquake records is outlined in this section. The ultimate objective is to obtain reliable estimates of the parameters which appear in the uncoupled modal equations of motion for planar, linear, structural models. For mode r, these equations may be written as

$$\begin{aligned} &\ddot{x}^r + a_2^r \dot{x}^r + a_1^r x^r = - a_3^r \ddot{z}(t) \\ &x^r(t_i) = a_4^r \quad ; \quad \dot{x}^r(t_i) = a_5^r \end{aligned} \tag{3.2}$$

The total response is the sum of the modal responses

$$x(t,\underset{\sim}{a}^1,\ldots,\underset{\sim}{a}^N) = \sum_{r=1}^{N} x^r(t,\underset{\sim}{a}^r) \tag{3.3}$$

In a terminology more conventional to structural dynamics, the parameters in Eq. 3.2 may be written as

$$a_1^r = \omega_r^2 \equiv (2\pi f_r)^2 \tag{3.4}$$

$$a_2^r = 2\zeta_r\omega_r \tag{3.5}$$

$$a_3^r = \phi_{ri} \frac{\underset{\sim}{\phi}_r^T[M]\underset{\sim}{1}}{\underset{\sim}{\phi}_r^T[M]\underset{\sim}{\phi}_r} \tag{3.6}$$

In the above, f_r is the modal frequency, ζ_r is modal damping and ϕ_{ri} is the component of the r^{th} mode shape vector $\underset{\sim}{\phi}_r$ measured at location i. Equation 3.6 is defined to be the effective participation factor, p_r for mode r at location i.

The optimal match between the model output $\underset{\sim}{m}$ and the real system output $\underset{\sim}{y}$ (ref. Eq. 3.1) is measured by an integral mean-square output

error J defined as

$$J(\underset{\sim}{a}^1,\ldots,\underset{\sim}{a}^N) = \alpha_1 V_1 \int_{t_i}^{t_f} (x_0-x)^2 dt + \alpha_2 V_2 \int_{t_i}^{t_f} (v_0-\dot{x})^2 dt$$

$$+ \alpha_3 V_3 \int_{t_i}^{t_f} (a_0-\ddot{x})^2 dt \qquad (3.7)$$

By choosing the α_i as either 0 or 1, the optimal estimate may be obtained by matching displacements, velocities or accelerations, or some combination of these three quantities, over the time interval $[t_i,t_f]$. The x_0,v_0 and a_0 are, respectively, the observed relative displacement, velocity and acceleration responses of the real structure. The V_i are chosen as normalizing constants so that comparisons may be made between J values for different response quantities and for different time intervals. The V_i are defined as the inverse of the mean-square of the observed relative responses (McVerry and Beck, 1983):

$$V_1 = \left[\int_{t_i}^{t_f} x_0^2 dt\right]^{-1} \quad ; \quad V_2 = \left[\int_{t_i}^{t_f} v_0^2 dt\right]^{-1} \quad ; \quad V_3 = \left[\int_{t_i}^{t_f} a_0^2 dt\right]^{-1} \qquad (3.8)$$

Thus, the measure-of-fit J is the ratio of the mean-square output error to the mean square of the recorded response over the time interval under consideration.

The degree of matching in the time-domain may be quantitatively evaluated by assessing the value of J for the optimal estimates. The optimal estimates of the modal parameters, $\hat{\underset{\sim}{a}}$, are those values which minimize the value of J for a given mode. The optimal value of J would be zero if there were a perfect match between the records of $\underset{\sim}{m}$ and $\underset{\sim}{y}$ (i.e., $\underset{\sim}{y} = 0$ in Eq. 3.1). In practice Beck and McVerry found that optimal values of J ranged from less than 0.1 for excellent matches to as high as 0.5 for poor matches. The poorer matches were most often associated with response records from earthquake damaged structures, whose effective periods and dampings varied with time.

To achieve optimal estimates of the modal parameters, the measure-of-fit J is minimized with respect to the constraints imposed by the class of model described by the theoretical equations in Eq. 3.2. A method developed by Beck which has been found to be numerically efficient and has reliable convergence properties is used to minimize J. In this method, called modal minimization, J is minimized by a series of modal sweeps to find new estimates for the r^{th} mode parameters $\underset{\sim}{a}^r$ (r=1,...N). Each modal sweep involves N single-mode minimizations. During the sweeps, updated estimates for the parameters of the r^{th} mode are obtained by matching a modified response in which the current estimates of all other modes s (s=1,...,N;s≠r) have been subtracted from the original record. Iteration is terminated when a fractional decrease in J is less than a specified amount ε. In later applications, ε is taken to be 10^{-4}.

Beck (1978) has used the above method to investigate a limited number of building response records, and McVerry (1979) has used a similar technique in the frequency domain on a larger sample of buildings. In these applications it was found that modal periods were always estimated very accurately, and the damping and effective participation factors for each mode were estimated quite accurately for the dominant modes of response. In other words, minimization of J is most sensitive to the estimation of modal frequency, and less sensitive to estimation of damping and effective participation factor. Sensitivity analyses (Beck, 1978; 1982) indicate that correlation between modal parameters $a_1^r,\ldots,a_5^r$ is generally insignificant, except for an interaction between ζ_r and p_r. This may be expected on the physical grounds that the amplitude of the transfer function is controlled by the ratio p/ζ. The interaction between p and ζ is generally not viewed as a serious problem for structural identification from earthquake records. Reasonable ranges for values of damping for a given structure are often known a priori, so it is usually easy to detect abnormally high or low values. Furthermore, the inherent uncertainties in attempting to describe the energy dissipation mechanisms of a real structure by a single parameter often override the effects that parameter interaction may have on estimation of damping values.

3.2 SYSTEM IDENTIFICATION USING THE SAN JUAN BAUTISTA BRIDGE RECORDS

This section is concerned with application of the single input-single output modal minimization algorithm to records of the seismic

response of the San Juan Bautista bridge during the 1979 Coyote Lake earthquake. Most applications of system identification techniques in the past have been related to building dynamics, or to laboratory models of structures, and hence, this application is one of the first instances where such an identification scheme has been applied to the strong-motion records from a bridge. In the initial attempt at using system identification on the San Juan Bautista bridge the recorded ground motions and superstructure responses were rotated into the global X-Y axes system, as defined in Fig. 2.2.

Several runs of the modal minimization program were completed using one-mode matches of displacement ($\alpha_1 = 1$; $\alpha_2 = \alpha_3 = 0$ in Eq. 3.7) and two-mode matches of acceleration ($\alpha_3 = 1$; $\alpha_1 = \alpha_2 = 0$). Fourier spectra of absolute accelerations in the global X and Y directions at the top of bent 5, shown in Fig. 3.1, were used to make initial estimates of 3.17 Hz and 6.0 Hz as the first and second modal frequencies of the bridge.

The outcome of these attempts at model identification were generally disappointing as none of the optimal models produced satisfactory matches to the recorded response time histories. In most cases the optimal measure-of-fit J was found to be greater than approximately 0.6 which, by comparison to results from similar identifications of models of buildings, is judged to be a fairly poor match. Optimal estimates of modal frequencies $\hat{f}_r$, dampings $\hat{\zeta}_r$, and effective participation factors $\hat{p}_r$, and the optimal measure-of-fit J for the time interval 0 to 20 seconds are summarized in Table 3.1.

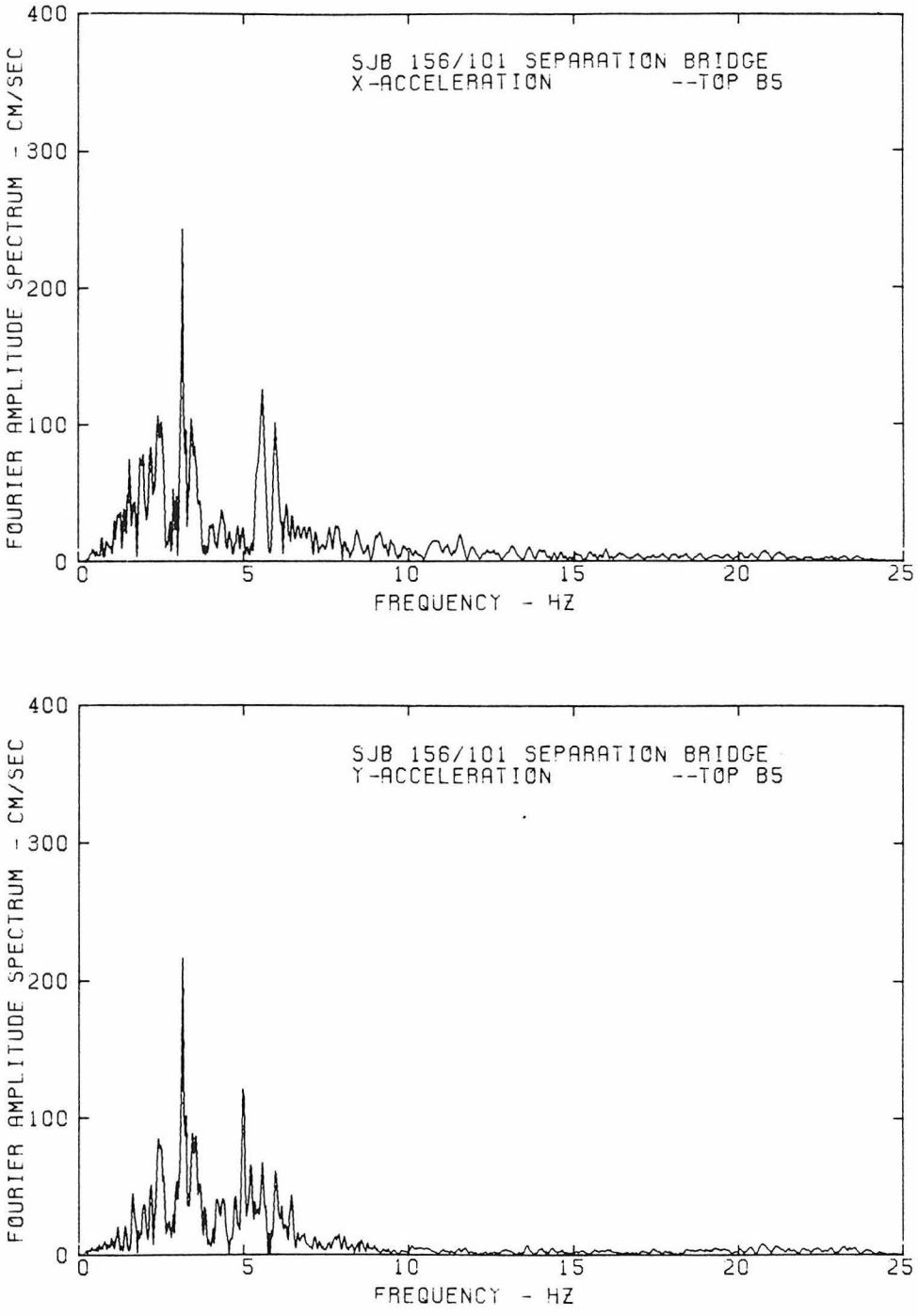

Figure 3.1 Fourier Spectra of Absolute Accelerations at the Top of Bent 5 in the X and Y Directions

TABLE 3.1

Optimal Models Using Global X-Y Records
for the Time Interval 0 to 20 Seconds

Modal Parameters	X-direction		Y-direction	
	1-mode model*	2-mode model**	1-mode model*	2-mode model**
$\hat{f}_1$ (Hz)	3.39	3.38	3.61	3.60
$\hat{\zeta}_1$ (%)	10.4	7.2	12.7	3.7
$\hat{p}_1$	0.84	0.53	0.87	0.31
$\hat{f}_2$ (Hz)		6.17		5.92
$\hat{\zeta}_2$ (%)		4.0		8.3
$\hat{p}_2$		0.50		0.74
J	0.70	.58	0.76	0.65

*1-mode models are displacement matches
**2-mode models are acceleration matches

The one-mode displacement matches in the X and Y directions have modal frequencies within about 7% of each other, and the damping values demonstrate a general consistency of being moderately high at 10% to 13%. On the other hand, although the first modal frequencies of the two-mode acceleration matches are in general agreement with the values found by displacement matching, the damping values are substantially different in both directions. Based upon these observations, the reliability of the estimates in Table 3.1 is open to some question.

Before proceeding with another approach to the use of system identification on these records, it is instructive to examine a single case from Table 3.1 in more detail. The optimal one-mode displacement match for the X-direction in Table 3.1 is shown in a comparative plot in Fig. 3.2. The observed relative response is shown by a solid line; the one-mode model response as a dashed line. The model appears to identify the higher frequency content of the relative displacement response quite well but does a poor job in capturing the long-period component; hence, the large J value of 0.70. Inclusion of a second "mode" with optimal parameters $\hat{f}_2 = 0.318$Hz, $\hat{\zeta}_2 = 8.1\%$, $\hat{p}_2 = .090$ improves the match considerably, as illustrated in Fig. 3.3, with a consequent reduction in J to a value of 0.31.

While the two-mode match appears to be a better representation of the response, evidence presented in Chapter II has indicated that the presence of motion with a period of about 3 seconds appears to be a result of a surface wave travelling across the bridge site. Also, three seconds is an unreasonably long period for such a bridge. The parameters associated with $\hat{f}_2 = 0.318$ Hz are therefore not considered to be a modal response, but rather, an imposed, pseudostatic deformation.

Since the real aim of using system identification techniques is to extract information on the dynamics of the structure, the artificial mode that was added to account for the long-period component really does not contribute to an understanding of the structural behavior. In the following section some refinements are introduced in the application of

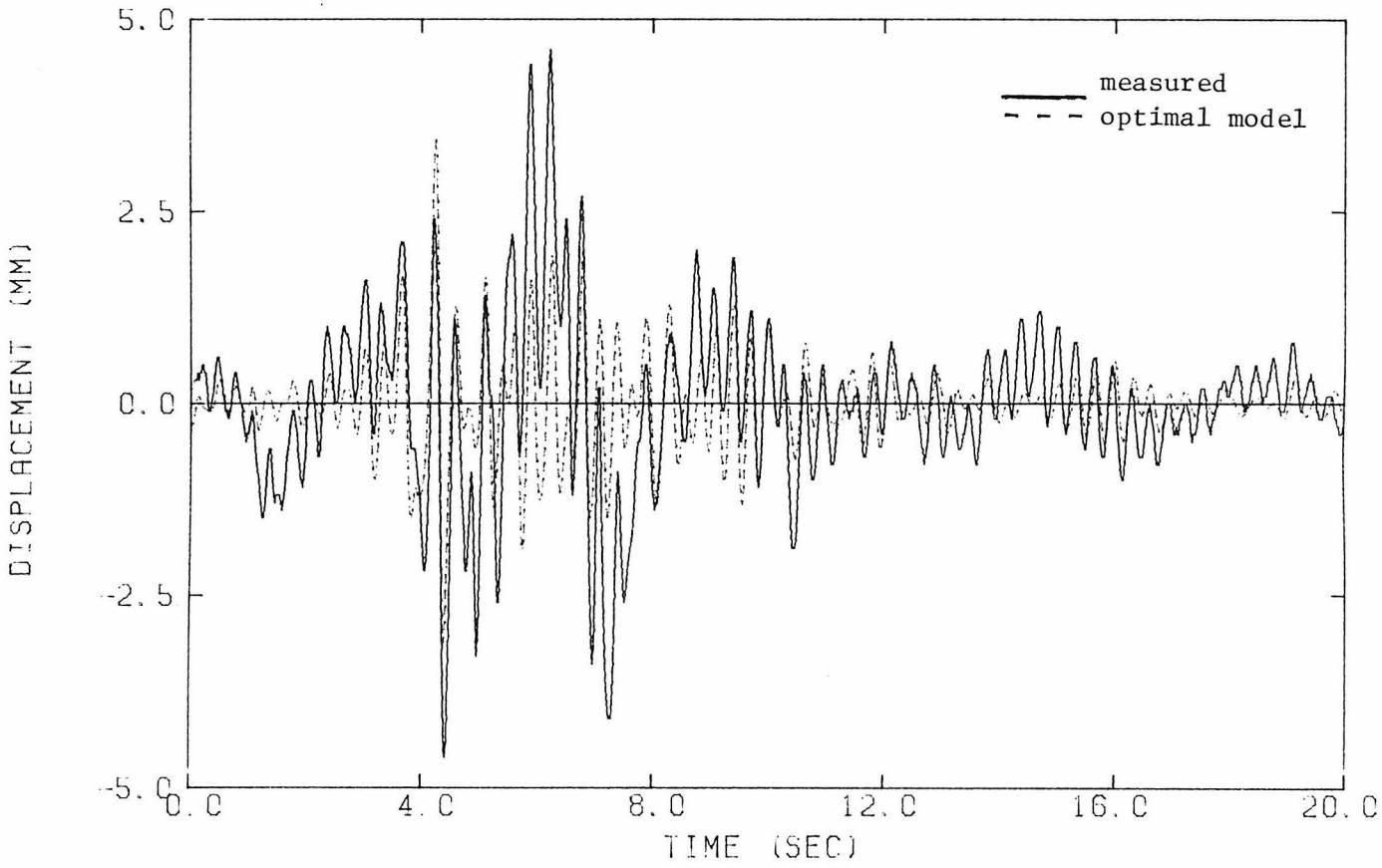

Figure 3.2 Relative Displacements for a One-Mode Displacement Match of Response in X Direction at Top of Bent 5

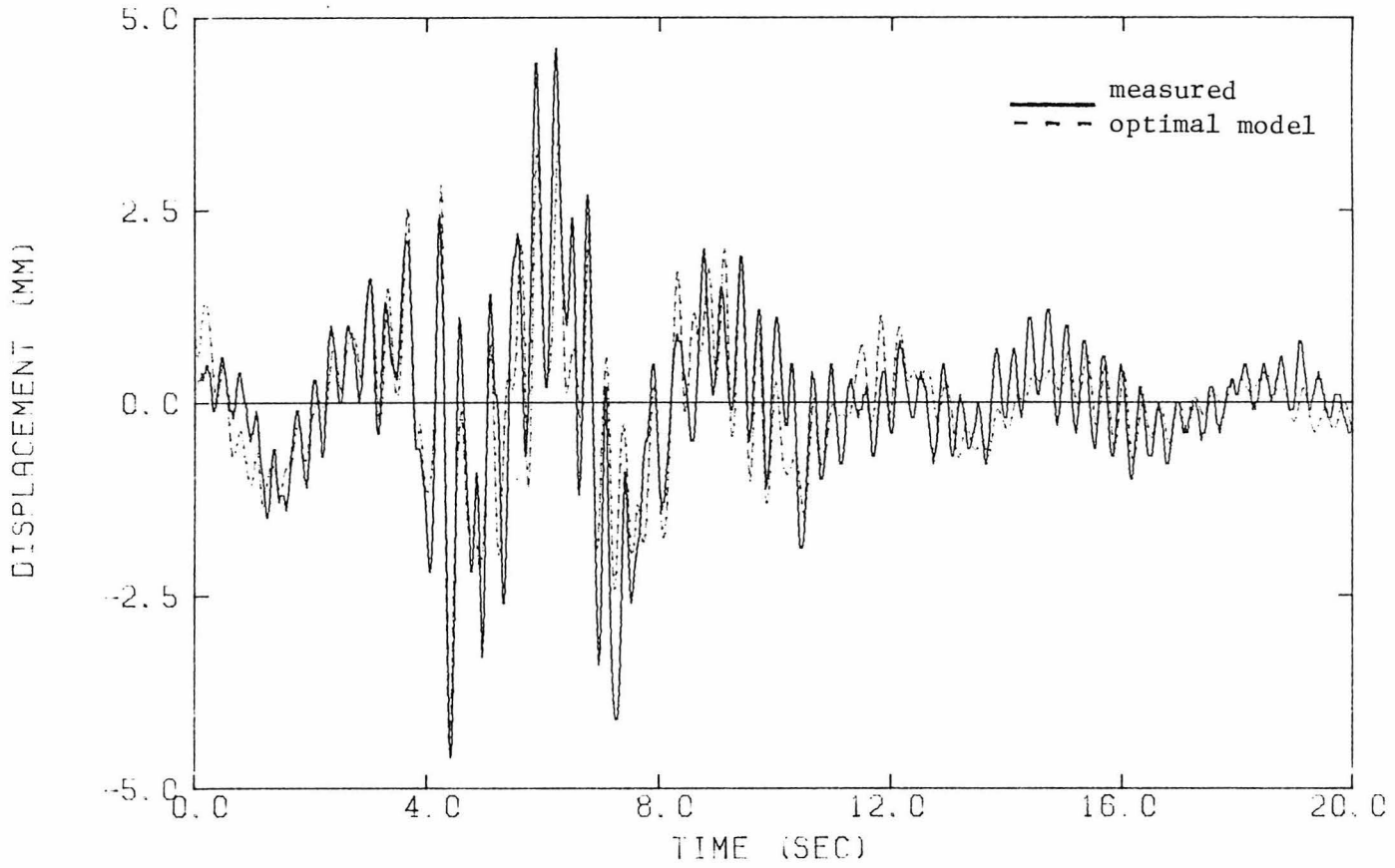

Figure 3.3 Relative Displacements for a Two-Mode Displacement Match of Response in X Direction at Top of Bent 5

the system identification technique to the bridge response records. These refinements lead to much better estimates of the modal parameters.

3.3 OPTIMAL MODAL PARAMETERS OF THE SAN JUAN BAUTISTA BRIDGE

The preliminary system identification analysis, summarized in Table 3.1, demonstrated that long-period motions (apparently due to multiple-support excitation by surface waves) had a significant influence on the ability of the identification procedures to achieve a reasonably good measure-of-fit J and simultaneously yield physically meaningful modal parameters. Additionally, for the cases investigated, it was not possible to achieve stable and reliable estimates of optimal parameters.

Another problem occurred with the orientation of the records. Rotation of the strong-motion data from the original recording orientations into the global X-Y coordinate system initially appeared to be a logical choice for system identification procedures as motions in these directions describe the longitudinal and transverse responses of the bridge as a whole. However, the system identification showed that the motions in the global X-Y system may have been coupled, a situation which is more complicated than can be handled by a single input-single output analysis.

Four refinements were introduced in applying the modal minimization approach to the San Juan Bautista bridge data in an attempt to improve the estimation of parameters of the dominant modes of response. The four refinements are:

(1) Since the fundamental frequency of the bridge is well above 1 Hz (Fig. 3.1), it was decided to high-pass filter all input and response data to eliminate frequency components below 1 Hz. The filtered data contains only frequency components in the range of interest for dynamic structural response.

(2) To reduce the effects of directional coupling in the bridge response records it was decided to use the records as originally recorded at the bridge site. That is, the components shown as channels 1,2,3,... on Fig. 2.2 were used. The directions of original recordings on Fig. 2.2 will be denoted by their true compass bearings for positive motions: N23W for channels 1 and 4; and N67E for channels 3 and 5.

Visual comparisons of the Fourier amplitude spectra in Fig. 3.4 with previous data for components in the X-Y system show that there is a distinct separation of frequency components when the N23W and N67E directions are used. This distinct separation is not evident in the X-Y directions; it indicates the presence of modes vibrating primarily in the original skew directions.

(3) A problem in application of the output-error technique is ensuring that the global minimum of J has been found during the nonlinear optimization. It is possible that a mode may be missed if the initial frequency estimate used to start the modal sweeps is not sufficiently accurate. To circumvent such a problem, preliminary calculations of the measure-of-fit J were made for a range of initial period values for both the N23W and N67E data sets. These calculations provided an easy and reliable aid for obtaining good initial estimates for

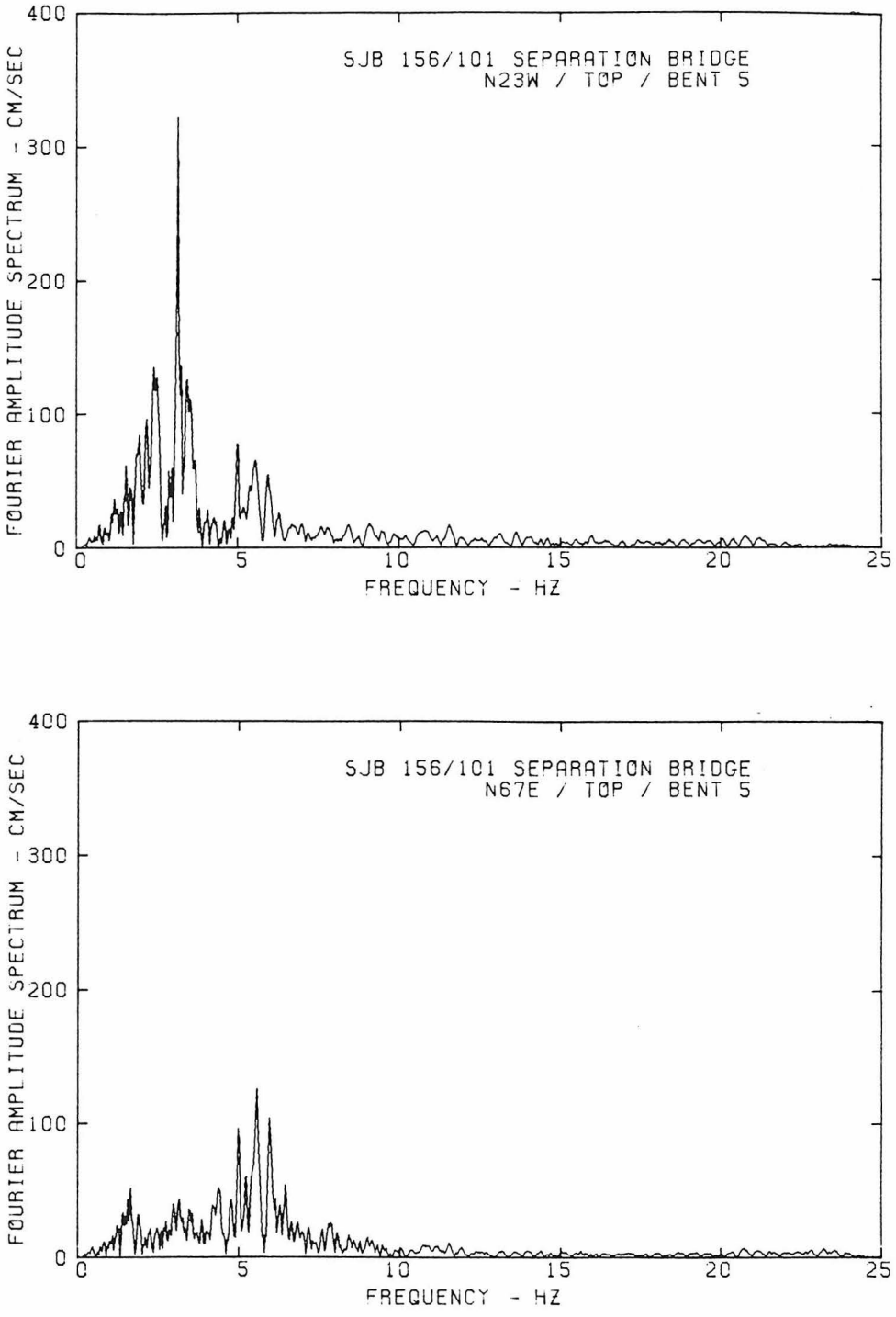

Figure 3.4 Fourier Spectra of Absolute Accelerations at the Top of Bent 5 in the N23W and N67E Directions

the frequencies of the dominant modes of response. A more sophisticated approach, not undertaken here, would be to use computer graphics to plot the surface defined by J in the f-ζ space.

(4) The analyses were extended to examine the time variation of modal properties during the earthquake by using a 4-second moving window. This technique helps identify any significant changes in modal properties during the duration of the response; for example, such as caused by sudden freeing of an expansion joint or onset of structural damage.

3.3.1 Time-Invariant Models

Incorporating modifications (1), (2) and (3) above, one-mode optimal models were determined by separate matches of displacement, velocity and acceleration over the time interval 0 to 20 seconds. Initial estimates of the modal frequencies were obtained by evaluating the measure-of-fit J for displacement matches over a range of frequencies at a fixed value of 5% damping. A sample plot of the measure-of-fit J as a function of period is shown in Fig. 3.5 for the N23W direction. From these evaluations, good initial estimates for modal periods are: 0.30 sec (3.33 Hz) for the N23W direction and 0.15 sec (6.66 Hz) for the N67E direction. These estimates are consistent with the frequency region in which the Fourier amplitude spectra (Fig. 3.4) have maximum amplitudes and are similar to the estimates used in section 3.2.

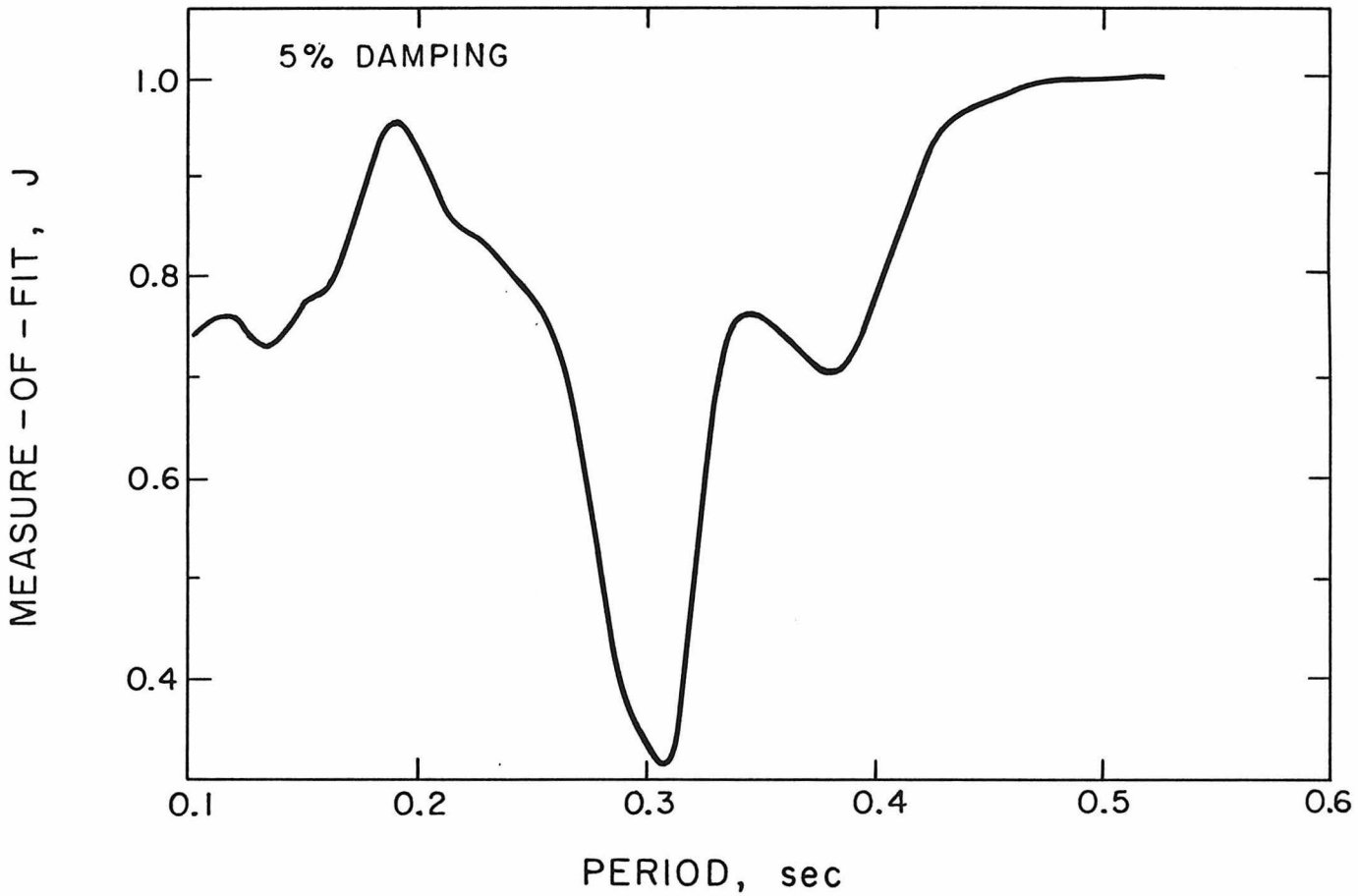

Figure 3.5 A Profile of J vs Model Period for a One-Mode Displacement Model Using N23W Response at Top of Bent 5

The separate identifications made for motions perpendicular to the bents (N23W, using filtered data of channels 1 and 4), and in the plane of the bents (N67W, using filtered data of channels 3 and 5) are summarized in Table 3.2.

TABLE 3.2

Optimal Time-Invariant One-Mode Models
Using Filtered Data in the N23W and N67E Directions

Direction	Match	$\hat{f}$ (Hz)	$\hat{\zeta}$ (%)	$\hat{p}$	$(\hat{p}/\hat{\zeta}) \times 100$	J
N23W	Displ.	3.50	11.0	1.24	11.3	0.13
	Velocity	3.47	10.3	1.13	11.0	0.21
	Accel.	3.46	8.7	0.92	10.6	0.40
N67E	Displ.	6.33	10.2	1.11	10.9	0.37
	Velocity	6.33	10.0	1.13	11.3	0.29
	Accel.	6.21	7.5	0.88	11.7	0.40

Optimal estimates of modal frequencies from both sets of data are clearly consistent for matches of all three response quantities, thereby providing a strong measure of confidence that they are reliable optimal values for the first two dominant modes of response.

In both directions, the variation in damping among the three matches is about 2½% of critical, with displacement matches giving the highest values in each case. It is noted, however, that the ratio $\hat{p}/\hat{\zeta}$

is approximately constant (variation is less than 8% in each direction) indicating that the individual variations in $\hat{\zeta}$ and $\hat{p}$ are likely due to interaction between the two parameters. This interaction is most likely the reason for a value of $\hat{p}$ less than 1.0 for acceleration matching in the fundamental mode in Table 3.2.

The accuracy of the match as judged by the measure-of-fit J ranges from a very good match (J = 0.13) of displacements in the N23W direction to several significantly poorer matches where J is greater than 0.3. It is interesting to note that the best fit in the N23W direction was obtained using displacements, while velocity matching worked best in the N67E direction. Acceleration matches gave identical J values in both cases. Figures 3.6 and 3.7 show the excellent agreements achieved for N23W displacement matching and N67E velocity matching, respectively. Despite the fact that different response matchings were used in the two directions, all three response quantities in Figs. 3.6 and 3.7 match very well over the entire 20 second duration.

The lower J values for N23W data as compared to N67E data are rather difficult to explain. One possible reason is that the dynamic response of the bridge in the N67E direction is not described as well by models of the class given in Eq. 3.2 as are the responses in the N23W direction. It is also possible that a higher mode, which would appear more strongly in the acceleration trace, is causing the larger J in the N67E direction. Another factor which may contribute is the difference in the signal-to-noise ratios in the N23W and N67E responses. In the N23W direction the peak relative displacement is about 5 mm, whereas in

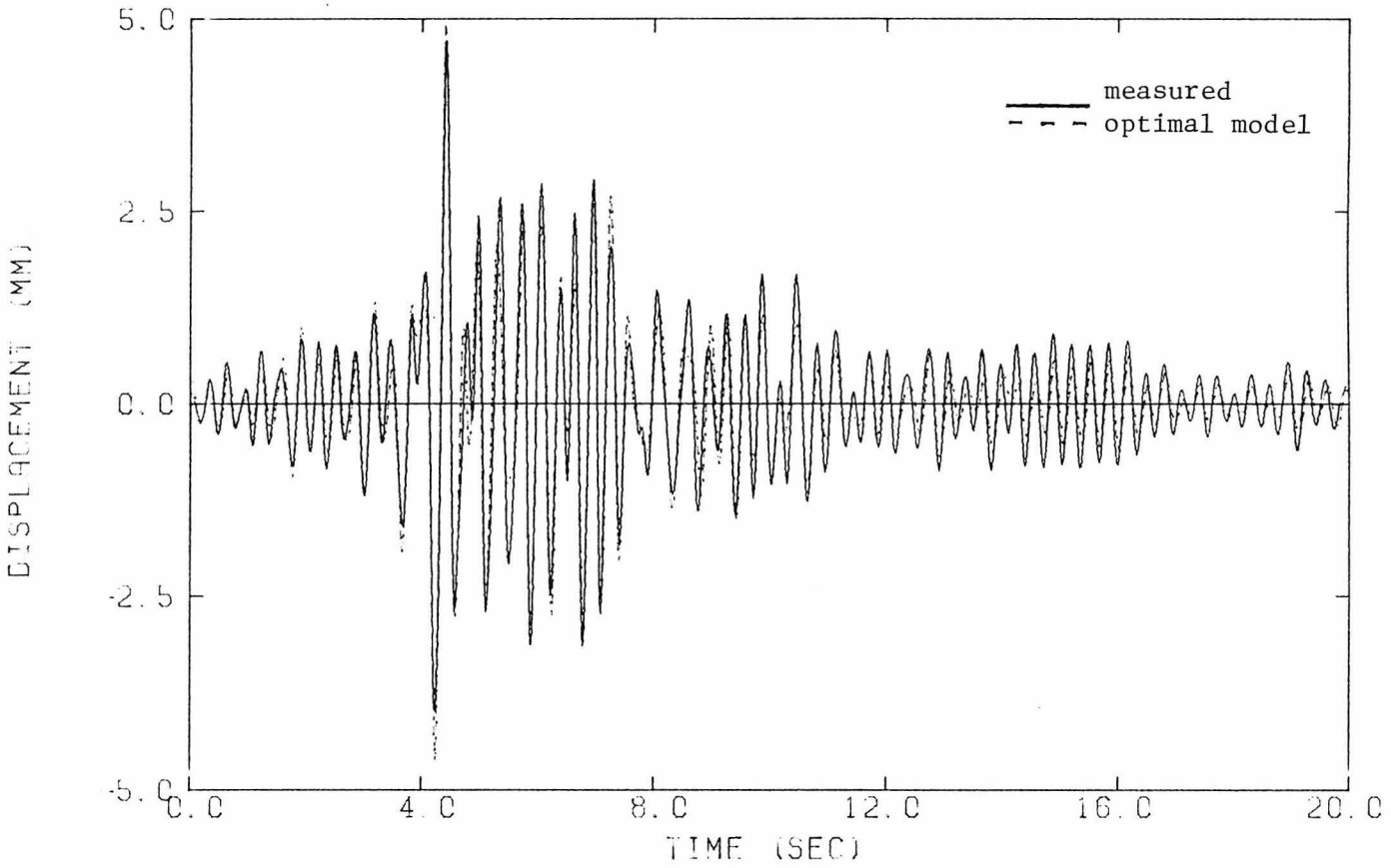

Figure 3.6a Relative Displacements for an Optimal One-Mode Displacement Match of N23W Response at Top of Bent 5

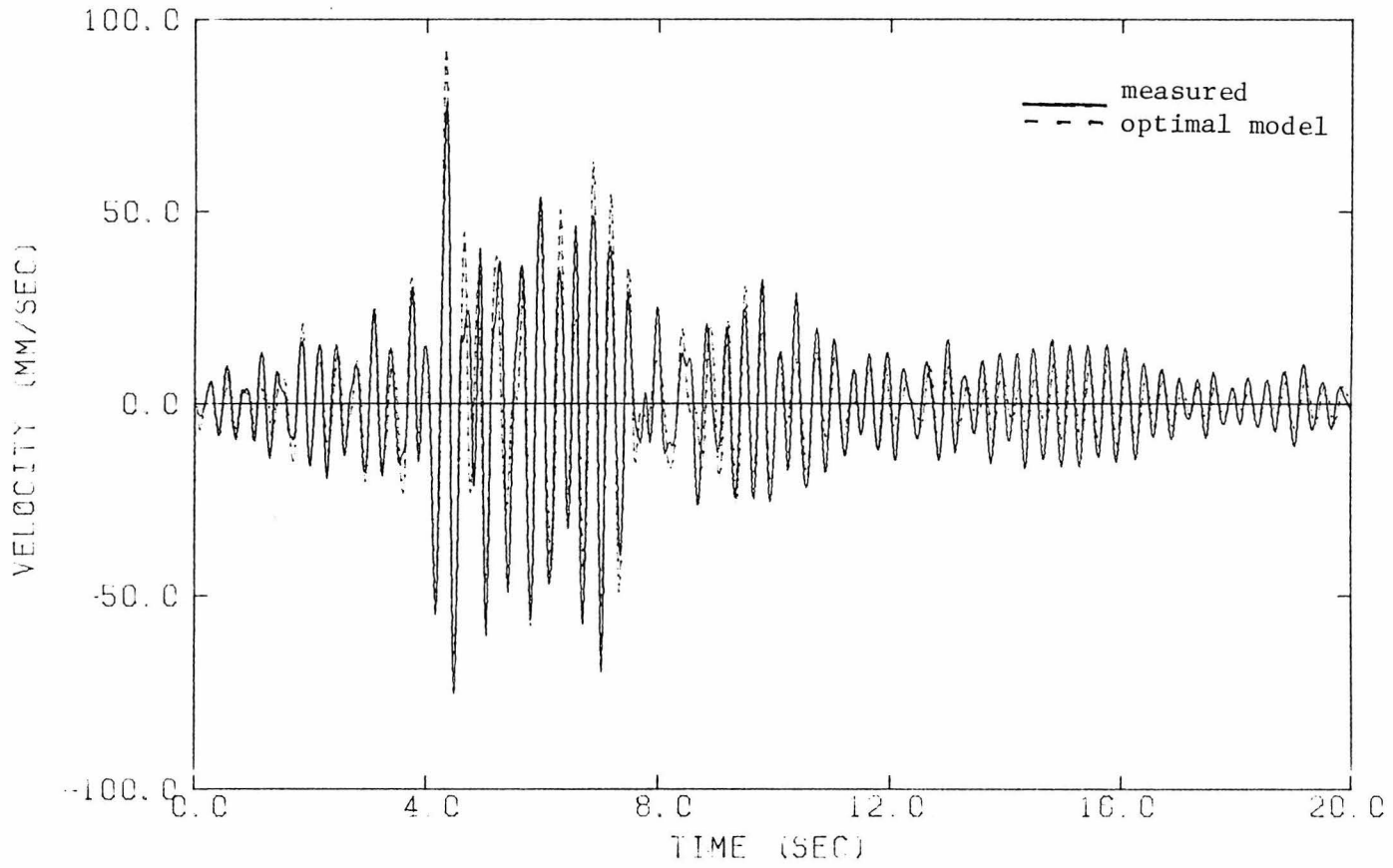

Figure 3.6b Relative Velocities of the Same Model as in Fig. 3.6a

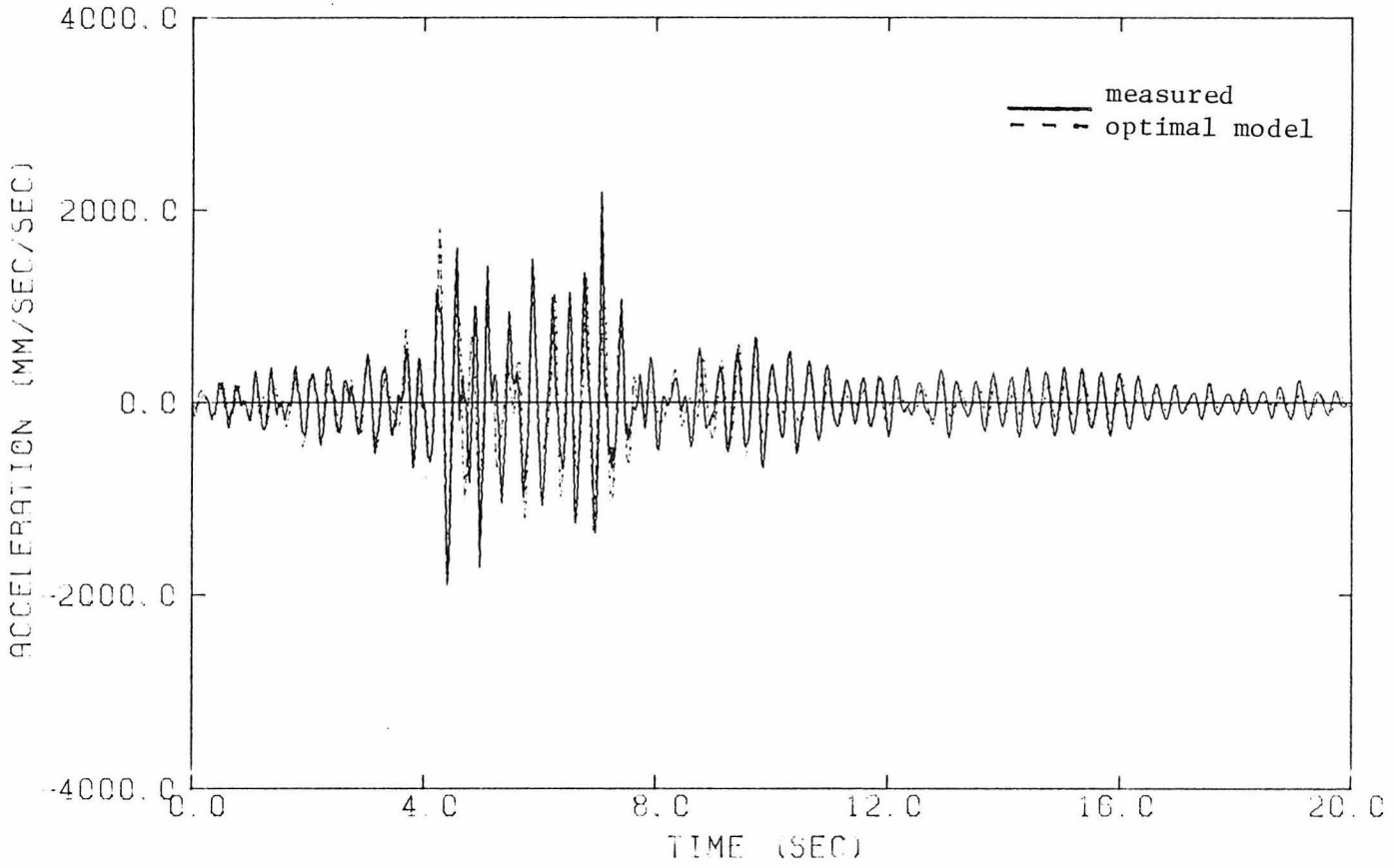

Figure 3.6c Relative Accelerations of the Same Model as in Fig. 3.6a

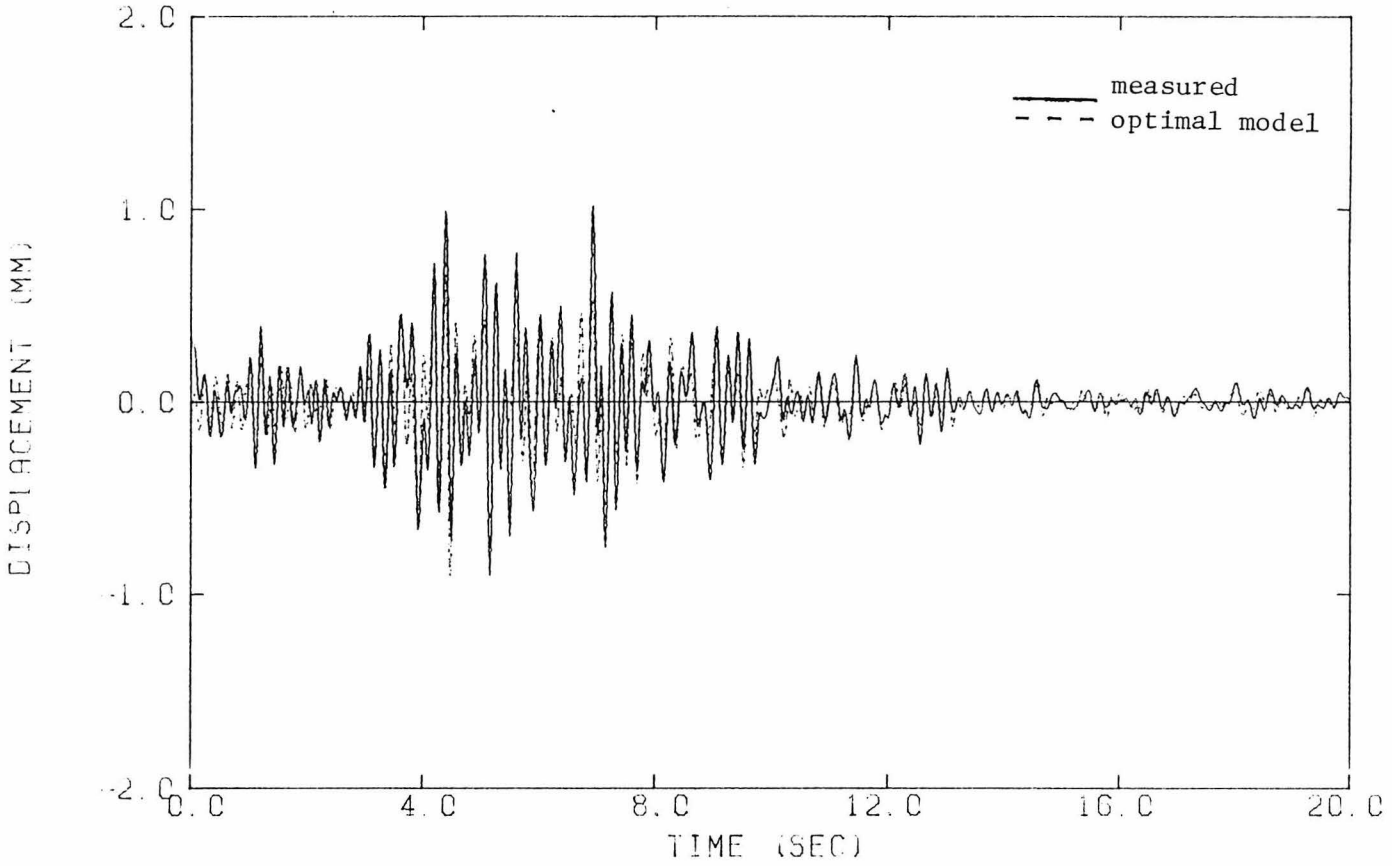

Figure 3.7a Relative Displacements for an Optimal One-Mode Velocity Match of N67E Response at Top of Bent 5

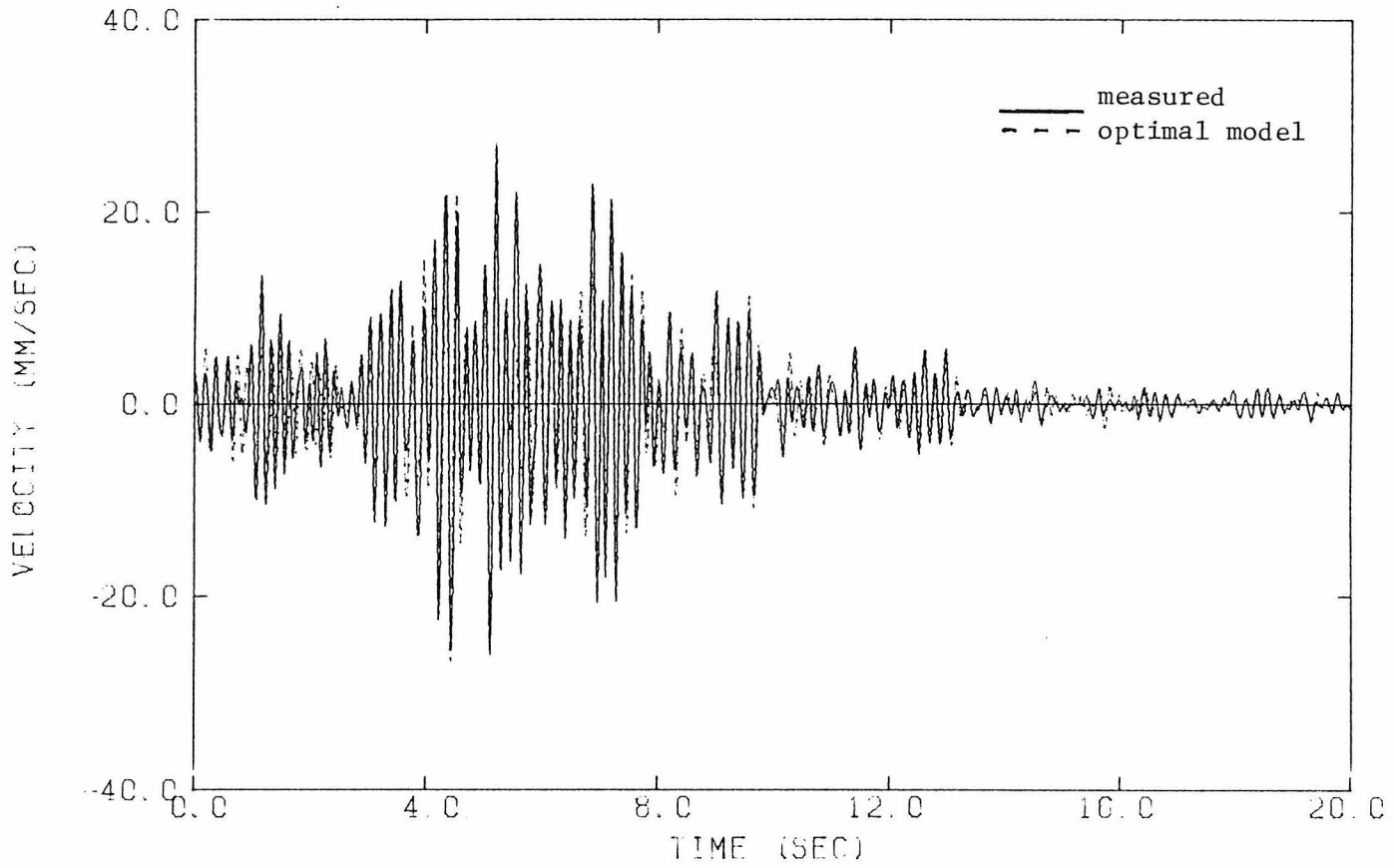

Figure 3.7b Relative Velocities of the Same Model as in Fig. 3.7a

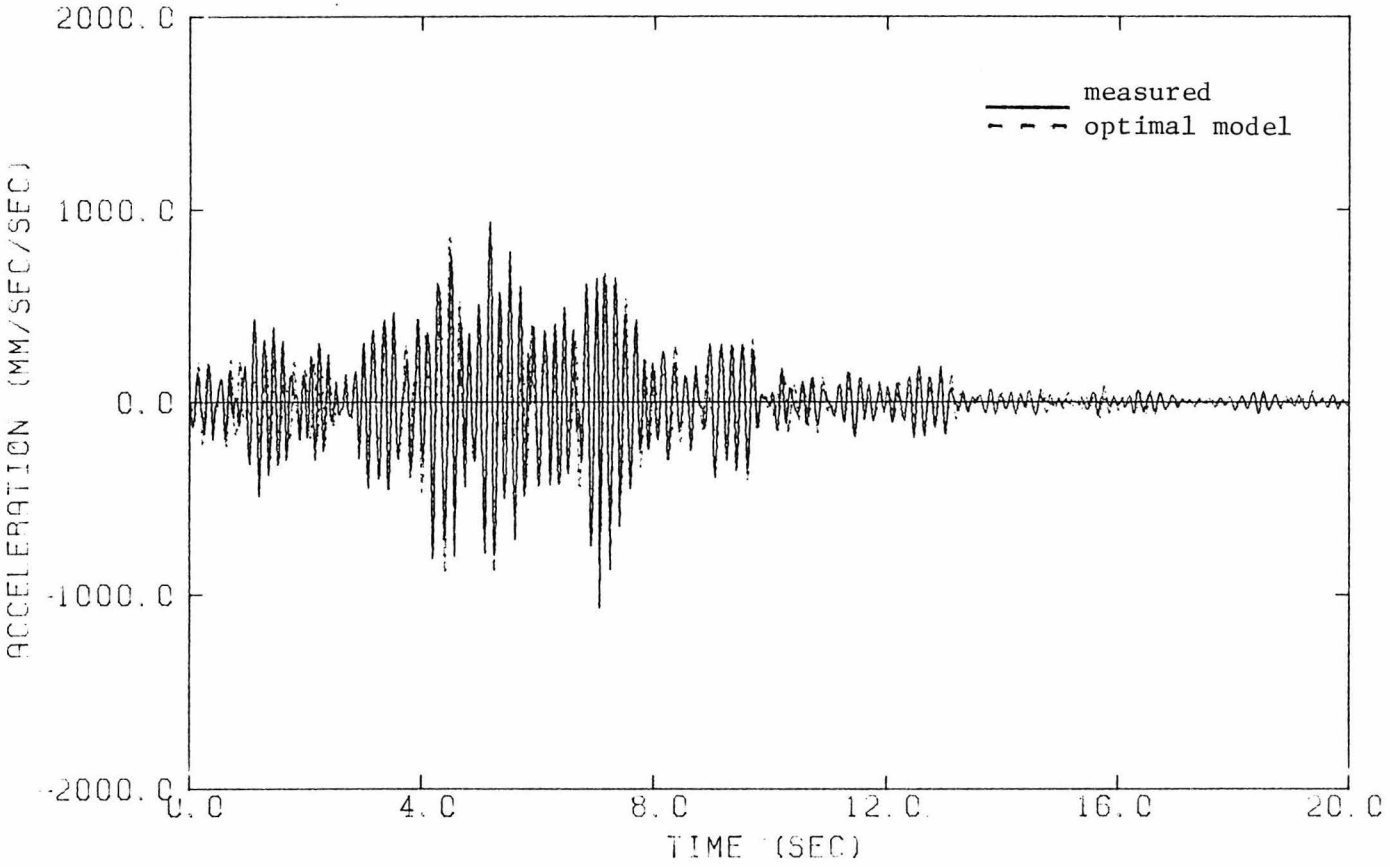

Figure 3.7c Relative Accelerations of the Same Model as in Fig. 3.7a

the N67E direction it is only approximately 1 mm. These factors may limit the accuracy of the determination of modal parameters in this direction.

3.3.2 Time-Varying Models

To investigate the possibility of changes occurring in the stiffness of the San Juan Bautista bridge during the earthquake, optimal linear models were determined for five successive time segments, each of four seconds duration. Changes in modal parameters from one time segment to the next provide an indication of changing structural properties. For this purpose, modal minimization in the time domain as proposed by Beck (1978) is preferrable to a similar approach in the frequency domain (McVerry, 1979) because of the limited resolution possible when short time segments are transformed to the frequency domain.

To obtain the most accurate assessment of the time variation of modal parameters, results from section 3.3.1 were used to select the type of match most likely to produce minimum values of J. For the N23W components this was displacement matching; for the N67W data velocity matching was used. Optimal modal parameters for nonoverlapping four second windows are presented in Table 3.3 for the N23W direction, and in Table 3.4 for the N67E direction.

There is a clear indication from these results that the frequencies of the two identifiable modes experienced a gradual decrease during the first twenty seconds of the Coyote Lake earthquake. In interpreting

TABLE 3.3

Optimal Time-Varying One-Mode Models
for the N23W Direction (Displacement Matching)

Time Interval (sec)	$\hat{f}$ (Hz)	$\hat{\zeta}$ (%)	$\hat{p}$	J
0-4	3.53	5.4	1.02	0.068
4-8	3.46	12.0	1.25	0.088
8-12	3.45	7.4	1.15	0.124
12-16	3.62	3.5	1.68	0.053
16-20	3.39	3.1	0.96	0.035

TABLE 3.4

Optimal Time-Varying One-Mode Models
for the N67E Direction (Velocity Matching)

Time Interval (sec)	$\hat{f}$ (Hz)	$\hat{\zeta}$ (%)	$\hat{p}$	J
0-4	6.85	13.4	1.44	0.41
4-8	6.21	7.3	0.94	0.22
8-12	6.21	11.0	1.04	0.27
12-16	6.76	12.6	1.61	0.33
16-20	6.13	8.1	0.77	0.40

these results, it should be recalled that the time from 0 to 12 seconds is of greatest engineering significance since it encompasses the interval of strongest response.

In the 12 to 16 second segment of response both modes show an unexpected increase in frequency, but beyond 16 seconds the frequency once again decreases. The increase in frequency in the 12 to 16 second interval is not completely understood. Since the strong ground motion is essentially over after about 12 seconds, it is possible that the low levels of excitation may have caused problems in accurately defining the modal parameters. During the first 12 seconds the change in the two modal frequencies amounts to a 2.3% decrease in fundamental frequency and a 9.3% decrease in frequency of the second mode. These percentage changes are similar to those found for time-varying models of the Union Bank building and JPL Building 180 during the 1971 San Fernando earthquake (Beck, 1978). Both buildings suffered only minor damage to nonstructural components.

The calculated displacements for optimal one-mode time-varying models, determined by matching displacements over four second segments, are compared with the measured responses in Fig. 3.8 for the N23W direction. A comparison of velocities is made in Fig. 3.9 for velocity matching of the N67E component.

Damping for the N23W response shows a large increase during the strongest segment of motion, the interval from 4 to 8 seconds. Over this time the damping approximately doubled from the initial value of 5.4% during the first four seconds. After the segment of strongest

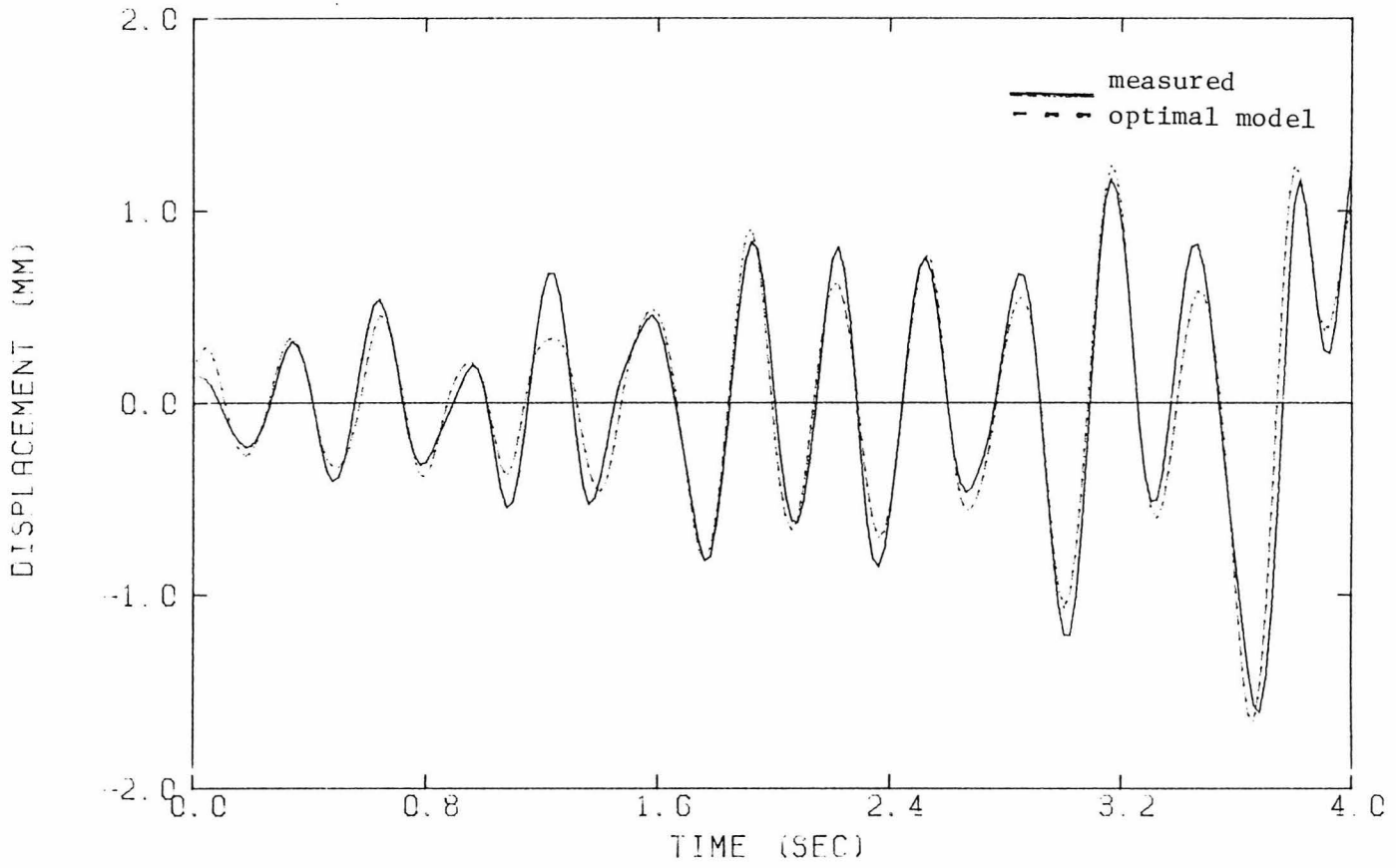

Figure 3.8a Relative Displacements for an Optimal One-Mode Displacement Match of N23W Response at Top of Bent 5 Over the Interval 0 to 4 Seconds

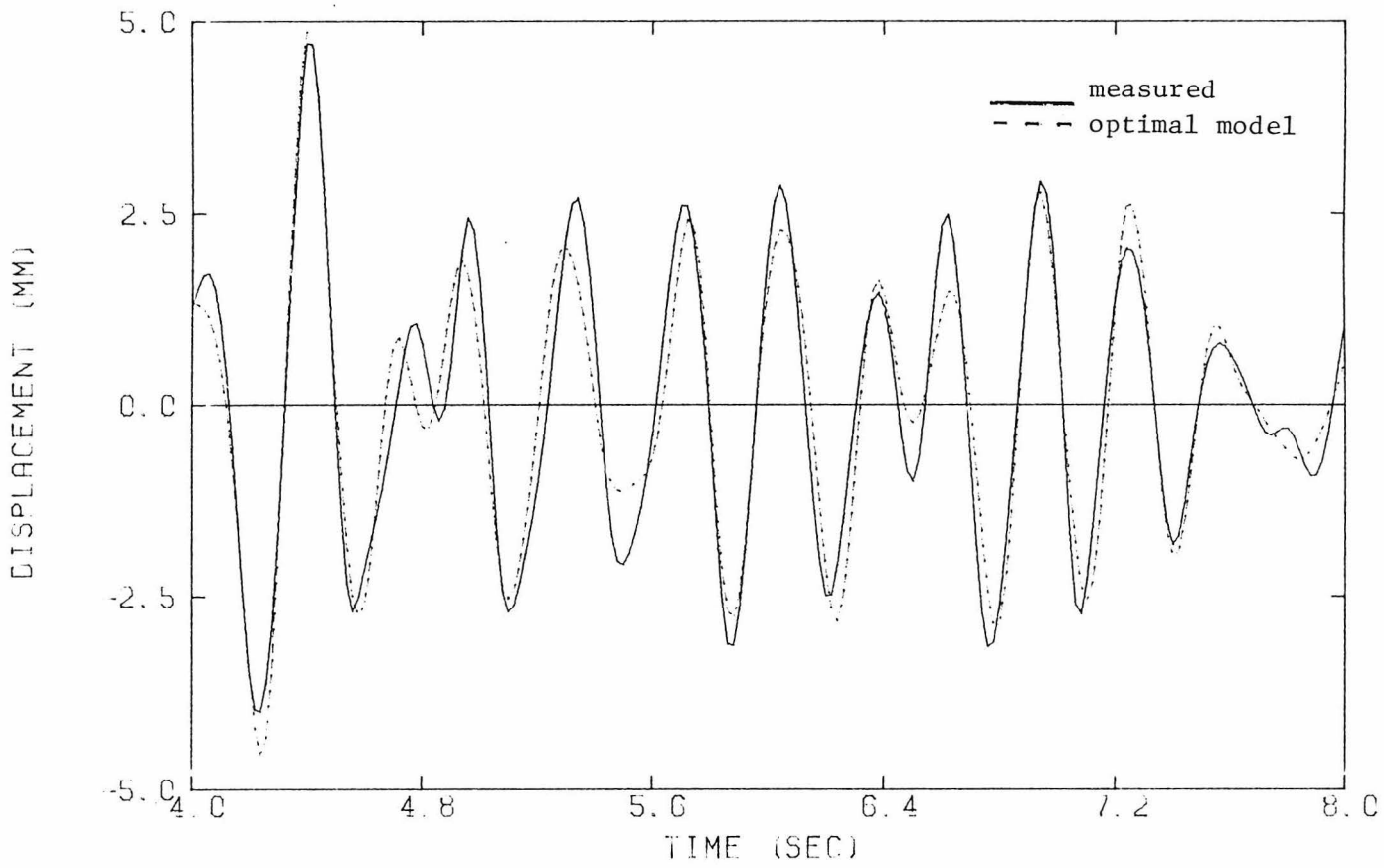

Figure 3.8b Relative Displacements for N23W Response Over the Interval 4 to 8 Seconds

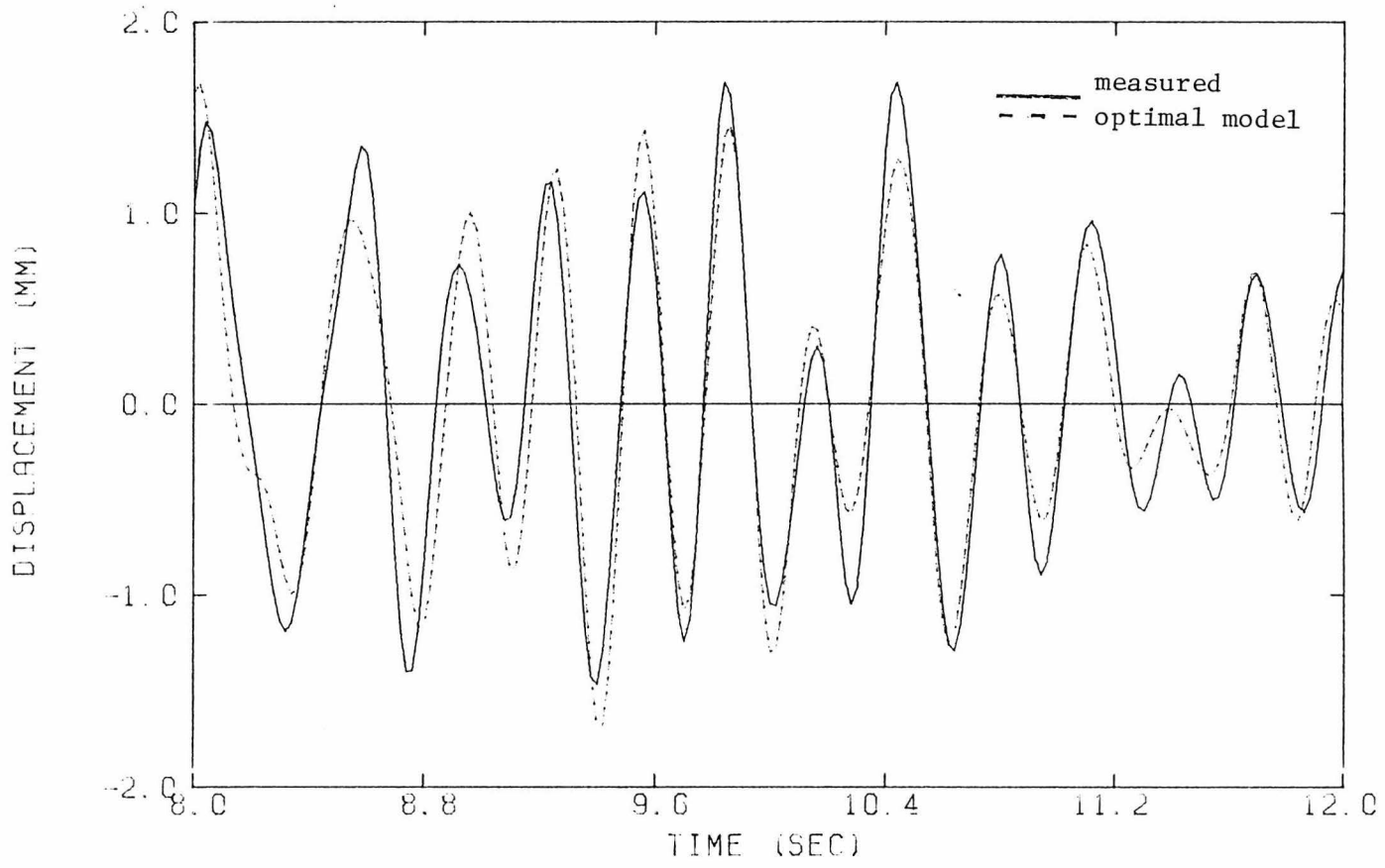

Figure 3.8c Relative Displacements for N23W Response Over the Interval 8 to 12 Seconds

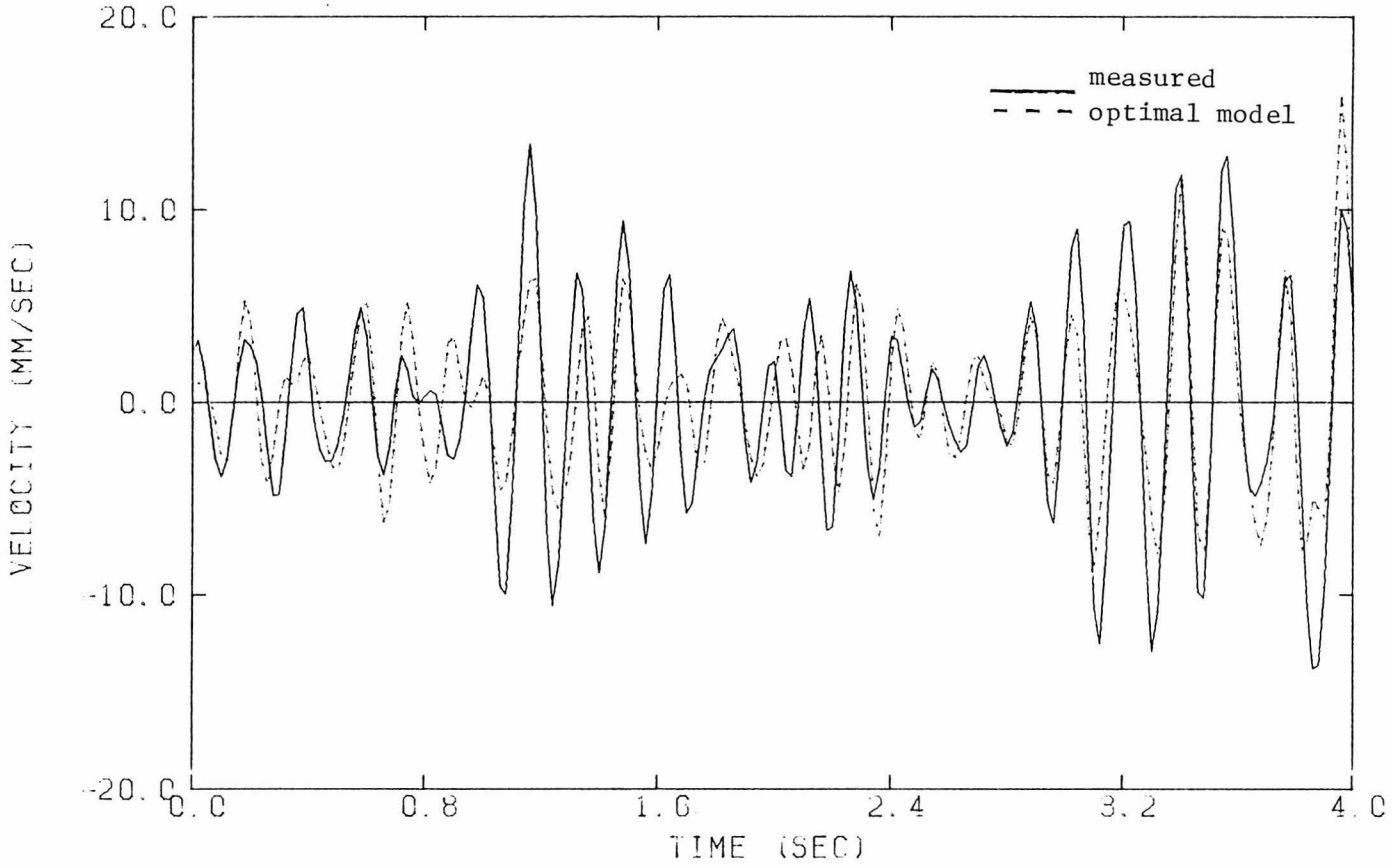

Figure 3.9a Relative Velocities for an Optimal One-Mode Velocity Match of N67E Response at Top of Bent 5 Over the Interval 0 to 4 Seconds

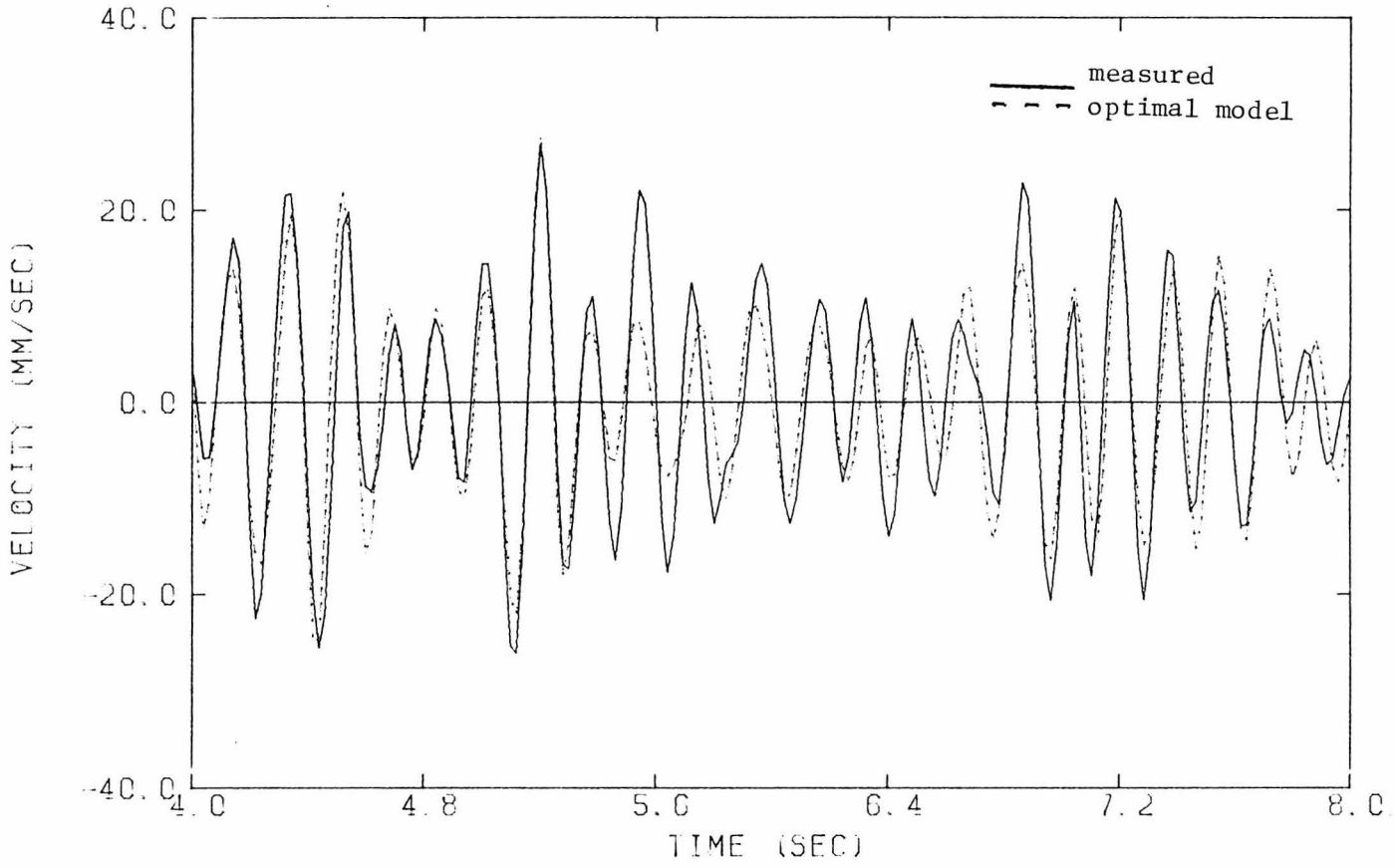

Figure 3.9b Relative Velocities for N67E Response Over the Interval 4 to 8 Seconds

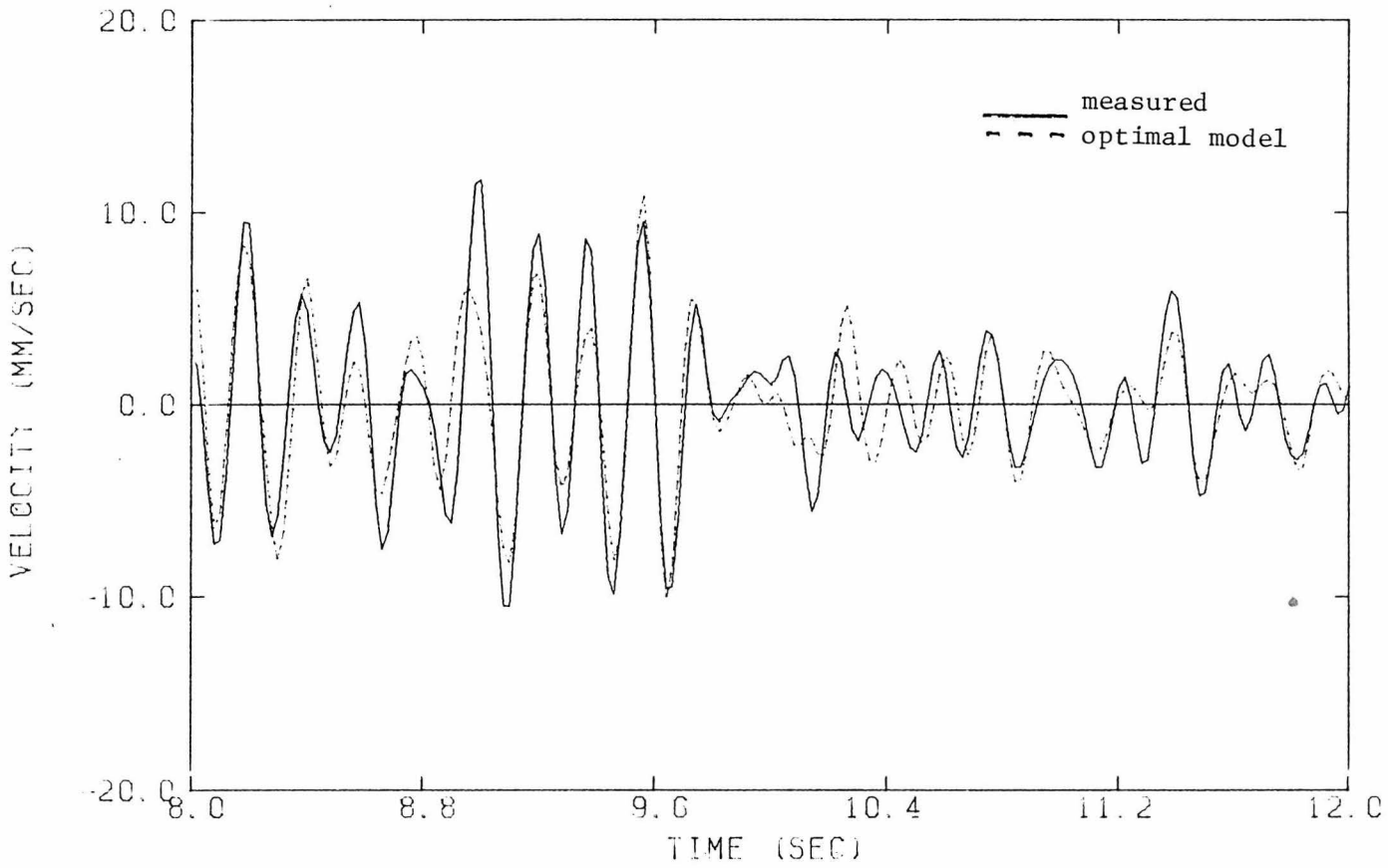

Figure 3.9c Relative Velocities for N67E Response Over the Interval 8 to 12 Seconds

motion, damping values again decreased, as the amplitudes of response diminished. The higher level of damping during the 4 to 8 second segment is an indication that certain energy dissipation mechanisms in the bridge became activated at the higher levels of response, or alternatively, these mechanisms have a nonlinear response with respect to amplitude. Possible mechanisms include some relative motion at the bearings, or increased energy loss with amplitude through soil-structure interaction.

The low-to-moderate levels of end of the N23W record when excitations are fairly low are probably indicative of the damping that would be observed in the fundamental mode of response during ambient or forced vibration testing. Thus, at low levels of dynamic response one might reasonably expect the bridge to be damped at 3% to 6% in the fundamental mode.

The very low measures-of-fit J attest to the exceedingly good matches that were achieved by time-varying modal properties. As a final comment on the N23W response, the modal frequency and damping for the time invariant model (Table 3.2) are very nearly the same as for the 4 to 8 second interval of the time-varying models. One may conclude in this case that the interval of strongest motion exerts a dominant influence on the optimization of a time-invariant model.

Optimal estimates of damping for the one-mode model in the N67E direction, as given in Table 3.4, tend to maintain a consistently high level (e.g., approximately 7% to 13%) throughout the 20 seconds of record. Each measure-of-fit J for the 4-second segments is

substantially higher than for the corresponding N23W response and indicates that optimal parameters for the second mode are not estimated as well as those for the first mode, although the calculated model responses in Fig. 3.9 match the observed bridge response very well.

The 13.4% damping in the first time segment of Table 3.4 seems excessively high. This is thought to be a result of a rapid change in frequency over the first few seconds of response. Since the system identification procedure attempts to find a "best-fit" to the changing frequency, the resulting damping and participation factors will be adjusted to try to make up for deficiencies in the frequency match. The overall effect is to produce a rather poor match over 0 to 4 seconds. This is reflected in the high J value of 0.41.

3.4 SUMMARY

Time-invariant models for the response of the San Juan Bautista bridge were found to work quite well under the following conditions: (1) long-period components were filtered from both input and response data, (2) input and response components were selected to be parallel and perpendicular to the direction of skew of the bents, and (3) reasonably accurate initial estimates of modal frequencies were available. The filtering of long-period components removed contributions from possible differential support motions at frequencies below 1 Hz and thereby "forced" the system identification to iterate to parameters for real structural modes, as opposed to attempting to fit pseudostatic ground motions. A selective choice of the orientation of the data made it

possible to obtain a separation of the effects of modal contributions from the two dominant modes of bridge response. Thus, the N23W component of superstructure response was essentially the response of the bridge in the fundamental mode, while the N67E component was predominantly the second mode.

The results of finding optimal modal parameters for a time-invariant model of the San Juan Bautista bridge indicate that reliable estimates of parameters for two dominant modes can be extracted from the strong-motion data. The optimal estimate of a time-invariant fundamental mode was 3.50 Hz and a second mode was estimated at 6.33 Hz. Both modes are damped at approximately 10% of critical. A three-mode analysis of the bridge was attempted by searching for a mode in the vicinity of the peak at 7.5 Hz on the Fourier spectra in Fig. 3.4, but it was not possible to obtain reliable estimates of parameters for modes beyond the second.

In conclusion, in spite of the observed changes in modal frequency and damping values during the earthquake, time-invariant linear models were able to simulate the response of the San Juan Bautista bridge very well.

CHAPTER REFERENCES

Beck, J.L. (1978). "Determining Models of Structures from Earthquake Records," Earthquake Engineering Research Laboratory, EERL 78-01, California Institute of Technology, Pasadena, California.

Beck, J.L. and Jennings, P.C. (1980). "Structural Identification Using Linear Models and Earthquake Records," International Journal of Earthquake Engineering and Structural Dynamics, Vol. 8, pp. 145-160.

Beck, J.L. (1982). "System Identification Applied to Strong Motion Records from Structures," in Earthquake Ground Motion and Its Effects on Structures, S.K. Datta (ed.), AMD-Vol. 53, ASME, New York.

McVerry, G.H. (1979). "Frequency Domain Identification of Structural Models From Earthquake Records," Earthquake Engineering Research Laboratory, EERL 79-02, California Institute of Technology, Pasadena, California.

McVerry, G.H. and Beck, J.L. (1983). "Structural Identification of JPL Building 180 Using Optimally Synchronized Earthquake Records," Earthquake Engineering Research Laboratory, EERL 83-01, California Institute of Technology, Pasadena, California.

Pardoen, G.C., Hart, G.C., and Bunce, B.T. (1981). "Earthquake and Ambient Response of El Centro County Services Building," Proceedings of the Second ASCE Specialty Conference on Dynamic Response of Structures: Experimentation, Observation, Prediction and Control, G.C. Hart (ed.), Atlanta, Georgia.

CHAPTER IV

DYNAMIC MODELING AND ANALYSIS OF THE SAN JUAN BAUTISTA BRIDGE

The results of Chapters II and III have provided a fairly detailed view of the dynamic response of the San Juan Bautista bridge during the 1979 Coyote Lake earthquake. Seismological investigations significantly aided in the implementation of the system identification procedures leading to the reliable identification of the first two modes of bridge response. In the present chapter the results from Chapters II and III are utilized, along with the original strong-motion records, to synthesize a realistic dynamic model of the bridge. Such a synthesis is a natural and important continuation of the research of previous chapters because it allows comparison of the computed response of a mathematical idealization of the structure with that observed during an earthquake. In a much broader context, the successful modeling of one type of bridge structure, such as the San Juan Bautista bridge, provides valuable knowledge and experience for predicting the earthquake response of other similar bridges. Systematic examination of the seismic response records is particularly important because so few bridges are instrumented to measure strong-motion response.

A finite element model of the San Juan Bautista bridge (model I), synthesized from the structural geometry and material properties of the bridge is presented in this chapter. The model includes an allowance for soil-structure interaction. Comparison of the dynamic response predicted by the model with the response observed during the earthquake

reveals a significant deficiency in the model which is attributed to dynamic behavior of the expansion joints. A second model (model II) with revisions to the expansion joints and soil-bridge interaction effects, predicts the first two horizontal modal frequencies in excellent agreement with the optimal values found by system identification procedures.

4.1 A FINITE ELEMENT MODEL OF THE BRIDGE

Bridges such as the San Juan Bautista bridge are well-suited to dynamic analysis by the finite element method wherein complex structural features such as skewed supports and abutments, expansion joints, multi-column bents and soil-bridge interaction can be incorporated into the model. While analytic models may serve adequately for continuous types of bridge construction, the complicating effects mentioned previously, especially the presence of many expansion joints in some bridges, generally makes the use of analytic models rather unwieldy.

4.1.1 Model Synthesis: Model I

A three-dimensional finite element beam model of the San Juan Bautista bridge was constructed using the features of the linear elastic finite element program SAP IV (Bathe, et al., 1973). This program (and subsequent versions of it) is a standard computer code for finite element analysis of many structural systems in civil engineering applications.

The superstructure was modeled using a series of beam elements to form each simply-supported span, one end pinned and one end on a roller, in conformity with the boundary conditions existing for each span of the bridge. The supporting bents were modeled as two columns spaced 28 feet apart and connected by a rigid bent cap. The deck-to-bent connection in the model was placed so that the centerline of the deck (the longitudinal axis of the deck beam elements) was connected to the bent cap midway between the columns. The effective column length was taken from the top of the footing to the center of the bearings supporting the deck. The complete finite element model of the bridge is shown in Fig. 4.1. Geometrical and material properties of the structure (as provided by Gates and Smith, 1982b) are summarized in Table 4.1. For the superstructure, the entries in Table 4.1 for areas, moments of inertia and weights/length are total values for each span. For the substructure (the bents) these quantities are for a single column of the bent. The moments of inertia for the superstructure are defined as follows: I_x for torsion of the deck about the X axis; I_y for bending in the vertical plane; I_z for transverse bending. The orientation of the local 1,2,3 axes for the columns is shown in Fig. 4.1 and the respective moments of inertia I_1, I_2, I_3 are defined for torsion about the local 1 axis and for bending about the local 2 and 3 axes. For analysis of the composite deck, the concrete was transformed to an equivalent area of steel using a modular ratio of n=9 ($n = E_{steel}/E_{concrete}$ where $E_{steel} = 4.18 \times 10^9$ lbs/ft^2).

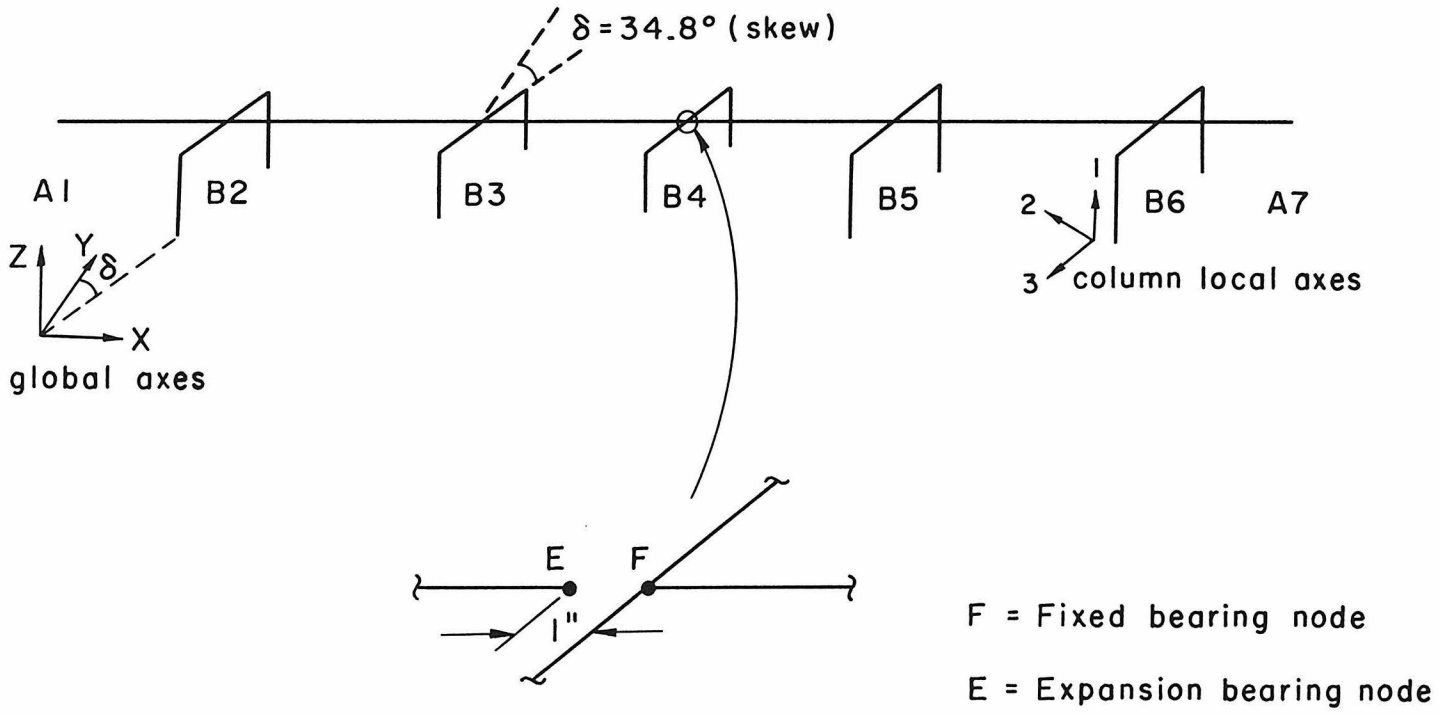

Figure 4.1 Finite Element Model of the San Juan Bautista Bridge

TABLE 4.1

Structural Properties of the San Juan Bautista Bridge

Superstructure

Span	Length (ft)	Area (ft^2)	I_x (ft^4)	I_y (ft^4)	I_z (ft^4)	Wt./Length (lbs/ft)
1	43.5	2.881	0.17	4.55	253.32	3759
2 & 5	68.5	3.158	0.17	6.85	280.58	3895
3 & 4	53.5	2.950	0.17	5.04	260.14	3793
6	33.5	2.881	0.17	4.55	253.32	3759

Substructure

Bent Structure	Length (Height) (ft)	Area (ft^2)	I_1 (ft^4)	I_2 (ft^4)	I_3 (ft^4)	Wt./Length (lbs)
Cap	28	12	19.44	16	9	1800
Columns						
bent 2	21.6					
bent 3	16.7					
bent 4	15.7	12	19.44	16	9	1800
bent 5	22.3					
bent 6	22.1					

Of major significance in determining the dynamic response of a structure is the allowable degrees-of-freedom assigned to each node in the model. The allowable degrees-of-freedom at the abutment nodes and column base nodes are discussed in section 4.1.2 under the topic of

soil-structure interaction. Elsewhere within the structure, six degrees-of-freedom per node were permitted.

The allowable degrees-of-freedom assigned to the ends of the spans (in modeling the expansion joints) requires special discussion. The expansion joints at each bent were modeled by allowing a gap of 0.1 foot to exist between the end nodes of adjacent spans. On all spans, the supports at the left end (orientations as in Fig. 2.2) provide a fixed bearing, having only a rotational degree-of-freedom about the Y axis; the right end support is an expansion bearing having degrees-of-freedom for X translation and rotations about both Y and Z axes. Details of the two bearings are shown in Fig. 4.2. The end nodes on adjacent spans are rigidly linked together to provide continuity across the joint for translations in the Y and Z directions and rotations about the X axis. The foregoing assumptions on the degrees-of-freedom of such bearings are consistent with the assumptions used by Caltrans in their standard dynamic analysis procedures (Gates and Smith, 1982a, 1982b). Hereafter, the above described finite element model of the San Juan Bautista bridge will be referred to as model I.

4.1.2 Soil-Structure Interaction

The earthquake response of all civil engineering structures is influenced, to some degree, by the dynamic characteristics of the soil medium on which the structures are founded. Often, the influence of the soil is judged to be minimal and the base of the structure is assumed to be rigidly attached at the surface of the ground. Earthquake

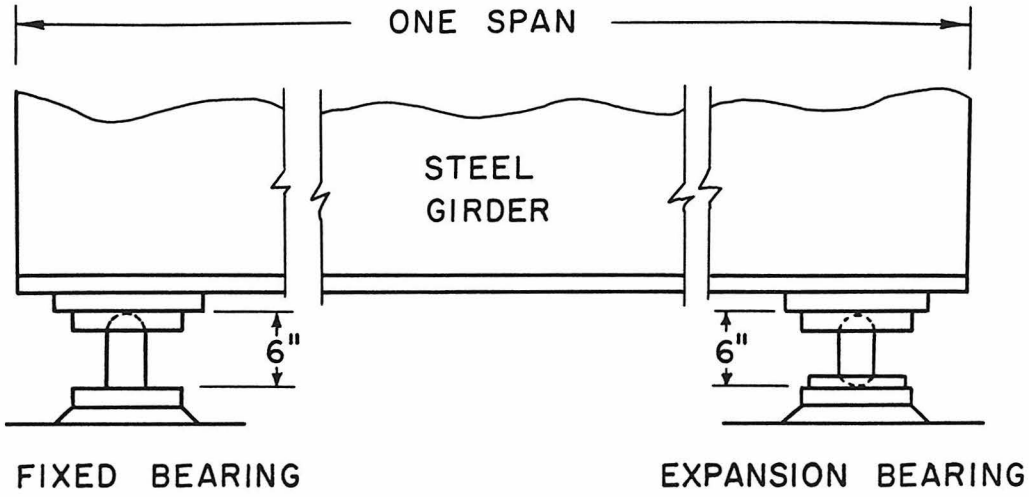

(a) SIDE VIEW

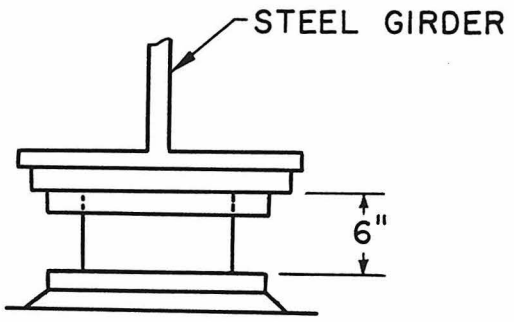

(b) TYPICAL END VIEW

Figure 4.2 Bearing Assemblies on a Typical Span

measurements and other experimental data suggest, however, that in many situations soil compliance can account for a substantial portion of the total response of the structure (e.g., Foutch and Jennings, 1978) and should be considered when accurate response calculations are attempted.

In the past decade or so, many approaches have been suggested to deal with the problem of soil-structure interaction. Often, these are based upon the simplified assumption that the soil can be represented by an elastic half-space (Jennings and Bielak, 1973; Luco and Westmann, 1971; Richart, et al., 1970; Veletsos and Wei, 1971). Veletsos and Wei (1971) and other researchers have examined the case of a rigid circular disc resting on an elastic half-space and have shown that the influence of the half-space may be represented by two pairs of frequency-dependent springs and dashpots; one pair for rotational motions of the disc and the other pair for translational motions. The stiffness and damping coefficients derived from an elastic half-space analysis are dependent upon the frequency of excitation of the disc. In translation, this frequency dependence is very small, but for rocking motions both the rotational stiffness and damping coefficients show a strong dependence upon the frequency. Fortunately, in many practical applications where the significant structural response is confined to the first few modes, reasonable approximations may be made by considering the stiffness and damping coefficients to be independent of the frequency of response.

Using results based upon an elastic half-space analysis, appropriate foundation springs and dashpots, with constant coefficients, may be estimated from a knowledge of the foundation dimensions

(represented by the disc) and the shear modulus and Poisson's ratio for the soil. For the San Juan Bautista bridge, it seems desirable to include the effects of soil-structure interaction by simply adding foundation springs to the finite element model. Because of the limited amount of data recorded at the foundations and on the superstructure, and the lack of abutment and free-field records, a greater complexity does not seem warranted.

Considerations of the geometry of the structure, the relative stiffness of the soil for rocking and for translational motions, and also experimental data from a Nevada bridge test (Douglas and Richardson, 1984) suggest that rocking of the bents about their footings is likely to be the most important feature introduced to the dynamic response of the bridge by a flexible soil foundation. The tendency for rocking of the bents to be accentuated is evident from the results of Chapter III wherein the dominant response of the bridge in the fundamental mode was found to be in a direction perpendicular to the direction of skew of the bents.

To incorporate soil compliance into finite element model I, rotational foundation springs were placed at the base of each column on all five bents, allowing rotation of each column footing about the X and Y axes of the bridge. The foundation dashpots were not included in the model because they were not needed in the subsequent modal analyses. Full base fixity is still assumed for column rotation about the Z axis (torsion) and for base translation along the X, Y and Z directions. The abutments are assumed fixed for all degrees-of-freedom. The arrangement

of soil springs for a single bent is shown in Fig. 4.3. In the finite element model, rotational springs k_θ are aligned along the local 2 axis ($k_{\theta 2}$) and local 3 axis ($k_{\theta 3}$) of each column, which are also the principal axes of the rectangular footings.

Using the results for a rigid disc on an elastic half-space, Veletsos and Wei (1971) express the rocking stiffness of the half-space as

$$k_\theta = \Gamma_\theta \frac{8GR^3}{2-\nu} \tag{4.1}$$

where G is the shear modulus of the half-space material, ν is Poisson's ratio (assumed herein to be $\frac{1}{3}$), and R is the radius of the disc. The Γ_θ is a constant dependent upon a dimensionless frequency parameter

$$a_o = \frac{\omega R}{\beta} \tag{4.2}$$

where ω is the (circular) frequency of excitation and β is the shear-wave velocity of the material in the half-space (see Eq. 2.3). An equivalent radius for rocking for a rectangular footing, based upon a moment of inertia equivalent to the circular disc, is given by

$$R = \left[\frac{ab^3}{3\pi}\right]^{1/4} \tag{4.3}$$

where a is the dimension of the footing parallel to the axis of rotation and b is the length of the other side. Assuming that the soil properties are isotropic it is obvious from Eqs. 4.1 and 4.2 that

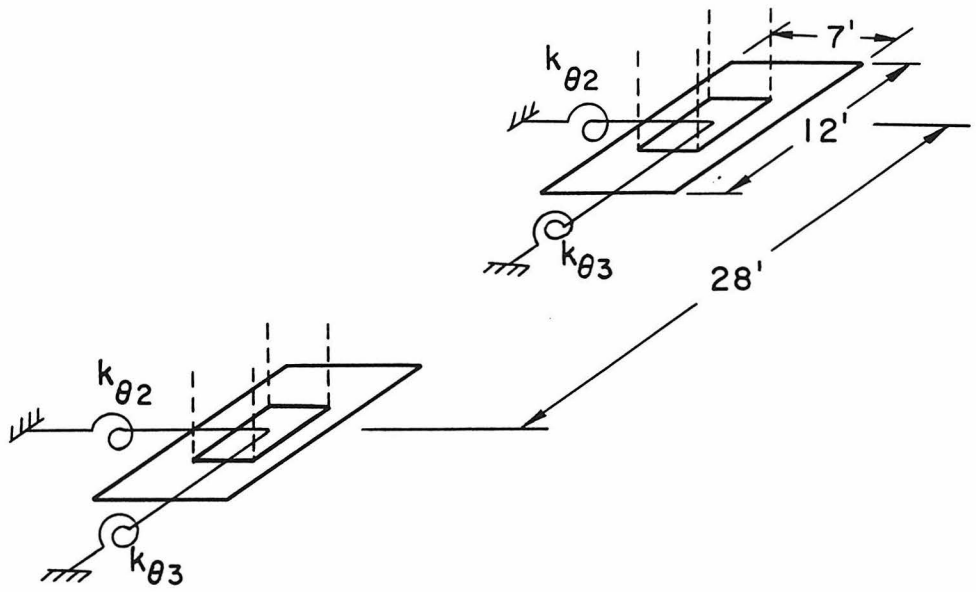

Figure 4.3 Rotational Soil Springs Added to Finite Element Model

$$\frac{k_{\theta 2}}{k_{\theta 3}} = \left[\frac{R_2}{R_3}\right]^3 \qquad (4.4)$$

where R_2 and R_3 are the equivalent radii for rocking about the local 2 and 3 axes, respectively. For the San Juan Bautista bridge R_2 = 6.00 feet and R_3 = 4.57 feet.

To complete the evaluation of foundation stiffness coefficients it is necessary to have available a suitable shear modulus for the bridge site. As cited in a previous section (2.2.1), geotechnical investigations at the bridge location prior to construction indicated standard penetration values of N of about 50. According to Scott (1983), N values in the range of 50 would correspond to a dense soil having a shear-wave velocity of approximately 1500 feet per second. In other studies, test data for soils presented by Okamoto (p. 19; 1973), and SPT tests and shear-wave velocity measurements by Shannon and Wilson Inc., and Agbabian Associates (1980), at selected U.S. sites, indicate a similar shear-wave velocity for soil deposits with N-values of about 50. Thus, an estimated shear-wave velocity of β = 1500 fps was used to compute the shear modulus G via Eq. 2.3 ($G \equiv \mu$ in Eq. 2.3). For the San Juan Bautista bridge, the dimensionless frequency parameter a_o is much less than unity for the values of β and R given above and for ω equal to the fundamental frequency of the bridge, approximately 3.5 Hz. Hence, from Veletsos and Wei (1971), Eq. 4.1 may be used with $\Gamma_\theta = 1.0$ to compute rotational foundation stiffness coefficients for an individual footing. The results are $k_{\theta 2} = 8.40 \times 10^9$ ft-lb/radian and $k_{\theta 3} = 3.71 \times 10^9$ ft-lb/radian.

Finite element model I, together with the rotational foundation springs determined above, is thought to represent the most straightforward, state-of-the-art finite element model for purposes of evaluating the dynamic response characteristics of the bridge. It is consistent with most of the common assumptions made about the behavior of structural components and with the information given in the structural drawings. Furthermore, its complexity is believed to be commensurate with the amount of strong-motion data available to evaluate the realism of the model.

4.1.3 Dynamic Bridge Response Predicted by Model I

Natural frequencies and mode shapes were computed for model I of the San Juan Bautista bridge. Owing to the simply-supported nature of the spans, the vertical modes are uncoupled from the horizontal modes of response. In the horizontal (X-Y) plane coupling is introduced due to the skewed supports and hence, each mode has components in both the X and Y directions. The instrumentation scheme (Fig. 2.2) is much better suited to gaining information on the longitudinal (X) and transverse (Y) responses of the bridge; for this type of bridge, horizontal response is usually of greater concern for earthquake engineering than is vertical response.

The natural frequencies computed for the first seven horizontal modes of model I are given in Table 4.2. Similar information is given for five vertical modes in Table 4.3. Only these modes are presented because examination of the Fourier spectra of the bridge response

TABLE 4.2

Horizontal Modal Frequencies Computed for Model I

Mode	Frequency (Hz)
H-1	2.49
H-2	3.20
H-3	3.70
H-4	3.80
H-5	4.37
H-6	6.74
H-7	8.11

TABLE 4.3

Vertical Modal Frequencies Computed for Model I

Mode	Frequency (Hz)
V-1	5.258
V-2	5.261
V-3	7.317
V-4	7.343
V-5	10.598

indicated very little contribution in either horizontal or vertical directions by frequency components above approximately 10 Hz. The horizontal mode shapes associated with the frequencies listed in Table 4.2 are shown in Fig. 4.4, and the vertical mode shapes are illustrated in Fig. 4.5.

One striking feature of the results in Table 4.2 is that the computed fundamental frequency of 2.49 Hz is substantially below both the peak of 3.16 Hz in the Fourier spectra and the optimal modal frequency determined for the first mode by the system identification procedures in Chapter III. The mode shape in Fig. 4.4 corresponding to 2.49 Hz indicates response, predominantly that of bent 5, with lesser responses at bents 4 and 6. The overall effect is a rather localized modal response, as opposed to a response of the entire bridge. If model I is to emulate the measured seismic response of the bridge adequately, it is necessary to review the manner in which the finite element model was synthesized to determine why the overall stiffness of the model is too low.

For structures such as the San Juan Bautista bridge, the complex assemblage of multi-column bents, deep bent caps, substantial size bearings and a deep girder-and-slab deck structure makes it difficult to define precisely the top of the column, and hence the effective column length that is needed for purposes of dynamic analysis. While the original effective column length, extending to the center of the bearings, appears to be a realistic choice based upon physical grounds, other reasonable alternatives are also possible.

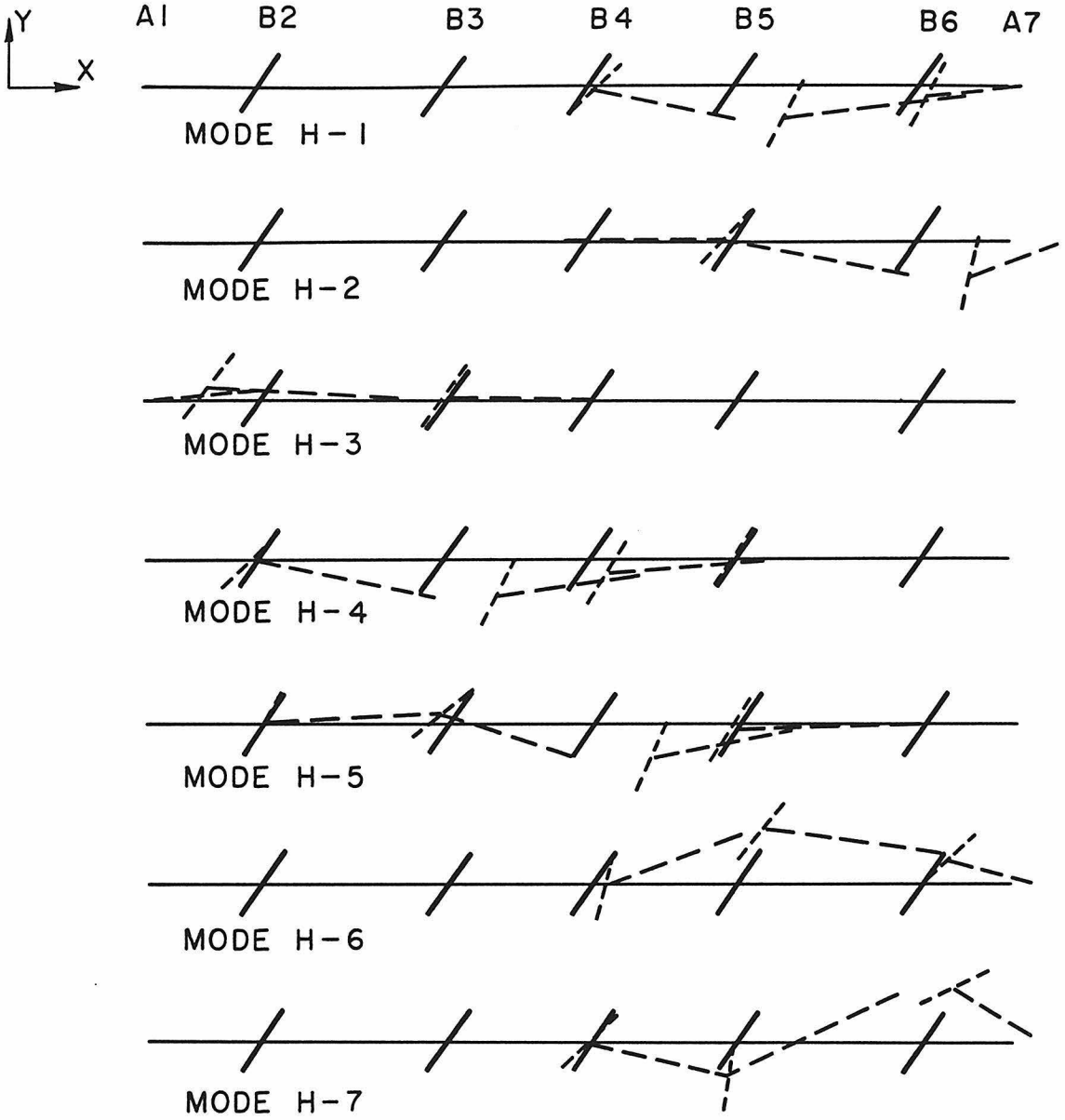

Figure 4.4 Horizontal Mode Shapes for Model I

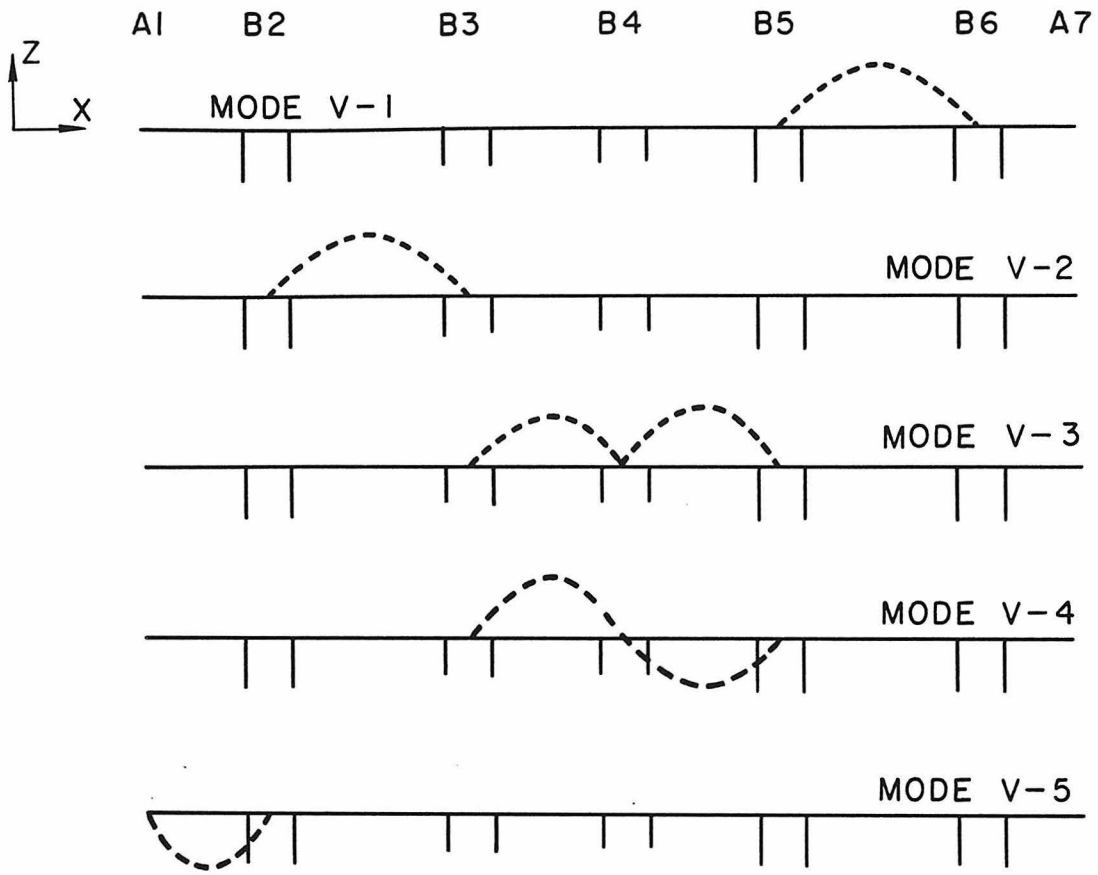

Figure 4.5 Vertical Mode Shapes

In order to bring the dynamic response predicted by model I, closer to the observed earthquake response, the stiffness of the finite element model was changed, increasing the fundamental frequency to 3.16 Hz. This frequency corresponds to the peak in the Fourier spectra for X and Y responses and is comparable to the fundamental bridge frequency found by system identification procedures. The increase in stiffness was achieved by decreasing the effective column heights to the distance from the tops of the footings to one foot beyond the bottoms of the bent caps. This represents a shortening of each column by 3.4 feet from its previous length. The natural frequencies for this modified version of model I are presented in Table 4.4 for the first seven horizontal modes. The mode shapes (not presented here) are virtually identical to those shown in Fig. 4.4.

The development of model I to this stage has assumed that the initial structural idealizations were appropriate for seismic analysis. These idealizations were drawn from the way in which various structural components were expected to behave under dynamic conditions. The uncertainty in the choice of an effective column length was examined, but was found to affect only the values of the horizontal modal frequencies; the column length did not have a significant influence on the calculated mode shapes of the bridge. An examination of the seismic response of the San Juan Bautista bridge shows, however, that its dynamic behavior is substantially different than the response predicted by model I. The main difference seems to arise from the modeling of the expansion joints.

TABLE 4.4

Horizontal Modal Frequencies for a Modified Model I

Mode	Frequency (Hz)
H-1	3.16
H-2	4.03
H-3	4.56
H-4	5.15
H-5	5.99
H-6	8.67
H-7	10.47

The fundamental mode shape predicted by model I, and the earthquake Fourier data at 3.16 Hz are compared in Table 4.5 where both sets of results have been normalized to a unit response in the X direction at the top of bent 5 (location XB5). From this comparison it is evident that the finite element model drastically underestimates the modal amplitudes for location XD5, and makes a major underestimation of the amplitudes at points YB5 and YD5. (XB5 is the X component of channels 4 and 5 on Fig. 2.2; XD5 is the X component of channels 6 and 8. Similar comments apply for Y components). Fourier data from the superstructure response indicate that the X motions of the bent and deck across the expansion joint at 3.16 Hz are nearly identical in both amplitude and phase. This result suggests that the expansion joint is "locked," with

TABLE 4.5

Comparison of Fundamental Modal Amplitudes for Modified Model I and Fourier Spectral Data

Component	Normalized† Fourier Amplitude	Normalized* Modal Amplitude
XB5	1.00	1.00
YB5	0.80	0.47
XD5	0.92	0.18
YD5	1.09	0.74

Notes: (†) from relative acceleration spectra at 3.16 Hz
(*) from modified model I (f_1 = 3.16 Hz) at nodes corresponding to instrument locations

very little relative motion occurring between the top of the bent (XB5) and the deck (XD5) in the fundamental mode. The normalized modal amplitudes predicted for the Y direction are also lower than observed during the earthquake; however, this discrepancy may be partly due to the deficiencies of the model in the X direction.

A more detailed look at the behavior of the expansion joints can be made by examining the relative motions which occur across the joint at bent 5. The instrumentation layout on the bridge is ideally suited for such a study. The absolute accelerations, recorded at the top of bent 5 and at the deck level of span 4 near bent 5 are shown in Fig. 4.6, after they have been rotated into the X and Y directions. Fourier spectra of these motions, presented in Fig. 4.7, show a distinct peak at 3.16 Hz and several smaller peaks in the 5 to 7 Hz range. Relative motions across the expansion joint were obtained by subtraction of the

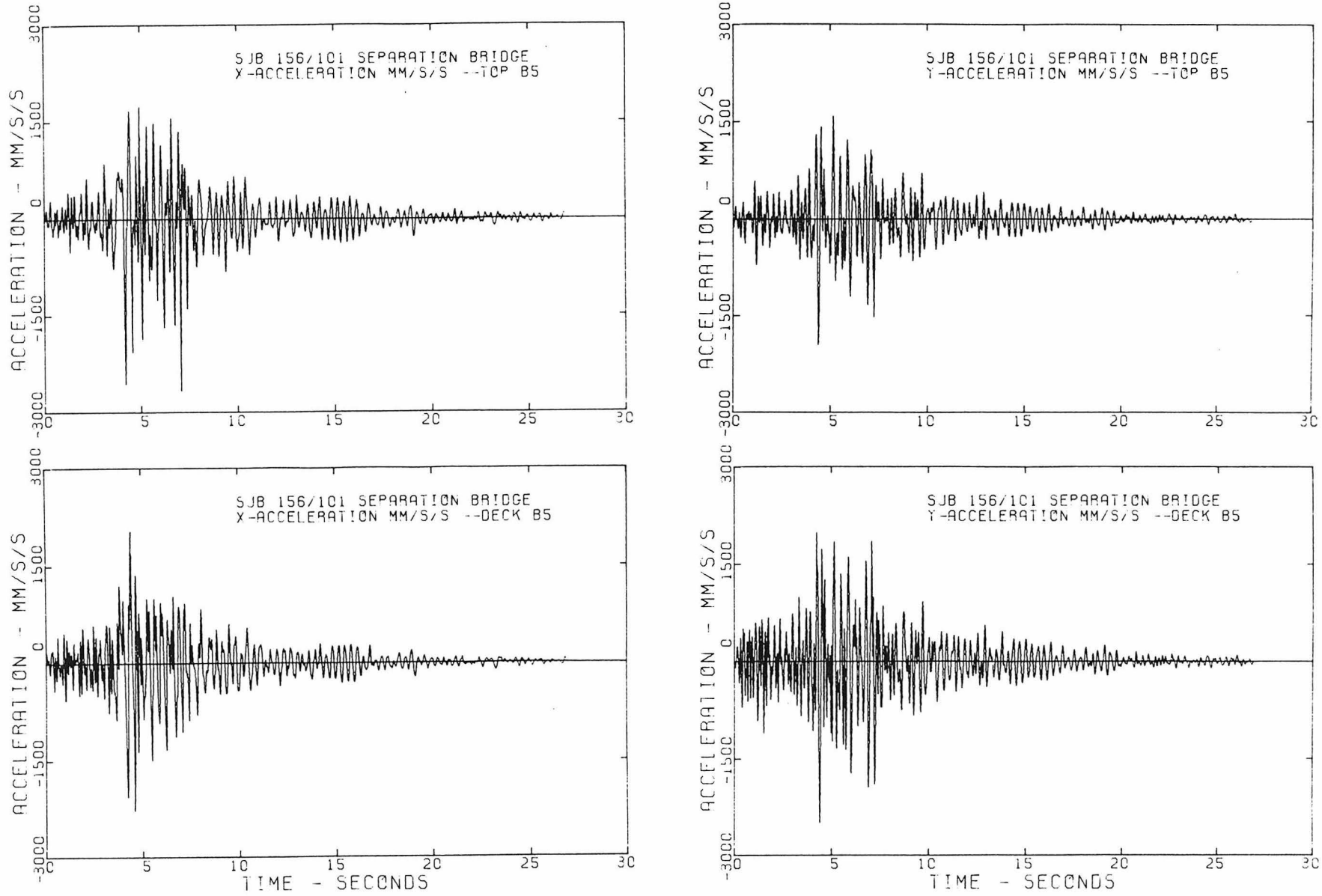

Figure 4.6 Absolute Accelerations of Superstructure at Bent 5

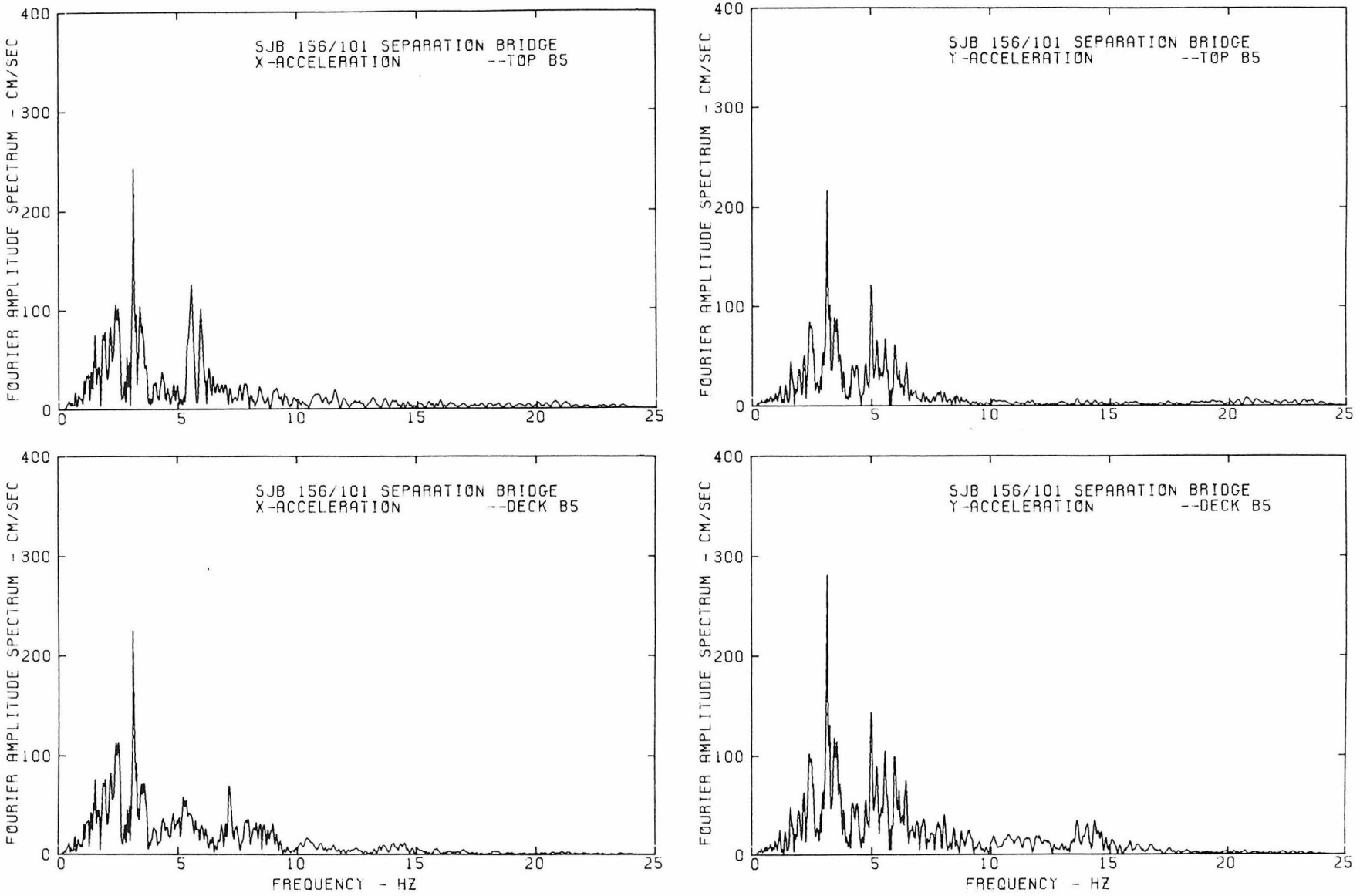

Figure 4.7 Fourier Spectra of Absolute Accelerations of Superstructure at Bent 5

respective X and Y records, with the results shown in Figs. 4.8 and 4.9. The Fourier spectra are transforms of the relative acceleration time-histories.

For motions in the longitudinal (X) direction the data presented in Fig. 4.8 supports the earlier observation that the expansion joints are essentially locked for response in the fundamental mode. The small peak in the Fourier spectrum near 3.4 Hz (Fig. 4.8b) may be a result of some slight rotation of the deck about a vertical axis in the fundamental mode, but the amplitude of the peak is similar to the amplitudes of many other peaks at higher frequencies (e.g., 9 Hz), which are probably noise-induced. The most noticeable features in the X direction are the peaks between 5½ and 6 Hz. This response dominates the Fourier spectra in Fig. 4.8b and is clearly visible in the time-history response in Fig. 4.8a. However, it is quite small in absolute terms. Considering the strongest segment of response in Fig. 4.8a, if one assumes this segment to be harmonic motion at 5.5 to 6 Hz, with acceleration amplitude of 1000 to 1500 mm/s^2, then the maximum estimated displacement occurring across the joint at this frequency would be no more than 1 millimeter.

The source of the motions at a frequency of about 5½ Hz is difficult to determine. In a later section (4.2.2) results of an ambient vibration survey show that the observed fundamental vertical frequency of the adjacent span (span 5) is 5.62 Hz. It is possible that the eccentric vertical loading on bent 5 due to the vertical vibration of span 5 has induced this small amount of relative longitudinal motion between the deck of span 4 and top of bent 5.

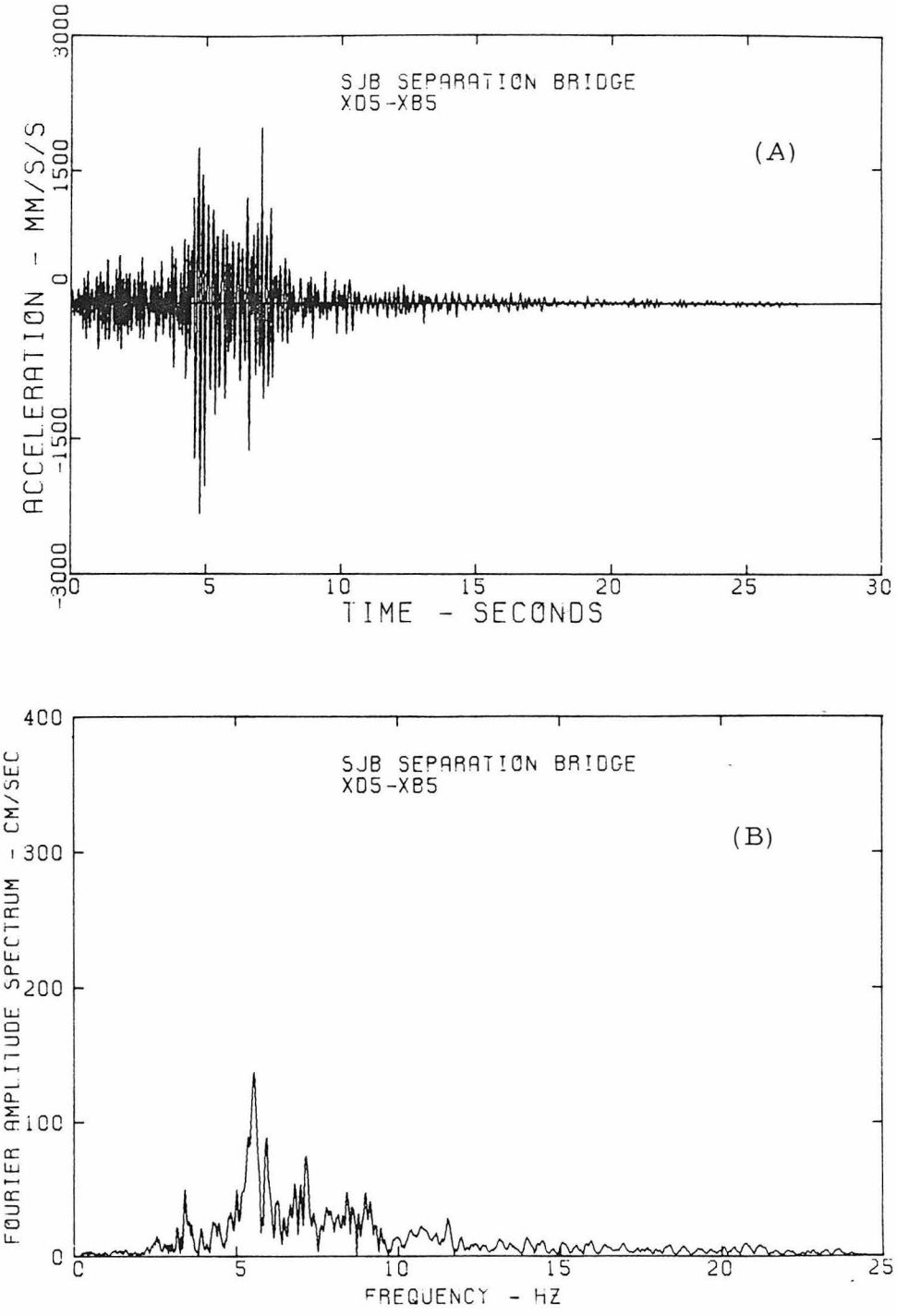

Figure 4.8 Relative Accelerations Across Expansion Joint in X Direction at Bent 5

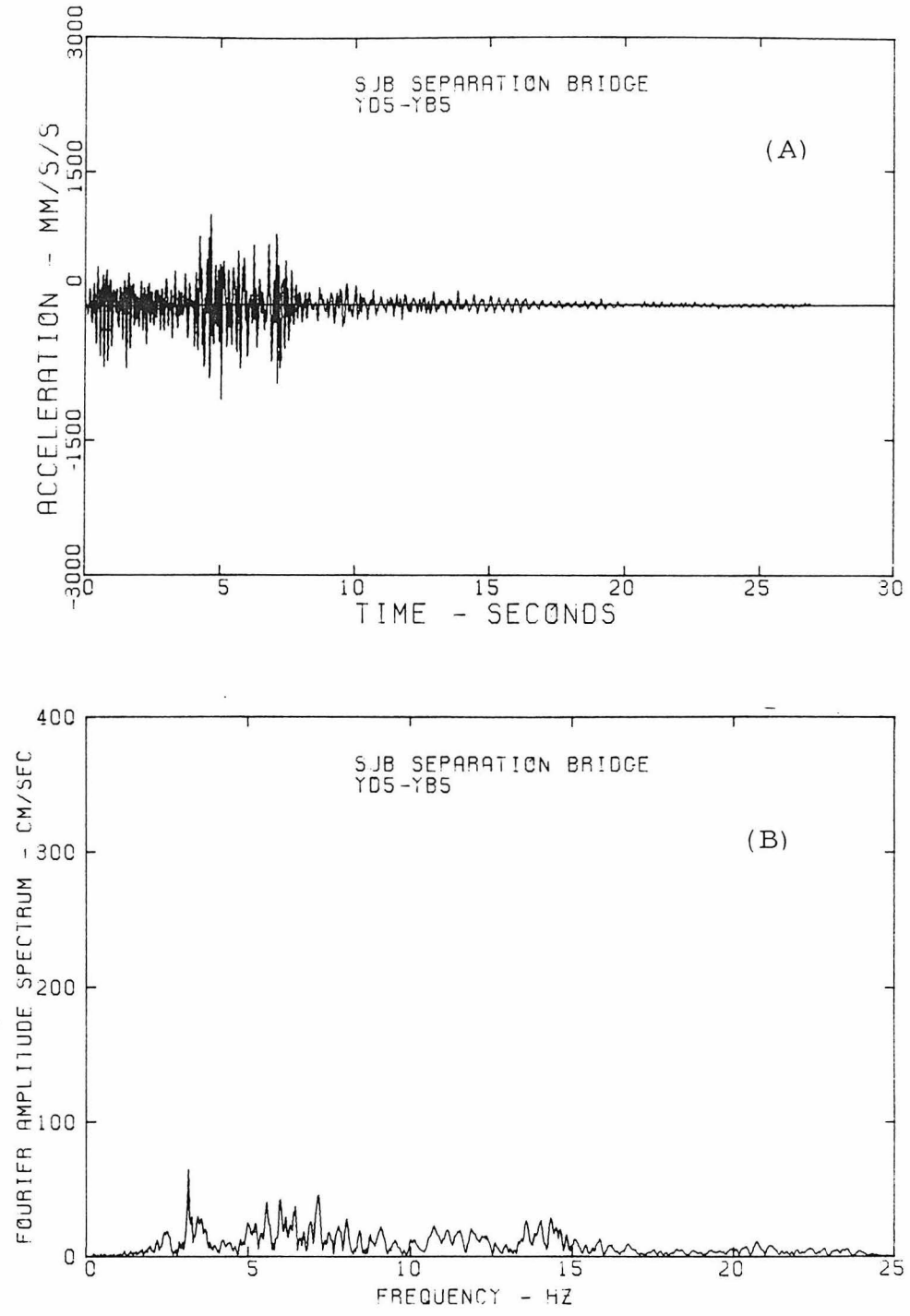

Figure 4.9 Relative Accelerations Across Expansion Joint in Y Direction at Bent 5

In the Y direction, the only peak to attract attention on the Fourier spectrum in Fig. 4.9b is at 3.16 Hz, but the amplitude of motion is relatively small, being comparable to the X amplitude at a similar frequency. The time-history response, shown in Fig. 4.9a, indicates a high-frequency relative acceleration with overall amplitudes less than in the X direction. The relative acceleration responses that were recorded in the Y direction represent displacements of substantially less than 1 mm and are believed indicative of the allowable displacements of the bearings in their transverse directions. The design of the expansion joints should prevent any larger relative motions between deck and bent in the Y direction.

From the observations in previous paragraphs it is apparent that the fundamental mode of bridge response (at least at these amplitudes of motion) is not modeled well by finite element model I. In particular, the problem appears to lie in providing the finite element model with the capability of correctly reproducing the behavior of the expansion joints. It would seem, from a study of the Fourier spectra and the recorded responses across the expansion joint, that a model with locked expansion joints would be more appropriate for describing the fundamental mode of the bridge. This observation is in direct contrast to the basic modeling assumption made for the expansion joints during synthesis of the finite element model from the structural plans, but seems to be the direction in which the earthquake response would point. The reason that such locking may occur is possibly a result of a certain amount of corrosion at the bearing interfaces, and the accumulation of windblown

debris over a period of years. Such locking behavior has been noticed by Douglas and Reid (1982) in tests of a bridge with neoprene bearing pads. Smith (1983) observed a significant amount of debris in the bearings of the San Juan Bautista bridge during a 1981 Caltrans field inspection and questioned their capability to move freely (in the intended, longitudinal direction). Consequently, further analysis of the San Juan Bautista bridge will be done using a finite element model which does not allow relative translations to occur between the ends of adjacent bridge spans.

4.2 A REVISED FINITE ELEMENT MODEL: MODEL II

Despite the modeling details, including soil compliances, introduced into model I, the computed modal responses do not correlate well with the observed bridge response during the Coyote Lake earthquake. The results of the previous section indicated that modeling of the expansion joints should be changed so that each simple span had pinned-pinned connections for longitudinal motions, rather than pinned-free connections. In this revised model, hereafter referred to as model II, the entire superstructure is involved in the modal responses in the horizontal (X-Y) plane, as contrasted with the previous model wherein modal responses were essentially vibrations of subsections of the bridge. Thus, in model II, there is continuity of displacements between the ends of adjacent spans in the X,Y,Z directions and continuity of rotation about the X axis. Both ends of each span are free to independently rotate about the Y axis, and the right end of each span is

free to rotate about the Z axis. Finally, there is continuity of rotation about the Z axis between the left end of each span and the associated bent structure below.

In model I the influence of longitudinal abutment stiffness is confined to span 1 because all other spans are isolated from abutment motions by the expansion bearings (roller) at the end of spans 1 and 6. Thus, for model I, it was reasonable to neglect soil-structure interaction at the abutments. In model II however, since the deck is continuous, forces may be transmitted longitudinally to the abutment, and hence their stiffnesses should be considered.

Evaluation of abutment stiffnesses for a highway bridge is a much more difficult task than the estimation of foundation stiffnesses for the intermediate supporting columns. Typically, methods developed for column footings (e.g., using results from elastic half-space analysis) are difficult to apply for determining abutment stiffness because of the complicated geometry and significantly different loading conditions. Only a few attempts have been made to determine experimentally the stiffnesses of typical highway bridge abutments (Douglas and Reid, 1982).

To include an allowance for abutment stiffness in model II of the San Juan Bautista bridge, a linear translational spring with stiffness k_A was placed in the X direction at both ends of the deck in the finite element model. Using the results of the system identification analyses in Chapter III as a guide, it was found that a spring constant of $k_A = 3 \times 10^6$ lbs/ft was required in order that the fundamental frequency

of model II matched the optimal fundamental frequency of 3.50 Hz. This value of k_A is somewhat low compared to recommended design values (Caltrans, 1982), and possibly indicates that the abutment stiffness during the Coyote Lake earthquake resulted from the mobilization of only a small amount of soil resistance due to the low displacement amplitudes.

Mode shapes for the first four horizontal modes of model II are shown in Fig. 4.10 and the corresponding frequencies are listed in Table 4.6.

TABLE 4.6

Horizontal Modal Frequencies for Model II

Mode	Frequency (Hz)
H-1	3.50
H-2	6.27
H-3	7.27
H-4	9.19

The vertical mode shapes and vertical modal frequencies of model II are unchanged from those of model I. The results for the horizontal modes indicate that, in addition to the forced match of the fundamental mode of the model with the results from system identification, the model predicted a second mode at a frequency of 6.27 Hz, very close to the

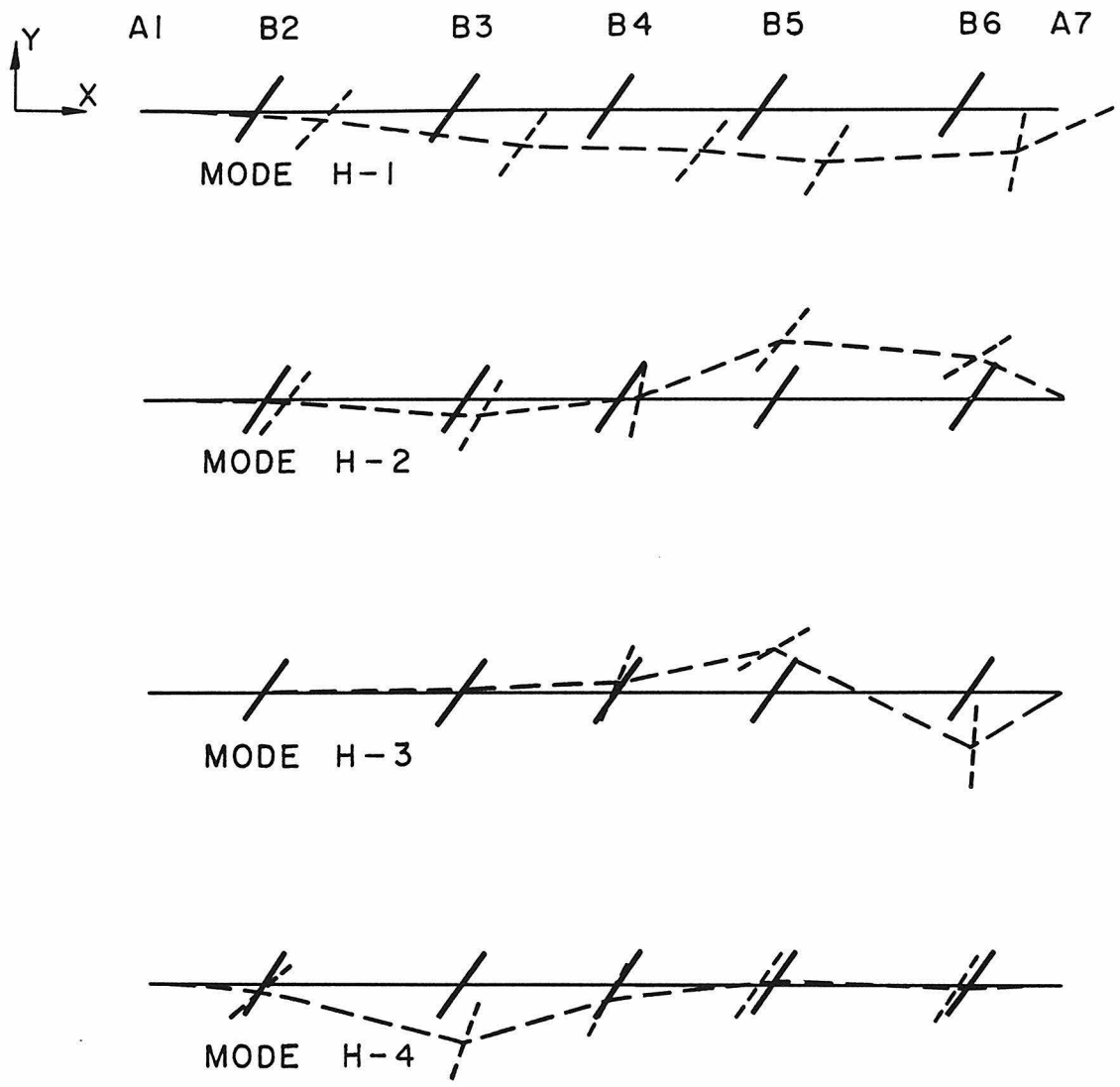

Figure 4.10 Horizontal Mode Shapes for Model II

6.33 Hz frequency found by system identification. Verification of more than two horizontal modes in the finite element model is not possible with the present data set, as it appears that longitudinal and transverse responses in higher modes are indistinguishable from high frequency recording noise.

4.2.1 Comparison of Observed and Modeled Responses in the Horizontal Direction

By comparing Fourier amplitudes from the earthquake records with the modal amplitudes at nodes of finite element model II, which correspond to instrument locations, it is possible to obtain an indication of how well the model simulates the actual seismic response of the bridge. Values of the Fourier amplitude and fundamental modal amplitude from model II, each normalized with respect to the amplitude in the X direction at the top of bent 5, are summarized in Table 4.7 (Fourier data are taken from Table 4.5). The motions at XB5 and XD5 and the motions at YB5 and YD5 are both in-phase, respectively.

The normalized modal amplitudes of model II are in reasonably good agreement with the Fourier amplitudes, and show a marked improvement over the results from model I, especially for the X direction where it is evident that very little relative motion is occurring across the expansion joint in the fundamental mode. From this comparison it appears that model II, which assumes locked expansion joints in the X direction, provides a substantially better representation of the funda-

TABLE 4.7

Comparison of Fundamental Modal Amplitudes for Model II and Fourier Spectral Data

Component	Normalized† Fourier Amplitude	Normalized* Modal Amplitude
XB5	1.00	1.00
YB5	0.80	0.75
XD5	0.92	1.08
YD5	1.09	0.80

Notes: (†) from Table 4.5
(*) from model II at nodes corresponding to instrument locations.

mental mode of response of the bridge than does model I, with its free expansion joints.

4.2.2 Dynamic Response in the Vertical Direction

The deployment of strong-motion instruments on the bridge, shown in Fig. 2.2, makes it clear that very little experimental information can be gained concerning the vertical modes of response because there is only one vertically-oriented transducer on the superstructure. This transducer is located on the underside of the concrete deck of span 4, very nearly above the expansion joint at bent 5 (see channel 7 on Fig. 2.2). Unfortunately, since the transducer is located very close to the end of the span, the amplitudes of vertical vibration are minimal. However, a Fourier spectrum of the motion on channel 7 does suggest a structural resonance of span 4 at a frequency of 7.13 Hz. Information

on the fundamental mode of vertical vibration for each span is summarized in Table 4.8, including a summary of data obtained during an ambient vibration survey (AVS) of the San Juan Bautista bridge conducted by Caltrans in April 1981 (Gates and Smith, 1981).

TABLE 4.8

Fundamental Vertical Mode Frequencies for Each Span

Data Source	Vertical Frequencies (Hz)					
	Span 1	Span 2	Span 3	Span 4	Span 5	Span 6
Finite Element Models	10.59	5.26	7.34	7.32	5.26	**
Caltrans AVS	10.01	5.57	7.81	7.91	5.62	18.65
Fourier Spectrum†	---	---	---	7.13	---	---
Theoretical*	10.59	5.15	7.34	7.34	5.15	17.86

--- not recorded
** not calculated
† from acceleration recorded during the Coyote Lake earthquake
* see text

The theoretical frequencies in Table 4.8 were calculated using the equation for the fundamental frequency of a simply-supported Bernoulli-Euler beam, $f = \frac{1}{2\pi} EI/m\ell^4$, m = mass/length, and using properties of the deck sections from Table 4.1. Average section properties were used for spans 2 and 5 in the beam equation, whereas the finite element solution accounts for the slight changes in girder size along the length of spans 2 and 5. The section properties of spans 1, 3, 4 and 6 are constant along their length.

The vertical frequency of 7.32 Hz computed by the finite element model for span 4 is in good agreement with the frequency of response (7.13 Hz) observed during the earthquake. The ambient vibration frequencies for spans 2 through 5 are from 6% to 8% greater than those predicted by the finite element analysis, possibly as a consequence of some minor amount of rotational restraint existing at the bearings during the low levels of ambient excitation. Overall, however, it appears that both the finite element model and Bernoulli-Euler beam theory predict the fundamental vertical frequency of each span quite well, with the maximum discrepancy between the ambient results and those of the models being less than 8%. The single vertical frequency observed during the earthquake, that of span 4, was within 3% of the frequency predicted by finite element model II.

Although the vertical seismic response of bridges such as the San Juan Bautista bridge are not of as great concern to engineers as are the longitudinal and transverse motions, the close agreement between results from the analysis and from experiments, including both ambient tests and the limited earthquake data, helps provide confidence in the structural idealizations and model synthesis described in earlier sections of this dissertation. The results also show that simple beam models can be used with reasonable confidence in examining the vertical responses of similar bridges. That is, bridge structures in which each span acts in a simply-supported manner, with vertical responses uncoupled from horizontal motions of the bridge.

CHAPTER REFERENCES

Bathe, K-J., Wilson, E.L. and Peterson, F.E. (1973). "SAP IV A Structural Analysis Program for Static and Dynamic Response of Linear Systems," Earthquake Engineering Research Center, Report No. EERC 73-11, University of California, Berkeley, California.

California Department of Transportation (1982). "Caltrans Seismic Design Criteria for Bridges and Commentary," Sacramento, California.

Douglas, B.M. and Reid, W.H. (1982). "Dynamic Tests and System Identification of Bridges," Journal of the Structural Division, ASCE, Vol. 108, No. ST10, October, pp. 2295-2312.

Douglas, B.M. and Richardson, J.A. (1984). "Maximum Amplitude Dynamic Tests of a Highway Bridge," to appear in Proceedings of the Eighth World Conference on Earthquake Engineering, San Francisco, California.

Foutch, D.A. and Jennings, P.C. (1978). "A Study of the Apparent Change in the Foundation Response of a Nine-Story Reinforced Concrete Building," Bull. Seism. Soc. Am., Vol. 68, No. 1, February, pp. 219-229.

Gates, J.H. and Smith, M.J. (1982a). "Verification of Dynamic Modeling Methods by Prototype Excitation," California Dept. of Transportation, Report No. FHWA/CA/ST-82/07, Sacramento, California.

Gates, J.H. and Smith, M.J. (1982b). California Dept. of Transportation, Sacramento, California, personal communication.

Jennings, P.C. and Bielak, J. (1973). "Dynamics of Building-Soil Interaction," Bull. Seism. Soc. Am., Vol. 63, No. 1, February, pp. 9-48.

Luco, J.E. and Westmann, R.A. (1971). "Dynamic Response of Circular Footings," Journal of the Engineering Mechanics Division, ASCE, Vol. 97, No. EM5, October, pp. 1381-1395.

Okamoto, S. (1973). Introduction to Earthquake Engineering, John-Wiley and Sons, Inc., New York.

Richart, F.E., Hall, J.R. and Woods, R.D. (1970). Vibrations of Soils and Foundations, Prentice-Hall, Inc., New Jersey.

Scott, R.F. (1983). California Institute of Technology, personal communication.

Shannon and Wilson, Inc., and Agbabian Associates (1980). "Geotechnical Data from Accelerograph Stations Investigated During the Period 1975-1979," NUREG/CR-1643, Report to the U.S. Nuclear Regulatory Commission, September.

Smith, M.J. (1983). California Dept. of Transportation, Sacramento, California, personal communication.

Veletsos, A.S. and Wei, Y.T. (1971). "Lateral Rocking Vibration of Footings," Journal of the Soil Mechanics and Foundation Division, ASCE, Vol. 97, No. SM9, September, pp. 1227-1248.

CHAPTER V

SUMMARY AND CONCLUSIONS

5.1 SUMMARY

In this dissertation, the earthquake response of a major six-span highway bridge has been studied using strong-motion records obtained on the bridge after a moderate earthquake. The bridge under study, the San Juan Bautista 156/101 Separation bridge in California, was subjected to moderate levels of ground shaking (0.12g maximum horizontal acceleration) at a distance of approximately 30 km from the epicenter of the 6 August 1979 Coyote Lake earthquake ($M_L = 5.9$). The shaking was not strong enough to damage the bridge. The set of twelve time-synchronized accelerograms was the first strong-motion data recorded on a highway bridge in California and provided a unique opportunity to study the earthquake response of such a structure. The moderate levels of shaking and the undamaged condition of the bridge after the earthquake provided reasonable grounds for assuming linear elastic behavior of structural components.

The study was subdivided into three parts, involving: (1) a study of the earthquake ground motions at the bridge site using techniques of engineering seismology; (2) a computer-oriented, systematic determination of best estimates of modal parameters (frequency and damping) of the bridge, using the strong-motion data; and (3) dynamic modeling and analysis of the bridge using a finite element approach. Although each of the three major parts viewed the earthquake response of the bridge

from a different perspective, and together involved several forms of analyses, the overall result is a fairly comprehensive evaluation of the seismic response of the San Juan Bautista bridge.

The location of transducers at two ground level stations made it possible to study variations in ground motion along the length of the bridge. By correlation of the P wave motions at the two instrument sites, the difference in arrival time of P waves at the abutments was estimated to be 0.021 seconds. The results indicated that, within the significant frequency band of the earthquake motion, differential vertical excitation of the bridge supports by travelling P waves would be minimal.

The calculated ground displacements did reveal, however, the presence of a seismic excitation having a period of approximately three seconds, much longer than any structural periods. Upon subtraction of the displacements at the two sites it was found that the three-second signal was responsible for a differential motion of the bridge foundation. A three-second period signal also appearing in the displacement of the superstructure relative to the ground at bent 5 was found to be correlated with the three-second differential ground motion. This is an indicator of pseudostatic response of the structure to differential movement of its supports. Furthermore, analysis of the ground displacements, using a horizontal component rotated into the radial direction with respect to the earthquake epicenter, demonstrated that the long-period ground displacements in the radial-vertical plane were retrograde during most of the strong shaking. These findings all support the

premise that the long-period superstructure displacements were a result of differential support motion induced by phase delays in a Rayleigh wave travelling across the bridge site.

In Chapter III, a computer-oriented system identification technique, based upon an output-error approach, was utilized to determine optimal estimates of frequencies and damping values of the dominant modes of response of the bridge. The modal minimization method, originally conceived for a single input-single output analysis of earthquake records from buildings, was found to work surprisingly well provided the strong-motion records were rotated into directions in which the dominant structural response was in a single mode. For the San Juan Bautista bridge, record orientations parallel to and perpendicular to the direction of skew of the bents were found to work best.

The contribution made to the structural response by the long-period differential support motion was not serious from the viewpoint of possible damage, but it significantly complicated modal identification from the strong-motion data. Systematic identification of frequencies and estimates of damping for the first two modes required that these long-period components be filtered from the data in order to obtain good definition of modal characteristics. Using time-invariant models, best estimates of frequencies of the first two horizontal modes of the bridge were found to be 3.50 Hz and 6.33 Hz, with associated damping values of approximately 10% of critical in each mode. A moving window analysis, used to study the time variation of frequencies and damping values, indicated a general trend towards a decrease in frequency of each mode

as the intensity of shaking increased. In the fundamental mode, at very low levels of excitation, the damping was found to be in the range of 3% to 6%, but increased to 12% during the time of strongest response.

In Chapter IV a three-dimensional finite element model of the bridge was developed to compare responses calculated from standard modeling procedures with the observed earthquake responses. It was found that such a model, which also included soil-structure interaction, was able to predict modal frequencies in agreement with the observed values only when the expansion joints were assumed to be locked, thereby preventing relative motion between adjacent spans in the longitudinal direction. This is in contrast to the common assumptions used in modeling such expansion joints in which freedom of longitudinal relative movement supposedly occurs at the joints. Springs, added to model the effect of abutment resistance, were adjusted to provide a fundamental modal frequency of 3.50 Hz, the same as the observed fundamental frequency of the bridge. The fundamental modal amplitudes predicted by this model were in reasonably good agreement with those observed as a result of earthquake shaking. Additionally, the finite element model predicted the second horizontal modal frequency to within 1% of the observed value of 6.33 Hz.

The only significant dynamic response in the vertical direction was that of the individual spans. Very close agreement was found in the fundamental vertical frequencies predicted by the finite element model, the Bernoulli-Euler beam analyses and the results of an ambient vibration survey. Together, the results for horizontal and vertical

responses suggest that the bearings were essentially free to work in rotation but not in longitudinal translation.

5.2 CONCLUSIONS

The comments and observations on earthquake response of bridges stated in previous chapters were directed specifically at the San Juan Bautista bridge. In a broader context, the results of the research also may be used to comment on the seismic response of highway bridges in general.

As previously stated, the response of the San Juan Bautista bridge was a result of only moderate earthquake ground shaking. In the horizontal directions the bridge responded to the shaking as a continuous structure with expansion joints locked for translational motions. It seems reasonable to conjecture that under similar levels of ground shaking many other bridges, particularly those similar to the San Juan Bautista bridge, may respond with locked expansion joints and with behavior described by a dynamic model which assumes this feature. At higher levels of earthquake ground shaking, however, the forces involved may be large enough that one or more expansion joints may suddenly become free to respond with large amplitudes. A bridge's dynamic response under these conditions would be significantly different than that shown by the San Juan Bautista bridge. Thus, a knowledge of the expected behavior of the bearing-expansion joint system under dynamic loading conditions is an important factor in an assessment of the seismic response of such bridge structures. Most significant are the

questions of when the bearings allow movement to occur, and in what degrees-of-freedom will movement occur. The research in this dissertation has addressed the later question. Future work and additional strong-motion records obtained for various intensities of shaking are needed before the former question can be answered adequately.

Current methods of upgrading the seismic resistance of bridges like the San Juan Bautista structure are aimed, in part, at providing positive connections across the expansion joints by means of restrainer bars or cables. Depending on the details of the restrainers, the assumption of locked expansion joints may be appropriate even under severe seismic loading conditions.

The responses of individual bridge spans in the vertical direction was predicted very well by both the theoretical beam models and the finite element model. The close agreement between the finite element results and the observed fundamental vertical frequencies provides encouraging support for the modeling techniques used in creating the finite element representation, especially in the use of a transformed deck section and in allowance for rotations about the Y axis of the bearings.

The presence of long-period surface waves complicated modal identification procedures; however, since the periods of all bridge modes were much shorter than the surface wave period, the response of the bridge to these waves was essentially static. The results of this research suggest that, for engineering purposes, effects of differential support motion could normally be neglected in computing the earthquake

response of moderate length highway bridges founded on uniform soil conditions. The more common assumption of rigid base excitation is likely to be sufficient for such structures. For very long span or very tall bridge structures, where the fundamental frequency may be close to the frequency of large amplitude surface waves, then long-period differential support motions may significantly influence the dynamic response of the bridge.

A major problem associated with measuring and evaluating some aspects of the response of structures to long-period earthquake motions is the accuracy with which long-period displacements can be recovered from recorded accelerograms. Furthermore, with current processing techniques, permanent offsets of a structure, such as rotations of skew bridges, cannot be evaluated from the time-histories, as permanent deformations are removed during routine processing of velocities and displacements. Digital recording strong-motion accelerographs are expected to improve this situation by increased recording resolution and by associated changes in processing techniques.

A few comments may be made regarding the placement of strong-motion transducers on the San Juan Bautista bridge. Although a substantial amount of data was collected at the bridge during the Coyote Lake earthquake, the research of previous chapters suggests that the present plan of instrumentation might be augmented or reconfigured in order to obtain additional earthquake response data which would both complement and supplement the existing data set. This is not meant as a criticism of the present placement of instruments, which were installed to study

one aspect of the bridge response, but rather as a way in which additional information might be obtained. Either an augmentation or rearrangement of instruments on the San Juan Bautista bridge is believed preferable to moving them to a new bridge site because the potential for future earthquakes to occur in the area is much greater than in many other areas of California, and because of the advantages of having repeated measurements on the same structure.

Based upon the research in this dissertation, it is recommended that the present twelve transducers be redeployed at the San Juan Bautista bridge site, if they cannot be augmented. In redeployment, one triaxial free-field station should be located at a distance of 200 to 300 feet from the bridge, along the median of U.S. Highway 101, and the other nine channels should be arranged on the superstructure and abutments of the bridge. The overall objective of the proposed redeployment of transducers is to place a greater emphasis on obtaining detailed measurements of the dynamic response of the superstructure/abutment system, rather than on measuring spatial variations in ground motions.

The exact placement of transducers on the superstructure will depend upon the practical constraints of installation of the instruments. It would, however, be highly desirable to locate at least two sets of biaxial transducers to measure motions in the horizontal plane. The results of finite element model II suggest that maximum modal information might be recovered if one set of superstructure instruments was located near bent 3, and a second set near bent 5.

Of course, even greater flexibility and scope would be possible by addition of a second central recording system to increase the number of data channels. Figure 5.1 illustrates a more ambitious plan involving rearrangement and augmentation of the present instrumentation system on the San Juan Bautista bridge. The plan, consisting of twenty-six transducers, is based upon the dual objectives of: (1) obtaining a second set of data from the same locations that were instrumented during the 1979 Coyote Lake earthquake; and (2) obtaining dynamic measurements for several additional degrees-of-freedom, involving both bridge and soil systems. The following paragraph outlines the intended purpose in the location of each of the transducers. To complement Fig. 5.1, the location of each transducer is described in Table 5.1.

It is recommended that a triaxial package (transducers 1,2,3 in Fig. 5.1) be located 200 to 300 feet from the bridge, along the median of U.S. Highway 101, to record free-field accelerations. Transducers 8, 9 and 10 are placed with the intent of measuring the motions at abutment 1 (A1) in X and Y translation and in rotation about the Z axis (using 8 and 10). Transducers 23, 24 and 25 have a similar function at abutment 7. Additionally, transducer 26 is placed for measurement of relative motions in the X direction across the abutment joint at A7. Transducers 11 to 16 are placed to obtain better definition of the bridge response in the horizontal plane. Pair 12 and 13, and pair 15 and 16 will provide a check on possible expansion joint movements. Transducers 4 and 5, and 17 to 20 are at the same location as several of the transducers during the Coyote Lake earthquake and hence will provide for a

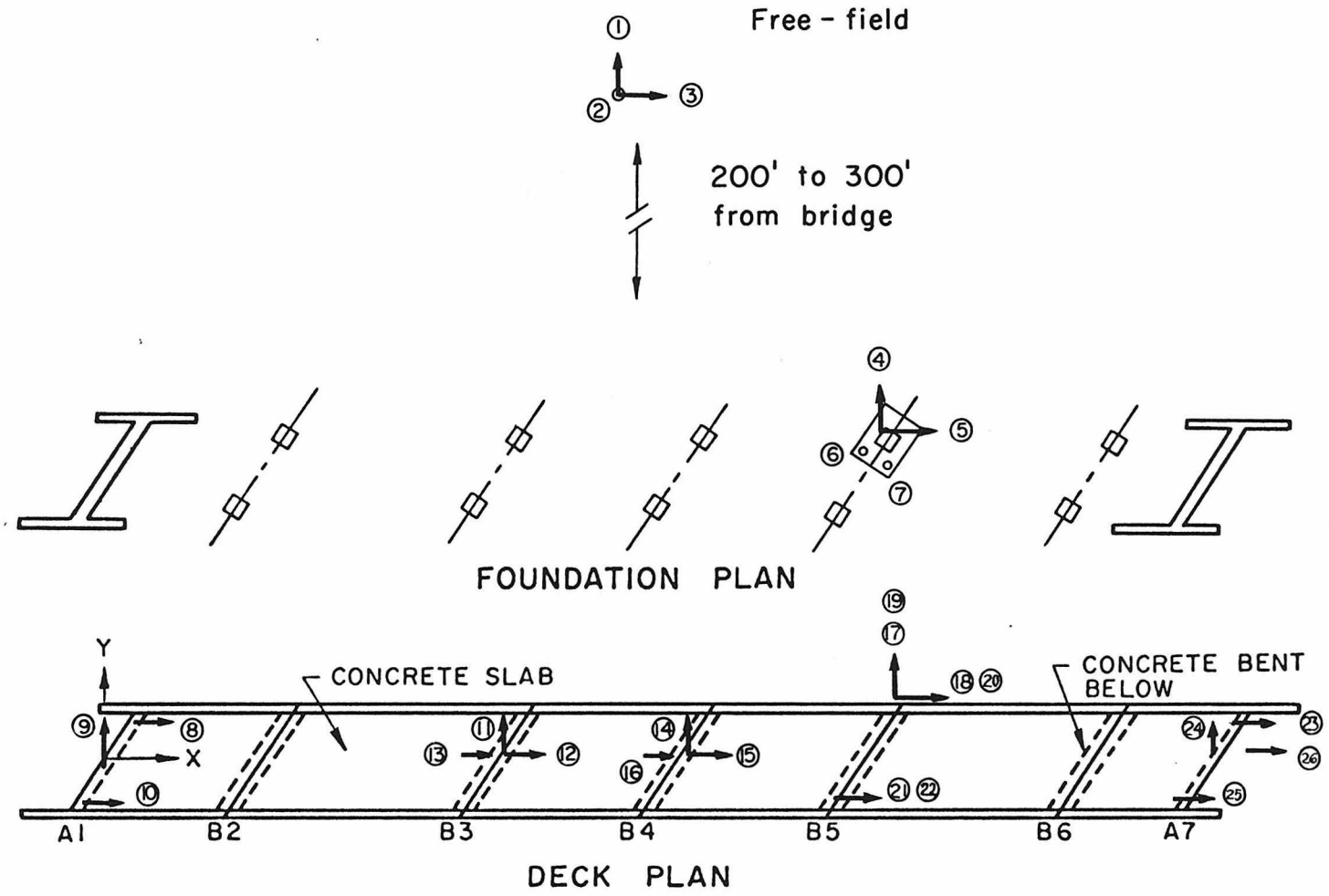

Figure 5.1 A Recommended Plan of Instrumentation for the San Juan Bautista Bridge

TABLE 5.1

Recommendation for Strong-Motion Instrumentation
of the San Juan Bautista Bridge

Transducer	Location
1,2,3	Free-field
4,5	Horizontal, on footing at B5
6,7	Vertical, on footing at B5
8,9,10	Deck of span 1, near A1
11,12	Top of B3
13	Deck of span 2, near B3
14,15	Top of B4
16	Deck of span 3, near B4
17,18,21	Top of B5
19,20,22	Deck of span 4, near B5
23,24,25	Deck of span 6, near A7
26	Near joint at A7

valuable comparison of bridge responses during different earthquakes. Transducers 21 and 22, together with 18 and 20, may be used to determine whether relative translational and/or rotational motions occur across the expansion joint at bent 5. Vertically oriented transducers 6 and 7, located on opposite sides of one of the footings at bent 5, are intended for measurement of rocking motions of the foundation.

In addition to strong-motion transducers, it is further recommended that scratch-plate devices be installed across one or more of the expansion joints to obtain direct measurement of any relative displacements occurring across the joints. These devices would provide for a valuable comparison with the maximum displacements computed by integration of the accelerograms.

The above described instrumentation plan should allow a comprehensive set of strong-motion records to be obtained for the San Juan Bautista bridge. In view of the results of the analysis of the bridge's response to the Coyote Lake earthquake, most of the emphasis has been placed on measurements for the horizontal (X-Y) plane. Only three transducers (2,6,7) have been oriented in the vertical direction. A deployment of twenty-six transducers affords enough flexibility to provide a check on the behavior of several of the expansion joints without unduly compromising the number of transducers available for the purpose of defining modal properties.

To date, research efforts to study the earthquake response of bridges have been small in comparison to the efforts put forth in other areas of earthquake engineering. From the research undertaken in the preparation of this thesis, it is felt that investigations in the near future in bridge earthquake engineering should be focused in two major directions, with the aims of: (1) increasing the number of bridges instrumented with strong-motion accelerographs; and (2) gaining an increased understanding of the dynamics of soil-bridge systems.

Since strong-motion accelerograms are the basic source of data for earthquake engineering research, it is necessary that the current plan of instrumenting highway bridges (ref: Table 1.1) be extended to include a variety of types of construction (steel, reinforced concrete, pre-stressed concrete), geometry, length and height. The current existence of only a few sets of response data necessarily limits the broader implications which can be drawn from the data. Of particular concern is the lack of strong-motion instrumentation on very long-span, high overcrossing bridges. This type of bridge has significantly different dynamic properties than a structure like the San Juan Bautista bridge.

One effective method of studying structural dynamics of bridges, in addition to utilizing strong-motion accelerograms, is to measure experimentally the dynamic response of full-scale structures. Ambient vibration surveys, while relatively quick and easy to perform, may not always furnish sufficient information. For example, under low levels of ambient excitation it is possible that not all of the modes of interest may be sufficiently excited to allow accurate measurements to be made. Forced vibration testing, although more expensive and time-consuming, affords the opportunity of exciting a structure under controlled conditions and at various applied force levels. Such studies have the potential of yielding valuable information on both structural dynamics and soil-bridge interaction. Again, it would be desirable to investigate bridge structures of various designs.

5.3 FINAL REMARKS

The observations and results presented in this dissertation have provided a detailed examination of the seismic response of a multiple-span highway bridge, subjected to moderate levels of earthquake ground motion. By a careful consideration of the nature of earthquake ground motions at the bridge site it was possible to identify both pseudostatic and dynamic components of bridge response. From the dynamic components, dominant modes of response were identified. It was also shown that standard finite element methods of dynamic analysis can describe the earthquake response of geometrically complicated highway bridge structures extremely well for moderate levels of earthquake excitation. In developing such models, attention must be given to the dynamic behavior of structural details, particularly expansion joints. Similar analyses, applied to the strong-motion records from other bridges, should lead to a substantially better understanding of the earthquake response of these structures.